DYNAMIC MODULATION OF *IN VIVO* SEROTONIN SIGNALING

Elyse Cathleen Dankoski

A dissertation submitted to the faculty at the University of North Carolina at Chapel Hill in partial fulfillment of the requirements for the degree of Doctor of Philosophy in the Curriculum in Neurobiology.

Chapel Hill
2014

Approved by:

R. Mark Wightman

Regina M. Carelli

Sabrina Burmeister

Paul Manis

Benjamin Philpot

ABSTRACT

Elyse C. Dankoski: Dynamic Modulation of *In Vivo* Serotonin Signaling
(Under the direction of Prof. R. Mark Wightman)

Serotonin signaling influences many neural processes and is highly implicated in the etiology and treatment of depression. Understanding how *in vivo* elements regulate serotonin signaling may provide insight into serotonergic function in the depressed brain. This work presents a modification to fast-scan cyclic voltammetric methods that enables rapid, spatially resolved, and chemically selective measurement of *in vivo* serotonin signaling in the substantia nigra *pars reticulata*. We used this modified technique to investigate the dynamics of serotonin neurotransmission. Initial investigations found that serotonin release can be evoked by electrical stimulations *in vivo*, but it is greatly attenuated in comparison to serotonin evoked in brain slices. We hypothesized that feedback from intact inhibitory circuitry restricted serotonin signaling *in vivo*. A comparison of *in vivo* dopamine and serotonin release revealed a critical role for the serotonin transporter (SERT) in limiting serotonin signaling. This process is likely involved in the therapeutic effects of selective serotonin reuptake inhibitors (SSRIs), which are common pharmacotherapies for depression. Further studies found that acute SSRI treatment uniquely enhances serotonin signaling by disrupting inhibitory feedback to the dorsal raphe nucleus. We hypothesized that this action plays an important role in the 3-6 week lapse between SSRI treatment onset and clinical efficacy. Indeed, in a study of chronic SSRI treatment, we found that long-term reductions in SERT function result in enduring enhancement of serotonin signaling. In a healthy brain, this signaling is the product of dynamic, multi-systemic modulation, and SERT

activity likely drives both ambient and transient serotonin concentrations in a coordinated, equilibrated manner. Our finding that the introduction of mild stress can significantly impact the effects of SSRIs implicates a more complex network of elements in the modulation of serotonin signaling. Future work will address how stress interacts with serotonergic function.

To my family, especially Mom, Dad, Grandpa, and Grandma. I love you.

ACKNOWLEDGEMENTS

Thank you to my mentor, Mark Wightman. My experience working with you has made me a better problem solver, writer, critical thinker, and an aspiring PBR connoisseur. You had confidence in my ability to work as an independent scientist, to make mistakes, and to learn from them, even when I didn't have confidence in myself. This was a training experience I feel lucky to have had.

I am sincerely grateful for the intellectual contribution and moral support of all my current and former labmates in the Wightman lab during my doctoral work. Above all, thank you to Dr. Nina Owesson-White, Dr. Anna Belle, Dr. Zoe McElligott, Jenny Ariansen, and Meg Fox for many hours of science mixed with fun (and sometimes just fun).

Many collaborators contributed to the research that made these chapters and publications a reality. I would especially like to acknowledge the contributions of Dr. Thorfinn Riday, Dr. Kara Agster, and Dr. Sheryl Moy.

7 years ago, I had no clue how to pursue a graduate education in science. For the inspiration, information, and confidence to follow my interest in neuroscience toward a Ph.D, I thank Dr. Paul Gold, Dr. Donna Korol, Dr. Gene Robinson, and the ISNI Program at the University of Illinois at Urbana-Champaign. For mentorship and guidance throughout my undergraduate studies, I thank Dr. Steve Pruett-Jones and Dr. Philip Lloyd at the University of Chicago.

Finally, I thank my family for their support and dedicate this dissertation to them. To my parents, who encouraged me to live "the life of the mind." To my grandfather, whose love of knowledge has always been an inspiration to me. To Rylan, whose continual support, kindness, and friendship make every day a good day.

Crescat scientia; vita excolatur.

TABLE OF CONTENTS

LIST OF ABBREVIATIONS xii

CHAPTER 1: MONITORING SEROTONIN SIGNALING WITH FSCV 1

Introduction 1

1. Fast-scan cyclic voltammetry of serotonin 2

2. Electrical stimulation 9

3. Release 11

4. Uptake 17

5. Future Directions 25

Conclusion 27

Support 28

CHAPTER 2: VOLTAMMETRIC DETECTION OF 5-HYDROXYTRYPTAMINE RELEASE IN THE RAT BRAIN 34

Introduction 34

Experimental Methods 38

Results and Discussion 42

Conclusion 51

CHAPTER 3: SIMULTANEOUS SEROTONIN AND HISTAMINE RELEASE FOLLOWING MEDIAL FOREBRAIN BUNDLE STIMULATION 61

Introduction 61

Materials and Methods 63

Results 68

Discussion 72

CHAPTER 4: DIFFERENTIAL MECHANISMS IN THE REGULATION OF IN VIVO DOPAMINE AND SEROTONIN RELEASE 85

Introduction 85

Methods 87

Results 88

Discussion 93
Conclusions 97
Supplemental Methods 98
Support 101
CHAPTER 5: THE DORSAL RAPHE NUCLEUS MEDIATES SSRI-INDUCED FACILITATION OF SEROTONIN SIGNALING 107
Introduction 107
Materials and Methods 108
Results 111
Discussion 115
Support 119
CHAPTER 6: FACILITATION OF SEROTONIN SIGNALING BY SSRIs IS ATTENUATED BY SOCIAL ISOLATION 123
Introduction 123
Materials and Methods 125
Results 128
Discussion 134
Supplemental Methods 137
Support 140
CHAPTER 7: CONCLUSION 148
Summary of findings 148
Discussion and Future Directions 154
Concluding Remarks 156
REFERENCES 158

LIST OF FIGURES

Figure 1.1 *In vitro* calibration of microelectrodes 29

Figure 1.2 Illustration of a carbon-fiber microelectrode in SNr 30

Figure 1.3 A model predicts serotonin release and uptake at different frequencies. 31

Figure 1.4 Sample trace of *in vivo* serotonin release and uptake. 32

Figure 1.5 A synopsis of the findings presented in this article. 33

Figure 2.1 Comparison of waveforms for detection of dopamine and serotonin 53

Figure 2.2 Comparison of cyclic voltammograms obtained *in vivo* vs. *in vitro* 54

Figure 2.3 Nafion-modified microelectrodes are more sensitive to 5-HT. 55

Table 2.1 Comparison of Responses of Bare vs. Nafion-Modified 56

Figure 2.4 Response of bare and Nafion-modified electrodes to common electronegative species 57

Figure 2.5 Determination of lp and D5-HT for a Nafion-coated carbon-fiber microelectrode using flow injection analysis 58

Figure 2.6 Electrochemical and anatomical validation of 5-HT detection. 59

Figure 2.7 Pharmacological validation of 5-HT signal with GBR 12909 and citalopram 60

Figure 3.1 Histology of Stimulating and Carbon-Fiber Electrode Placements in the MFB and SNpr 79

Figure 3.2 5-HT Color Plot, CV and Time Profile of Response in SNpr with DRN and MFB Stimulation. 80

Figure 3.3 Comparison of *In vivo* Signal to a Mixed *In vitro* 5-HT and Histamine Signal 81

Figure 3.4 Effect of Varying Scan Rate and Upper Potential Limit on Histamine Response *In vitro*. 82

Figure 3.5 Pharmacological Characterization of Histamine with SKF 91488 83

Figure 3.6 A Comparison of 5-HT Experimental Data and Kinetic Analysis Between DRN and MFB Stimulation 84

Figure 4.1 Comparison of dopamine and serotonin release evoked by electrical stimulation of MFB 102

Figure 4.2 Comparison of dopamine and serotonin release evoked by varying stimulation parameters. 103

Figure 4.3 Effects of manipulating dopamine and serotonin synthesis, packaging and release. 104

Figure 4.4 Effects of uptake and MAO inhibitors on dopamine and serotonin release. 105

Figure 4.5 Dual uptake and MAO inhibition disregulates serotonin signaling. 106

Figure 5.1 Serotonin release is not frequency-dependent in vivo 120

Figure 5.2 Inhibiting SERT induces frequency-dependent serotonin release 121

Figure 5.3 DRN mediates enhancement of serotonin signaling by SSRIs 122

Figure 6.1 Voltammetric determination of serotonin release in the substantia nigra pars reticulata of the mouse brain. 141

Figure 6.2 Effects of cCIT or VEH treatment on marble-burying and OF assays in pair- and single-housed mice 142

Table 6.1 Maximal serotonin release measured in SNpr 143

Figure 6.3. Comparison of serotonin release and uptake evoked by electrical stimulation of the DRN 144

Figure 6.4 Comparison of electrically-evoked serotonin release following acute CIT challenge 145

Figure 6.S1. Comparison of liquid consumption before and during CIT/VEH treatment and tissue content analysis. 146

Figure 6.S2. 5-HT concentration traces evoked by each stimulation frequency 147

LIST OF ABBREVIATIONS

$[5\text{-HT}]_{max}$	maximal evoked serotonin amplitude
$[5\text{-HT}]_p$	serotonin released per stimulus pulse
5-HIAA	5-Hydroxyindoleacetic acid; a metabolite of serotonin
5-HT	5-Hydroxytryptamine, serotonin
CIT	citalopram; a selective serotonin reuptake inhibitor
DRN	dorsal raphe nucleus
FSCV	fast-scan cyclic voltammetry
K_i	Inhibition constant denoting affinity of ligand for target
K_M	Michaelis constant for half maximal activity
MAOI	monoamine oxidase inhibitor
MFB	medial forebrain bundle
SERT	serotonin transporter
SNpr	substantia nigra *pars reticulata*
SSRI	selective serotonin reuptake inhibitor
$t_{1/2}$	decay time between peak and half-maximal amplitude
V_{max}	maximum velocity of uptake

CHAPTER 1: MONITORING SEROTONIN SIGNALING WITH FSCV [1]

Introduction

The neurotransmitter serotonin (also called 5-hydroxytryptamine or 5-HT) can be found in nearly every region of the central nervous system. Its functions are as diverse as the areas it innervates, and it is a complex component of many psychiatric disorders. This pervasive involvement in brain-wide neurocircuitry is supported by an exceptionally large family of receptors whose collective functional scope enables the multifarious actions of serotonin throughout the brain (Barnes & Sharp, 1999). Much of our knowledge about serotonin comes from studies investigating its actions via these receptors, which remain the target of many pharmacotherapies involving serotonergic signaling. However, the release and uptake dynamics of serotonin precipitate its downstream effects, and exploring how these dynamics are modulated has provided key insights to the serotonin system and its therapeutic potential.

A number of techniques have been used to characterize serotonin signaling in the brain. *In vivo* microdialysis has provided key insights into natural and pharmacologically-induced fluctuations in ambient extracellular levels of serotonin. However, even recent advancements in microdialysis sampling rates provide markedly lower temporal resolution than required to examine individual release and uptake events (Schultz & Kennedy, 2008).

[1] This chapter previously appeared as an article in Frontiers in Integrative Neuroscience. The original citation is as follows: Dankoski EC and Wightman RM. "Monitoring serotonin signaling on a sub-second time scale." *Front. Integr. Neurosci.* 7, 44 (Jun 2013).

Electrophysiological measurements can infer some properties of neurotransmitter release by measuring postsynaptic response, and this method works well for neurotransmitters like glutamate and GABA, whose ligands effect instantaneous changes in ionic current or membrane potential. However, most serotonin receptors in the brain are G-protein coupled and activate intracellular cascades over time periods of 400 ms or more, resulting in postsynaptic effects that are too slow or heterogeneous to reveal information about small, fast changes in concentration. Rigorous characterization of serotonin signaling requires a technique that operates on the same temporal and spatial scales as its release and uptake processes.

Electroanalytical techniques, which combine chemical selectivity with high temporal resolution, are often used in brain tissue to monitor small, fast changes in neurotransmitter concentrations concurrent with release and uptake. Serotonin signaling has been studied using several electroanalytical techniques, including differential pulse voltammetry and chronoamperometry (for a review, see (Stamford, 1985)). Among these techniques, fast-scan cyclic voltammetry (FSCV) is the best combination of temporal and chemical sensitivity for measuring endogenous changes in serotonin concentration in brain tissue. This article will review the findings of voltammetric studies and discuss their contribution to current understanding of the mechanisms modulating serotonin release and uptake.

1. Fast-scan cyclic voltammetry of serotonin

FSCV is an electrochemical technique that detects changes in endogenous neurotransmitter levels rapidly enough to distinguish release and uptake events in brain tissue. The monoamine neurotransmitters dopamine, norepinephrine, and serotonin are well-suited to voltammetric detection because they oxidize predictably and at low potentials. To

evaluate changes in neurotransmitter concentration, FSCV measures the current generated by the oxidation of a neurotransmitter. Oxidation is driven by a potential waveform applied to a carbon-fiber sensor. The current generated is proportional to the concentration of analyte at the carbon surface, so the current-to-concentration relationship can be quantified by calibrating microelectrodes in authentic standards before or after experimental use. Chemical selectivity, or the ability to identify the neurotransmitter being measured, is facilitated by analyzing the plot of generated current vs. applied potential. This current-voltage curve is termed the cyclic voltammogram. Monoamines oxidize and reduce at predictable potentials, and their cyclic voltammograms have a characteristic shape that is easy to recognize. An example of a voltage waveform, cyclic voltammograms, and *in vitro* calibration is shown in **Figure 1.1**. The "fast-scan" in the technique's name refers to the potential waveform, which is applied rapidly and repeatedly, producing up to 10 cyclic voltammograms per second. The carbon-fiber microelectrode sensors used in FSCV have small dimensions (5 x 100 μm), and this small size enables sampling from as few as 100 synapses at a time, with the electrode targeted to a discrete brain region. Thus, FSCV is a technique for which temporal and spatial scales of data collection are compatible with monitoring neurotransmission.

1.1. Brain regions with measurable serotonin release

In brain slices, changes in serotonin concentration can be evoked using local electrical stimulation in brain regions containing serotonergic neurons or their axonal projections. The dorsal raphe nucleus (DRN), a tiny hub in the core of the medulla, contains the majority of serotonin-producing neurons that send ascending projections into the brain.

Voltammetric measurements detect serotonin efflux from both axonal and somatodendritic sites in this region because a subset of serotonergic neurons synapse locally. Although axonal serotonin release is prevalent throughout the central nervous system, experiments employing FSCV are typically constrained to brain regions dense with serotonergic terminals and limited interference from other neurotransmitters and metabolites. These studies predominantly take place in the substantia nigra, a midbrain region composed of the *pars compacta*, packed with dopamine-synthesizing neurons, and the *pars reticulata* (SNpr), a networked relay region that includes the densest serotonergic projections from the DRN to any forebrain region (9×10^6 sites per mm^3) (Moukhles et al., 1997). In the SNpr, serotonin is the predominant electroactive neurotransmitter evoked by electrical stimulations, frequently observed in the absence of somatodendritic dopamine release (Cragg, Hawkey, & Greenfield, 1997). However, Moukhles et al. (1997) reported that serotonergic processes form synaptic junctions at a high rate in the SNpr than any other brain region. It should be considered, therefore, that serotonin dynamics described in this region may be dissimilar to the dynamics in other brain regions, including the cerebral cortex, neostriatum, and hippocampus, where a majority of serotonin terminals form non-junctional synapses (Descarries et al., 1990). Serotonin efflux has also been described using FSCV in brain slices containing the suprachiasmatic nucleus (SCN) and ventral lateral geniculate nucleus (vLGN), hypothalamic and thalamic areas with similarly robust serotonergic innervation.

Serotonin measurements in *in vivo* FSCV experiments have taken place exclusively in the SNpr. Thick vasculature and meninges above the DRN make targeting this region in the intact brain with a fragile carbon-fiber microelectrode difficult. Other serotonergic regions of interest, such as the hippocampus and prefrontal cortex, have not been explored due to

significant chemical interference from other monoamines. However, recent advancements in neuronal stimulation technology may help circumvent this problem, and these potential future directions will be discussed in more detail in the conclusion of this article.

1.2. Electrochemical identification

Electrochemical methods, including FSCV, lack absolute chemical specificity. Some chemical species, particularly those with similar structure, can interfere with detection of the desired substance by oxidizing at similar or identical potentials. Therefore, voltammetric measurements rely on five criteria for identification of endogenously released substances: First, cyclic voltammograms obtained under experimental conditions must have high correlation with cyclic voltammograms of the authentic compound. Second, presence of the neurotransmitter must be validated by independent chemical identification, such as microdialysis, tissue content analysis, or radioligand binding in the targeted brain region. The third criterion requires precise anatomical positioning of the sensor into the brain region of interest. Fourth, observed release should follow known physiological properties for the neurotransmitter and target brain region. Finally, identification of the released substance is dependent on pharmacological validation.

O'Connor and Kruk (1991a) systematically addressed the criteria for electrochemical validation in the first published report of endogenous serotonin measured in rat brain slices using FSCV (O'Connor & Kruk, 1991a). The cyclic voltammogram obtained from electrically-evoked serotonin is highly correlated to the one obtained after adding known concentrations of serotonin to the bath solution. Stimulation trains (500 ms in duration) elicited transient flux in serotonin levels in the DRN, where serotonin-synthesizing neurons

are located, and SCN, a region dense in serotonin projections from the DRN (Fuxe, 1965). The evoked concentrations measured in both brain regions was completely and reversibly abolished by removal of calcium from the buffer solution or addition of sodium-channel blocker tetrodotoxin, complying with known physiological properties of exocytotic release. RO 4-1284, an irreversible vesicular monoamine transporter 2 (VMAT2) inhibitor, attenuated release, confirming that observed release was vesicular in nature. Inhibition of monoamine oxidase had no effect on stimulated efflux, ruling out interference from serotonin's metabolite, 5-HIAA. Finally, the clearance rate of serotonin in the DRN and SCN could be decreased after application of citalopram, a selective serotonin uptake inhibitor, but not by benztropine, a norepinephrine uptake inhibitor, to bath solution. Similar procedures validate the identity of serotonin detected in subsequent experiments by this and other groups.

Bunin and Wightman (1998) later investigated an aspect of serotonin's physiological release properties that had not been addressed by initial voltammetric characterizations. The dimensions of carbon-fiber microelectrodes are considerably larger than the synaptic cleft into which neurotransmitters are released (**Figure 1.2**). Consequently, FSCV detects extracellular, not intrasynaptic, changes in concentration, and its measurements are limited to the neurotransmitter concentration that diffuses into the extrasynaptic space following release. A number of neuromodulators diffuse beyond the synaptic space to reach their receptors and transporters in a process called volume transmission (Fuxe et al., 2010), and prior evidence from non-voltammetric techniques implicated serotonin as a volume neurotransmitter. Ultrastructural studies of serotonergic terminals throughout the brain suggest that they form predominantly non-junctional synapses (Chazal & Ralston, 1987).

This terminal architecture, together with reports that expression of serotonin transporters and receptors occurs primarily on extrasynaptic regions of neuronal processes (Kia, Brisorgueil, Hamon, Calas, & Verge, 1996; Zhou, Tao-Cheng, Segu, Patel, & Wang, 1998), is indicative of volume transmission. In light of this information, Bunin and Wightman (1998) hypothesized that electrically-evoked serotonin should reach the extracellular space via diffusion, without buffering from uptake and receptor binding sites. This was found to be the case for both somatodendritic and terminal release, where the concentration of serotonin evoked per stimulation pulse during 20-pulse trains was equivalent to the concentration evoked by a single pulse (Bunin & Wightman, 1998). Therefore, the authors concluded that serotonin concentrations measured by voltammetry reflect physiological volume transmission from the synapse to its extrasynaptic targets.

1.3. Technical considerations

Since O'Connor and Kruk's first report of voltammetric detection of serotonin, several modifications have been implemented to adapt and improve the use of FSCV for novel applications. The voltage potential waveform (-1 to +1.4 to -1) used by the Stamford and Kruk labs, as well as others, in serotonin studies cited throughout this review was adjusted by Jackson and Wightman (1995) to improve temporal resolution. This modification to an N-shaped waveform, which scans from +0.2 to +1.0 to -0.1 back to +0.2 (Figure 1.1A), was designed to reduce serotonin adsorption to the electrode surface, as this slows electrode response times. It also avoids fouling reactions of serotonin's oxidative and reductive byproducts, improving electrode sensitivity and stability over time (Jackson, Dietz, & Wightman, 1995). The modified waveform's improvement enhanced electrode response

times and enabled more accurate measurements of release and uptake rates, facilitating closer examination of the kinetic parameters of serotonin release.

Improvement of carbon-fiber microelectrode sensors has been another ongoing adaptation to voltammetric measurements of serotonin. Brazell and Adams (1987) first reported that dip-coating a carbon-fiber microelectrode in Nafion, a cation-selective polymer, improves serotonin and dopamine detection (Brazell et al., 1987; Jackson et al., 1995). Nafion enhances serotonin detection in two ways: first, by directly increasing the electrode's sensitivity to (positively-charged) serotonin, and second, by reducing its sensitivity to interfering anionic species such as uric acid and serotonin's metabolites. Years later, the success of the first *in vivo* voltammetric measurements of endogenous serotonin concentrations in a rat owe their success to the enhanced sensitivity and temporal resolution facilitated by Nafion-coated sensors and the modified voltage potential waveform (Hashemi, Dankoski, Petrovic, Keithley, & Wightman, 2009).

It is important to note that many labs continued their investigations of serotonin release without adopting either modification. Because each study reports on electrically-evoked changes in serotonin concentration, which are derived from *in vitro* calibrations, comparing findings between labs is not considered an issue within this review. It is important to note that these calibrations do not take into account the deleterious effects of electrode fouling that may be appreciably different over the course an experiment depending on the waveform used. Regardless of waveform choice, however, demonstration of a linear relationship between concentration applied and the current evoked establish the suitability of a waveform for stable detection of serotonin.

2. Electrical stimulation

Many of the optimal electrical stimulation parameters for evoking somatodendritic and terminal serotonin in brain slices are consistent with previously established physiological principles. Serotonergic fibers are not myelinated and, like other unmyelinated fibers, are maximally excited by wider stimulation pulse widths, up to 2 ms in length (Anden, Fuxe, & Ungerstedt, 1967; Bunin, Prioleau, Mailman, & Wightman, 1998; Merrill, Wall, & Yaksh, 1978; Millar, Stamford, Kruk, & Wightman, 1985). The amplitude of evoked serotonin concentration is also strongly dependent on increases in stimulation intensity (up to 380 μA) and number of pulses in a stimulation train. Maximal release amplitudes are also positively correlated with increasing frequency, up to 100 Hz (Bunin & Wightman, 1998; Iravani & Kruk, 1997; O'Connor & Kruk, 1991b), although a detailed investigation by John, et al. (2006) found that electrically-evoked concentrations were less sensitive to stimulation frequencies above 30 Hz (John, Budygin, Mateo, & Jones, 2006). These constrained ranges of frequency dependence could reflect limitations in vesicular availability, but Aghajanian et al. (1990) has posited that processes in terminal regions store enough serotonin to sustain long, high frequency release (Aghajanian, Sprouse, Sheldon, & Rasmussen, 1990). Although serotonergic neurons are typically thought to fire at a rate of 0.5-5 Hz, burst-firing in the DRN has been measured at a rate of 100 Hz (Aghajanian, Wang, & Baraban, 1978; Hajos, Gartside, Villa, & Sharp, 1995; Vandermaelen & Aghajanian, 1983). Differences in the range of frequency sensitivity between studies may therefore reflect dynamic, physiological fluctuations and could point to yet another regulatory component within the serotonin system. Future investigation of the mechanisms influencing frequency dependence would be an interesting addition to our understanding of serotonin signaling.

Although voltammetric studies of serotonin have used a wide array of stimulation parameters, one type has been used repeatedly in the studies reviewed in this article. Pseudo-one-pulse (El Yacoubi et al.) stimulations consist of 5-10 pulses applied at 100-200 Hz and are shorter than 100 ms in duration. They are designed to approximate a single electrical impulse but evoke more consistent efflux. In brain slice experiments, POP stimulations are often used to avoid creating an endogenous "tone" at receptors, which facilitates more direct investigation of selective agonists and antagonists effects on autoreceptor-mediated modulation of release (Limberger, Trout, Kruk, & Starke, 1991; Thienprasert & Singer, 1993).

Endogenous serotonin concentrations have been evoked *in vivo* using electrical stimulation of the DRN as well as the medial forebrain bundle (MFB). A subset of serotonergic neurons that project to the SNr also send axon collaterals to forebrain structures via the MFB (van der Kooy & Hattori, 1980). Electrical stimulation of these collaterals excites SNr-projecting neurons in a retrograde direction, eliciting serotonin in the desired region (Hashemi, Dankoski, Wood, Ambrose, & Wightman, 2011). While targeting a stimulation electrode to the MFB is less challenging than targeting the DRN, this stimulation site can also be used to evoke neurotransmitter release in many brain regions. This may have indirect effects on serotonin signaling, complicating interpretation of data. Many optimal stimulation parameters are consistent between *in vitro* and *in vivo* measurements, including pulse width, stimulation intensity, and stimulation length. However, the concentration of serotonin evoked in the SNr is remarkably lower than predicted by brain slice measurements, prompting curiosity about the potential for serotonergic regulatory mechanisms that require intact brain tissue.

3. Release

Local electrical stimulations of serotonin terminals in brain slices typically evoke concentration changes in the 100 nM range. *In vivo*, however, serotonin concentrations evoked in the SNpr rarely reach 100 nM, even after pharmacological manipulations (Hashemi et al., 2012). *In vivo* serotonin release, measured in an intact brain, is presumably limited by negative feedback from somatodendritic and terminal autoreceptors as well as inhibitory neurotransmitters that are released concurrently, which may account for some of the disparity in release amplitudes. In brain slices, concentration flux coincides with onset of the stimulation pulse train and this rising phase reaches its maximum within milliseconds of the stimulation's end. Serotonin evoked *in vivo* tends to overshoot the duration of stimulation. The overshoot is partially an effect of the broader area of release sites activated by a remote stimulation location, but is also due to limited diffusion rates through a Nafion polymer coating that is applied to enhance sensitivity *in vivo* (Hashemi et al., 2009).

As mentioned in a previous section, electrically-evoked serotonin concentrations measured in brain slices are sensitive to stimulation frequency. A proposal by Wightman et al. (1988) explains this observation: more uptake occurs in the time between stimulation pulses during low frequency stimulations, which limits the summation of extracellular neurotransmitter concentration (R. M. Wightman et al., 1988). Jennings et al. (2010) hypothesized that shifts in uptake rate associated with differential serotonin transporter expression would predictably alter this frequency dependence. Mice with either gain or loss of SERT expression both displayed significantly lower sensitivity to stimulation frequency than their wild-type littermates. Furthermore, in wild-type mice, a selective serotonin transporter inhibitor reduced sensitivity to stimulation frequency (Jennings, Lesch, Sharp, &

Cragg, 2010). These findings underscore the importance of SERT in establishing a functional, dynamic equilibrium between release and uptake that enables coherent serotonin signaling.

Time-resolved measurements with FSCV also enable examination and comparison of the kinetic parameters of serotonin transmission. Neurotransmitter uptake is assumed to follow Michaelis-Menten dynamics, and uptake as well as concentration evoked per stimulus pulse can be calculated using a modified model of enzyme kinetics. **Figure 1.3** shows the equations used to model (i) uptake and (ii) release and representative signals predicted for stimulations of varying frequency. In brain slice preparations, the concentration evoked per stimulation pulse ($[5\text{-HT}]_{pulse}$) was found to be 100 ± 20 nM in DRN, and significantly lower in the SNpr, at 55 ± 7 nM. Differences in $[5\text{-HT}]_{pulse}$ are proportional to differences in tissue content between the two brain regions, indicating that local stores of serotonin may influence the concentration that can be evoked by electrical stimulation (Bunin et al., 1998). *In vivo* $[5\text{-HT}]_{pulse}$ in the SNpr is much lower, comparatively: 1.5 nM per pulse using DRN stimulation, and 1.1 nM per pulse from the MFB. **Figure 1.4** shows an averaged recording of *in vivo* serotonin signals in the SNr; note that the concentration evoked is strikingly lower than predicted by the model in Figure 1.3. Given that both Bunin et al. (1998) and Hashemi et al. (2011) conducted experiments in the SNpr, the nearly 50-fold difference cannot be attributed to differences in tissue content. Instead, this discrepancy between brain slice and *in vivo* preparations suggests powerful regulatory mechanisms acting on serotonin release *in vivo* which may depend on intact circuitry.

Hashemi et al. (2012) investigated mechanisms that may limit *in vivo* neurotransmission by using a common MFB stimulation to compare serotonin and dopamine

efflux in the SNpr and nucleus accumbens, respectively. The dopamine system serves as a good basis for comparison with the serotonin system because the two monoamines share parallel features in the mechanisms controlling their synthesis, release, modulation, uptake, and metabolic degradation. Inhibition of the monoamine synthesis enzyme aromatic amino acid decarboxylase and VMAT2 considerably decreased the concentration of evoked dopamine to 18% and 6% of control amplitudes, respectively, but affected serotonin to a much lesser extent (48% and 72%, respectively). Serotonin efflux was also resistant to short term depression after repeated stimulation pulse trains, while dopamine efflux was attenuated by 38% after 20 stimulations. This suggests that a relatively small proportion of the available vesicular serotonin is mobilized for release by each electrical stimulation train, a finding which may partially explain the low concentrations observed *in vivo*.

3.1. Modulation by autoreceptors

Three subtypes of serotonin receptors, all 5-HT1-type, are expressed on serotonergic axons, soma, and dendrites and function as autoreceptors that provide inhibitory feedback. 5-HT1-type receptors are found throughout the brain as autoreceptors, expressed on pre-synaptic serotonin terminals, and also as heteroreceptors, expressed on post-synaptic targets. The most well-studied autoreceptors, 5-HT1A, 1B, and 1D are seven transmembrane, G-protein coupled receptors (GPCRs). 5-HT1B and 1D autoreceptors negatively couple to adenylyl cyclase (Yocca & Maayani, 1990). 5-HT1A heteroreceptors throughout the brain also inhibit adenylyl cyclase activity, but autoreceptors in the DRN apparently function through a different G_i-coupled mechanism (Clarke, Yocca, & Maayani, 1996). *In vivo* studies of these autoreceptors are challenging because even highly-selective drugs inadvertently target pharmacologically-identical heterosynaptic receptors, which are often expressed at

high levels in the same brain region as the autoreceptor. Intact circuitry thus makes it difficult to extricate direct effects of autoreceptor activity from indirect regulation by heteroreceptors.

Voltammetric measurements in brain slices avoid some of the problems associated with 5-HT1-type receptor pharmacology. In slices, the absence of spontaneous activity in serotonergic cells , due either to separation from cell bodiesin a terminal slice or to elimination of noradrenergic inputs in a DRN slice, results in loss of endogenous serotonin tone (Judge & Gartside, 2006). Therefore, these experiments avoid tonic activation of autoreceptors and can also avoid transient autoreceptor activity, when appropriate, using POP stimulations. This provides an opportunity to study the timing and function of these receptors in relative isolation. O'Connor and Kruk (1991b) showed that the non-selective autoreceptor antagonist methiothepin did not affect the concentration of serotonin evoked by POP stimulations, but increased serotonin elicited by longer stimulations. Further exploration with stimulations of varying frequency and duration determined that activation of autoreceptors requires a stimulation period of at least 400 ms (O'Connor & Kruk, 1991b). This time frame is comparable to the activation window for dopamine autoreceptors in striatal and limbic regions. Phillips et al. (2002) found that the activation delay observed for dopamine autoreceptors reflects timing of intracellular cascades added to the rate of neurotransmitter diffusion in a given brain area (P. E. Phillips, Hancock, & Stamford, 2002).

5-HT1A, 1B, and 1D receptors are expressed at high levels in the DRN, where they negatively influence neuronal firing rate and extracellular levels of serotonin (Adell, Celada, & Artigas, 2001; Moret & Briley, 1997; Pineyro, Castanon, Hen, & Blier, 1995; Sprouse & Aghajanian, 1987). Voltammetric studies corroborate the inhibitory functions of all three receptors in this region by demonstrating that their selective agonists can reduce the

amplitude of electrically-evoked serotonin release (Davidson & Stamford, 1995b; Hopwood & Stamford, 2001). Although its heteroreceptor analogues are prominently expressed in limbic regions, 5-HT1A autoreceptors are only expressed in the DRN and median raphe nucleus (Verge et al., 1985). Serotonin levels in forebrain terminal regions are affected by 5-HT1A-mediated changes in DRN unit activity (Casanovas, Lesourd, & Artigas, 1997; Kreiss & Lucki, 1994), but only 5-HT1B and 1D autoreceptors are expressed locally to functionally inhibit release in these regions. Voltammetric measurements in the SCN and vLGN confirm absence of 5-HT1A autoreceptor function in these terminal regions. 5-HT1B and 1D receptors, and not 5-HT1A receptors, negatively influence serotonin efflux in vLGN brain slices (Davidson & Stamford, 1996; O'Connor & Kruk, 1992).

The 5-HT1A receptor may be the trump card in this family of autoreceptors: 5-HT1A receptor mRNA is expressed in nearly 100% of serotonergic cells and up to 15% of GABAergic interneurons in the DRN (H. E. Day et al., 2004). This receptor robustly regulates both neuronal firing rates and extracellular serotonin levels in the DRN (Hjorth & Sharp, 1991; Sprouse & Aghajanian, 1987). Voltammetric measurements find that antagonists for 5-HT1A and 1B have a supra-additive effect when administered together: increase in serotonin efflux is greater when both receptors are blocked than would be expected given the effect of each antagonist alone (Roberts & Price, 2001). In addition, the effects of 5-HT1B receptor antagonists on serotonin efflux are overpowered by 5-HT1A receptors unless they are also blocked, suggesting that these receptors compensate for reductions of 5-HT1B activity. Given these results, it is suggested that 5-HT1A and 1B receptors exhibit a functional interaction that is facilitated by proximal expression sites on serotonin neurons. Interest in 5-HT1A receptors has increased in the last decade, as they may

play a role in depression and anxiety-related disorders (Ohno, 2010). Use of FSCV in future studies could meaningfully contribute to our understanding of how 5-HT1A receptor-mediated modulation of serotonin release plays a role in the etiology and treatment of these disorders.

Much speculation has occurred regarding the explanation for seemingly parallel functions of 5-HT1B and 1D autoreceptors. Both receptors are expressed in most serotonergic brain regions and have superficially redundant effects. One theory posits that these autoreceptors differ in their affinity for serotonin: one high affinity and the other low affinity. However, it has since been demonstrated that their affinities are nearly identical (Boess & Martin, 1994). More likely, the two receptors are expressed in different anatomical locations, and thus provide site-specific regulation of serotonin release, e.g. dendritic vs. axonal localizations in the DRN. Stamford et al. (2000) have reviewed the evidence supporting this hypothesis (Stamford, Davidson, McLaughlin, & Hopwood, 2000).

The SNr expresses the highest concentration of 5-HT1B autoreceptors and heteroreceptors in the murine brain (Pazos & Palacios, 1985). 5,7-HT-induced lesions of serotonin neurons reduced 5-HT1B expression level by 37%, presumably due to degradation of serotonin terminals (Verge et al., 1986); this suggests that over 1/3 of 5-HT1B receptors expressed in the SNr could function as autoreceptors. Heterosynaptic function of 5-HT1B receptors on presynaptic sites in the SNr has been well-documented and may yield important therapeutic findings (Sari, 2004), but its functionality as an autoreceptor in the SNr remains controversial. Iravani and Kruk (1997) found no effects of 5-HT1B receptor antagonists on electrically-evoked serotonin concentrations in SNr slice preparations (Iravani & Kruk, 1997). However, Threlfell and Cragg (2010) report that these autoreceptors influence short-

term depression of serotonin efflux. In paired stimulation trains, the concentration of serotonin evoked by the second stimulation (S2) reached 30% of that evoked by the first stimulation (S1) when there was a 1 second delay between S1 and S2. Antagonists of 5-HT1B receptors relieved this depression by up to 20% (Threlfell, Greenfield, & Cragg, 2010). 5-HT1B autoreceptors are thus apparently functional in the SNpr, although their modulatory effects may be less robust than in other brain regions.

It is possible that the role of autoreceptors could be better elucidated by *in vivo* voltammetric studies, where endogenous serotonin tone is undisturbed and autoreceptor function is closer to normal physiological levels. However, a limited number of studies currently address the effects of serotonin's autoreceptors *in vivo*. In practice, it is difficult to selectively target 5-HT1-type receptors on serotonin terminals when pharmacologically indistinct 5-HT1-type heteroreceptors are expressed throughout the brain. As with *in vivo* microdialysis, the direct roles of the autoreceptor would be difficult to extricate from indirect modulation by *in situ* circuitry. Recent technological advancements in iontophoresis enable spatially-resolved, quantitative drug delivery at the site of voltammetric measurements (Herr & Wightman, 2013). Future studies using FSCV combined with this drug-delivery method have great potential to answer important questions about serotonin's autoreceptors.

4. Uptake

Serotonin clearance is achieved primarily via active transport. Its transporter, SERT, is a member of the Na^+/Cl^- transporter family, which includes dopamine, norepinephrine, GABA, and glutamate transporters (Bennett, Logan, & Snyder, 1973; Iversen, 1974). SERT displays high affinity for serotonin in the nanomolar concentration range (Blakely et al., 1991). Inhibitors of SERT, or selective serotonin reuptake inhibitors (SSRIs), have been a

significant target of research efforts for decades, owing to their widespread use as antidepressant medications. Given acutely, SSRIs exert striking effects on the serotonin system: they elevate extracellular serotonin levels in the DRN (Bel & Artigas, 1992), which in turn decreases rate of cell firing due to activation of 5-HT1A autoreceptors (Chaput, de Montigny, & Blier, 1986; Gartside, Umbers, Hajos, & Sharp, 1995). However, in therapeutic practice, SSRIs relieve depressive symptoms only after a chronic period of 3-6 weeks. It is during this period that the effects of transport inhibition on serotonin transmission become less clear. FSCV provides an ideal method for deciphering the effects of SSRIs because it can distinguish between changes in released serotonin and changes in rate of uptake.

Electrically-evoked changes in serotonin concentration are cleared from the extrasynaptic space within seconds of stimulation termination. The term $t_{½}$ is often used to compare rates of clearance; $t_{½}$ is the time elapsed between peak concentration of neurotransmitter and its decay to half this amplitude. Across brain regions, brain slice and *in vivo* voltammetric measurements report similar values of $t_{1/2}$ ranging from approximately 1 to 3 s (Davidson & Stamford, 2000; Hashemi et al., 2012; Iravani, Muscat, & Kruk, 1999; O'Connor & Kruk, 1994). Rates of neurotransmitter clearance may positively correlate with the density of transporter sites in a given brain region: Bunin et al. (1998) report clearance rates of 1,300 ± 20 nM/s in the DRN and 570 ± 70 nM/s in the SNr, and quantitative autoradiographic studies report two to four-fold greater SERT binding levels in the DRN (Kovacevic, Skelin, & Diksic, 2010; Kovachich, Aronson, Brunswick, & Frazer, 1988). However, some comparisons of SERT density across brain regions do not support this conclusion, particularly in species other than rat, so more thorough investigation of the relationship between transporter expression and SERT density is needed. In addition to

influencing uptake rate, brain slice studies in mice that either lack or overexpress SERT have demonstrated a negative correlation between transporter expression level and concentration of serotonin evoked by electrical stimulation (Jennings et al., 2010; John et al., 2006). The disparity observed between clearance rates in the DRN and SNpr is conspicuously proportional to differences Bunin et al. (1998) reported in release rates. This suggests a consistent relationship between transporter expression levels, uptake rates, and release rate. Modeling serotonin signaling kinetics in more brain regions could confirm whether this relationship holds true throughout the brain.

SSRIs decrease rate of neurotransmitter clearance while increasing the maximum amplitude of electrically-evoked serotonin concentrations. In brain slices, SERT inhibition slows clearance (measured as an increase in $t_{½}$) by 150-700%. This wide spread of responses may be attributable to experimental variability between studies, particularly differences in stimulation parameters. Indeed, *in vivo* studies of SSRI effects in the SNr using identical stimulation parameters report comparable changes in $t_{½}$ using MFB and DRN stimulation sites (increasing by 324% and 306%, respectively)(Hashemi et al., 2012; Hashemi et al., 2009). SSRIs also increase evoked serotonin concentrations by 200%-450% in SNr brain slices, and up to 410% *in vivo* (Hashemi et al., 2012; Iravani et al., 1999; John et al., 2006). In this case, the intensity of the SSRI's effect is associated with different stimulation frequencies or pulse number. Structure and selectivity differences between SERT inhibitors may also contribute to variable responses between voltammetric studies; however, differences between SSRIs have not been specifically investigated using FSCV. Serotonin efflux in SNr brain slices has been modeled to describe the effects of an SSRI, fluoxetine, on apparent K_M, the Michaelis-Menten constant (John et al., 2006). Quantifying changes to K_M,

V_{max} and $[5\text{-HT}]_p$ may be a more effective way to contrast the effects of various SERT inhibitors on serotonin signaling in future studies in brain slices and *in vivo*. Thorough comparison of these effects could inform clinical usage of these pharmacotherapies.

4.1. Autoreceptors mediate some effects of acute uptake inhibition

In addition to their inhibitory influence on release, serotonin's autoreceptors appear to modulate response to SERT inhibition. A number of studies report that autoreceptor antagonists can potentiate the rise in extracellular serotonin levels elicited by SSRIs (Artigas, Perez, & Alvarez, 1994; Hjorth, 1993), and 5-HT1A autoreceptors also mediate reduction of firing rate by SSRIs in the DRN (Gartside et al., 1995). The concentration change evoked by POP stimulations, deliberately rapid enough to avoid creating an endogenous tone, typically does not activate autoreceptors and is thus not affected by their antagonists. However, in brain slices of the DRN, paroxetine-induced increases in serotonin efflux were potentiated by 5-HT1A and 1B/D receptor antagonists (Davidson & Stamford, 1995a). Therefore, it is hypothesized that SERT inhibition causes an increase in extracellular serotonin levels sufficient to activate autoreceptors, even in brain slices. This produces an inhibitory tone, such that autoreceptor antagonists can further unmask SSRI-induced increases in release. 5-HT1B and 1D autoreceptors appear to similarly potentiate the effects of SSRIs in distal brain regions, as the Stamford lab also reports increases in paroxetine's effects in the vLGN when co-administered with 5-HT1B and 1D receptor antagonists (Davidson & Stamford, 1997b). The interaction between regulation of release and uptake functions may also be an important detail in understanding how chronic uptake inhibition functions in treating depressive disorders.

4.2. Chronic uptake inhibition

The gap between onset of acute physiological effects and the therapeutic efficacy achieved in a chronic treatment period implies that SSRI-induced increases in serotonin levels are not directly producing antidepressant effects. Instead, elevated serotonin levels may influence long-term changes in serotonin signaling and its downstream targets to relieve symptoms of depression (Blier, de Montigny, & Chaput, 1987). The effects of long-term SERT inhibition are conflicting: some find increases in extracellular serotonin levels, and some find no changes. Associated with these outcomes are variable reports of autoreceptor desensitization or hypersensitization of 5-HT1A and 1B autoreceptors (Bosker, Klompmakers, & Westenberg, 1995; Bosker, van Esseveldt, Klompmakers, & Westenberg, 1995; Chaput, de Montigny, et al., 1986; R. Invernizzi, Belli, & Samanin, 1992; R. Invernizzi, Bramante, & Samanin, 1995; Moret & Briley, 1996). Studies examining the effects of chronic SSRI treatment using FSCV have produced more consistent findings.

FSCV measurements of serotonin signaling after 21 days of SSRI exposure reveal that rate of clearance, measured by $t_{½}$, is unchanged by this treatment. This lack of change is intriguing because radioligand binding studies report brain-wide reductions in SERT density after chronic inhibition (Kovacevic et al., 2010). It may reflect compensation by other clearance mechanisms, such as low affinity serotonin transporters. High and low affinity transport systems have been described for other monoamine neurotransmitters (Hagan, Schenk, & Neumaier; Iversen, 1974; Stamford, Kruk, & Millar, 1990; Stamford, Kruk, Millar, & Wightman, 1984). Although studies suggest that these transporters may play an important role in serotonin signaling (Daws, 2009), there are presently no FSCV studies describing their role in modulating release and uptake. The role of non-selective uptake

transporters in modulating serotonin signaling, particularly following chronic SSRI treatment, would be interesting to investigate using FSCV.

Long-term SSRI treatment increases stimulation-evoked serotonin concentrations in the DRN and other brain regions by 20-100%, depending on the experiment and brain region studied (Davidson & Stamford, 1998, 2000; O'Connor & Kruk, 1994).These findings concur with the results of Schoups and De Potter (1986), who found that electrically-evoked release of tritiated serotonin (^{3}[H]5-HT) in the hypothalamus increased after 21 days of SSRI treatment (Schoups et al., 1986). Although increases in serotonin efflux are observed after acute SERT inhibition, these can be explained by changes in rate of uptake. However, $t_{½}$ was not altered in any voltammetric investigation of long-term SSRI treatment. Therefore, increases in evoked concentrations induced by chronic treatment must rely on another mechanism. Changes in other aspects of release may contribute to this effect, for example: the quantity or composition of serotonin stored in vesicles, regulation of intracellular calcium, or excitability of the synaptic membrane. In-depth exploration of these mechanisms has not yet been explored using voltammetric methods.

Alterations in 5-HT1A autoreceptors contribute to the effects of chronic SSRIs on serotonin signaling. Under normal conditions, activated 5-HT1A receptors inhibit serotonin release and neuronal firing rates, and chronic SSRI treatment may modify this activity. Selective suppression of 5-HT1A autoreceptors can produce antidepressant behavioral effects in the absence of SSRIs (Bortolozzi et al., 2012). Many investigations have described functional desensitization of 5-HT1A receptors after chronic SERT inhibition, but to varying degrees across brain regions (Bosker et al., 2001; Cremers et al., 2000; Kreiss & Lucki, 1994, 1997; Rossi, Burke, McCasland, & Hensler, 2008). Davidson and Stamford (1998) compared

serotonin release and uptake and neuronal firing rates in the DRN of rats treated with water or paroxetine for 21 days. Paroxetine-treated rats had significantly higher serotonin release rates but exhibited no differences in firing rate. Interestingly, application of a 5-HT1A receptor agonist revealed that firing rate was *less* sensitive, and release amplitude *more* sensitive, to this manipulation. Contradictory findings of 5-HT1A receptor sensitivity was not a total surprise: prior studies found similar desensitization of 5-HT1A receptors in the control of firing rate after chronic paroxetine treatment (Blier, de Montigny, & Chaput, 1988, 1990; Chaput, de Montigny, et al., 1986), and O'Connor and Kruk (1994) had previously reported sensitization of 5-HT1A receptors controlling release amplitude. The dichotomous effect of chronic SSRIs on 5-HT1A receptor sensitization indicates a functional distinction between the receptors mediating neuronal firing and those controlling release. Given the complex effects of chronic SSRIs on 5-HT1A autoreceptors in the DRN, it would be interesting to see how these changes translate to serotonin release in an intact brain. Currently, however, no studies employing FSCV have examined the effects chronic SERT inhibition *in vivo*.

5-HT1B and 1D receptors also desensitize after chronic SERT inhibition, although the extent to which this occurs appears to vary between brain regions. O'Connor and Kruk (1994) reported desensitization of 5-HT1B receptors in SCN after chronic treatment with fluoxetine. In contrast, the Stamford lab found no changes in the sensitivity of 5-HT1B receptors in the vLGN, instead finding desensitization of 5-HT1D receptors after chronic paroxetine. This inconsistency may reflect differences in autoreceptor expression in the SCN and vLGN, or result from difficulty in selectively targeting the 5-HT1B receptor pharmacologically (O'Connor and Kruk do not address the effects of 5-HT1D receptors in

their study). Additionally, while O'Connor and Kruk (1994) found no desensitization of 5-HT1B receptors in the DRN, Davidson and Stamford (2000) later demonstrated that 5-HT1B receptor desensitization was apparent only when the 5-HT1A autoreceptor is antagonized (Davidson & Stamford, 2000). This adds further weight to the conjecture that 5-HT1A and 1B receptors functionally interact in the DRN.

4.3. Monoamine oxidase

Metabolic degradation of serotonin by the enzyme monoamine oxidase (MAO) also contributes to serotonin clearance, especially in the developing brain (Cases et al., 1998; Cases et al., 1995). However, MAO inhibition in brain slices has no reported effect on release amplitudes or uptake (O'Connor & Kruk, 1991a), a finding used to confirm absence of serotonin's metabolites from the voltammetric signal. Owesson and Stamford (2002) showed a greater role of MAO in regulating serotonin efflux using transgenic mice lacking MAO-A expression. MAO-A is the isoenzyme that preferentially degrades norepinephrine, epinephrine, dopamine, and serotonin, and mice lacking this enzyme have decreased neuronal firing rates in the DRN and increased extracellular serotonin levels (Evrard et al., 2002). In brain slices of the DRN, MAO-A-deficient mice displayed significantly greater serotonin efflux and reduced clearance rates compared to wild-type controls. Additionally, the effects of citalopram were smaller and radioligand binding showed significantly lower expression of SERT in these mice (Owesson et al., 2002). This suggests that serotonin signaling is subject to regulation by MAO under the right experimental conditions. *In vivo* work supports this idea, as a recent study has shown that MAO inhibitors dramatically increase serotonin efflux in the SNpr (Hashemi et al., 2012). MAO inhibition also has a much greater effect on serotonin than dopamine efflux when compared *in vivo*, suggesting a unique

role for metabolic degradation in the regulation of serotonin transmission compared to other monoaminergic systems.

5. Future Directions

Most of the studies reviewed in this article focused on describing the role of autoreceptors and transporters in modulating serotonin signaling throughout the brain. However, signaling is also considerably influenced by many other neurotransmitter systems, including norepinephrine, glutamate, GABA, and a number of neuroendocrine modulators. These external influences are highly implicated in serotonin's involvement in a number of psychiatric disorders and, while they have been investigated by other techniques, their functions have not been fully described using subsecond voltammetric measurements. Evaluating the effects of external modulatory mechanisms on the subsecond dynamics of serotonin signaling could provide important clues about their role in neurological disorders.

Ongoing methodological developments continue to progress voltammetric measurements beyond the current experimental limits. While electrochemical techniques have been optimized for serotonin detection (Lama, Charlson, Anantharam, & Hashemi, 2012), multi-electrode arrays are being developed which would enable measurements of multiple neurotransmitters in multiple locations simultaneously. Additionally, iontophoretic methods adapted for FSCV now enable localized, quantitative drug delivery, enabling investigation of recording-site specific effects *in vivo*. FSCV can also be paired with concurrent electrophysiological measurements to couple information about neurotransmitter release to single-unit responses of post-synaptic neurons. Iontophoretic and electrophysiological methods have already been applied to voltammetric studies of dopamine release in anaesthetized and freely-moving animals (Takmakov, McKinney, Carelli, &

Wightman, 2011), and the Wightman group is currently working to adapt these methods for serotonin detection.

It has previously been challenging to selectively study serotonin's autoreceptors *in vivo* because homologous receptors are expressed throughout the brain. However, many novel drug-delivery and transgenic methods have been developed to avoid this type of complication. DREADDs, designer receptors with exogenous ligands, have been used to target specific G-protein-activated cascades in serotonergic neurons (Dong, Allen, Farrell, & Roth, 2010). A light-activated 5-HT1A receptor has been generated that can be expressed only on serotonergic neurons (Oh, Maejima, Liu, Deneris, & Herlitze, 2010). Furthermore, transgenic mice and rats offer many opportunities to study signaling in models of neurological disorders and targeted deletions. The effects of SERT deletion or overexpression on serotonin signaling have been investigated in brain slices of the SNr but not in an *in vivo* preparation. Many conditional knockout mouse models, which avoid confounding developmental effects, are now available for serotonin's transporter and receptors. These techniques could lead to more selective targeting and better characterization of serotonin's receptors and their downstream effectors in combination with voltammetric measurements.

Voltammetric measurements have, until recently, been limited to brain regions with high levels of the neurotransmitter of interest and limited presence of other electroactive compounds. This is because electrical stimulations indiscriminately excite all proximal nerve terminals. Use of optogenetic stimulation circumvents this barrier by enabling selective excitation of a specific population of neurons. Channelrhodopsin-2-mediated serotonin efflux has been measured in fly larvae using FSCV in a technique developed by the Venton group.

The light-evoked efflux is vesicular and subject to regulation by synthesis and uptake transport in a manner that is similar to mammalian serotonin release (Borue, Condron, & Venton, 2010; Borue, Cooper, Hirsh, Condron, & Venton, 2009). Selective stimulation of serotonergic neurons in a mammalian model would permit measurements in brain regions with significant interference from other electroactive neurotransmitters, such as the hippocampus.

Finally, while voltammetric measurements of serotonin have presently only occurred in brain slices and anaesthetized animals, an exciting future direction for research will be monitoring serotonin signaling in an awake, freely moving animal. FSCV has been used to measure endogenous dopamine and norepinephrine release in freely moving animals, and this research has led to groundbreaking information coupling real-time neurotransmission to specific facets of behaviors. Many questions remain about serotonin's role in both basic and complex nervous system processes, and coupling FSCV to relevant behavioral paradigms may yield important clues about its function.

Conclusion

Serotonin signaling is an important component in the etiology and treatment of many neurological disorders. By combining sub-second temporal resolution with nanomolar sensitivity to concentration changes, FSCV has revealed a great deal about dynamic serotonin transmission. These findings are summarized by the illustration in **Figure 1.5**. Studies using voltammetric methods have emphasized the importance of autoreceptor-mediated inhibitory feedback mechanisms in normal signaling as well as response to SSRIs. Further, recent *in vivo* measurements suggest that intact brain circuitry supports the involvement of multiple modulatory mechanisms in the control of serotonin signaling.

The work presented in this dissertation describes some of the mechanisms that control serotonin release and uptake in an *in vivo* preparation. In chapter 2, we present modifications to existing voltammetric methods which enable detection of endogenous serotonin release in an intact brain for the first time. In chapter 3, we model this release, finding that it is significantly smaller than concentrations evoked in brain slices. Chapter 4 describes how the similar biochemical components of dopaminergic and serotonergic systems differentially modulate release of the two neurotransmitters, and the work suggests that SERT plays a significant role in regulating both release and uptake. In chapter 5, we further elucidate this role, showing how SERT inhibitors can potentiate serotonin release by dysregulating the control over serotonin signaling that occurs at a neuronal level. Finally, in chapter 6, we show how long-term SERT inhibition, modeled after chronic antidepressant therapies, causes enduring plasticity in the regulation of serotonin signaling. Importantly, this effect can be attenuated by ongoing stress throughout SSRI treatment. Taken together, chapters 5 and 6 suggest that acute responses to SERT inhibition may predicate the therapeutic effects of long-term treatment. Non-serotonergic neurochemical responses to stress may modify serotonin signaling following acute and chronic SSRIs in a way that influences chronic therapeutic outcomes. Future work will focus on how environmental stress is transduced by the serotonergic system into adaptive behavioral responses.

Support

The authors wish to thank the Electronics Facility at University of North Carolina for their contribution to selected studies cited in this review. Our work was funded by the National Institute of Health (R01 NS38879 to RMW).

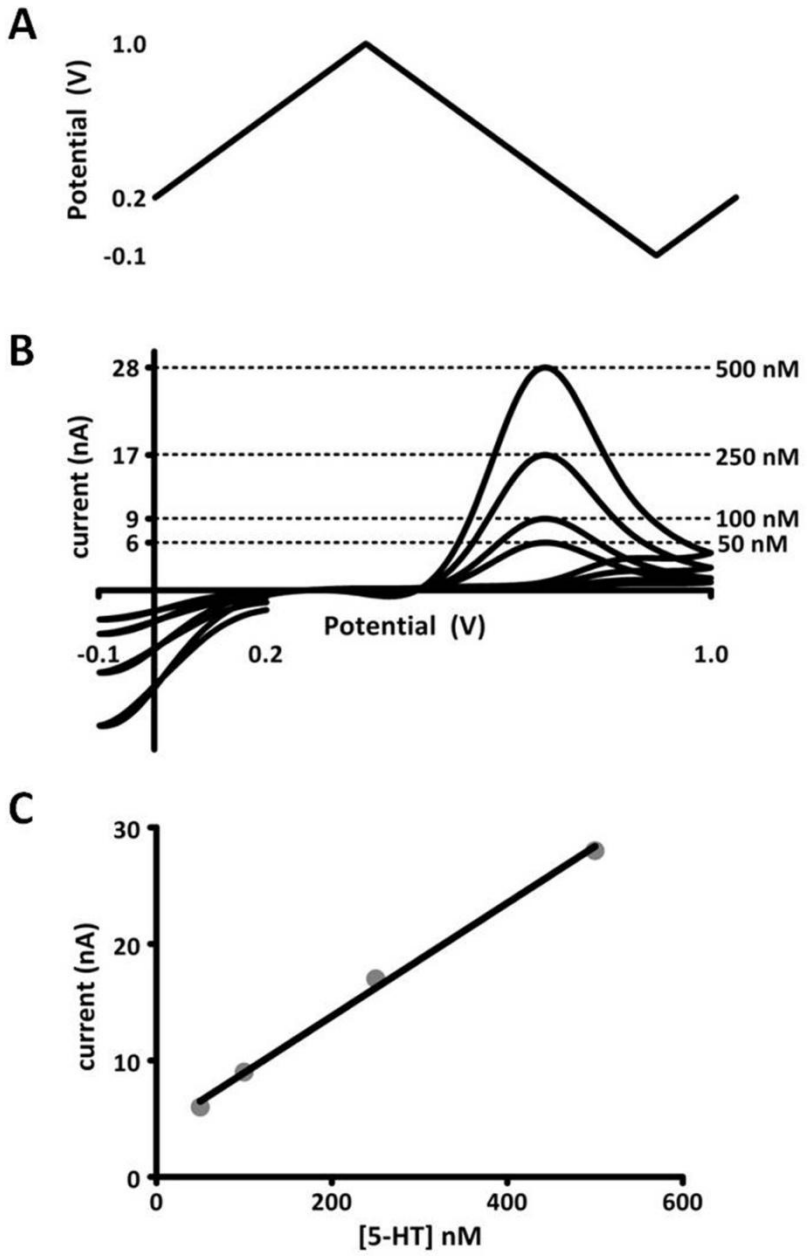

Figure 1.1 *In vitro* calibration of microelectrodes. (A) Voltage potential waveform, described by Jackson, et al. (1995), for detection of serotonin. (B) Cyclic voltammograms (current-voltage curves) obtained for known concentrations of serotonin injected into a flow cell apparatus. The concentration (right) and its corresponding oxidation current amplitude (left axis) are noted by dashed lines. (C) Maximal oxidation current *vs*. concentration of serotonin. The data is fit to a linear regression (black line), the slope of which gives a calibration factor for serotonin measured at these electrodes.

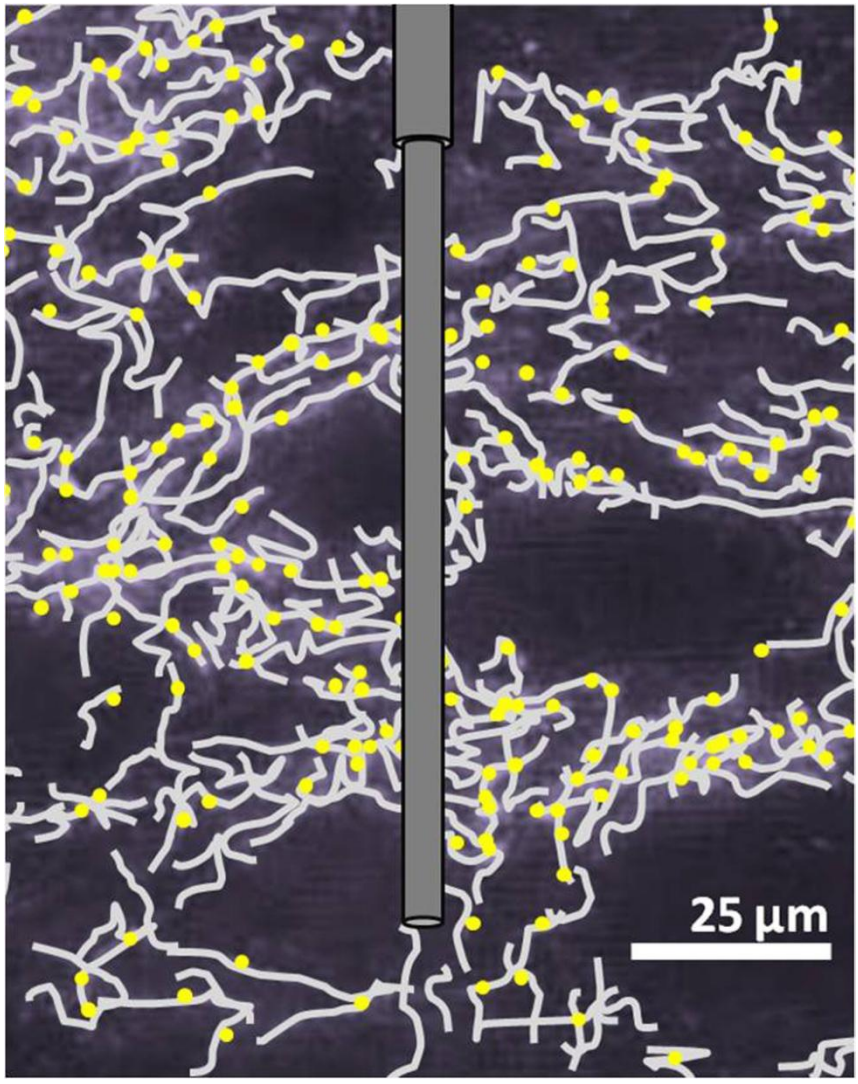

Figure 1.2 Illustration of a carbon-fiber microelectrode in SNr. Scaling of the microelectrode to *in situ* serotonergic fibers (gray) and uptake sites (yellow) is a representation based on Moukhles, et al. (1997).

(i) $$v = \left\{\frac{d[\text{5-HT}]}{dt}\right\}_{uptake} = \frac{V_{max}}{\frac{K_M}{[\text{5-HT}]} + 1}$$

(ii) $$\frac{d[\text{5-HT}]}{dt} = \left([\text{5-HT}]_p * f\right) - v$$

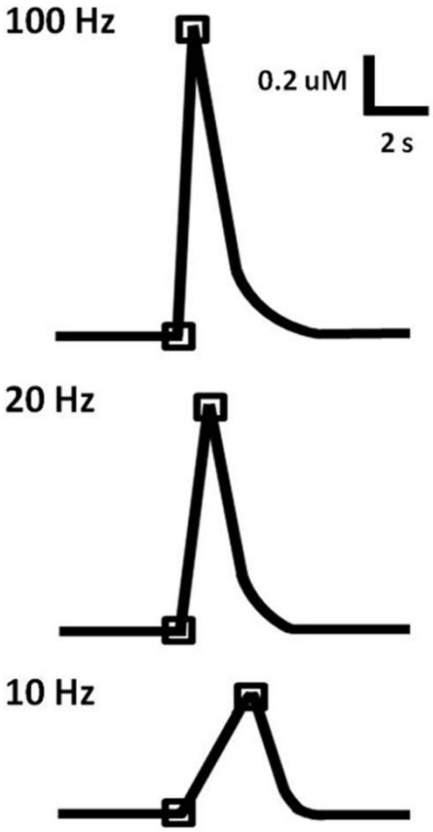

Figure 1.3 A model predicts serotonin release and uptake at different frequencies. Top panel: Equation (i) describes rate of uptake (*v*) as a function of maximal uptake rate (V_{max}), the Michaelis constant for SERT (K_M), and concentration of released serotonin ([5-HT]). Equation (ii) describes the expected concentration of released serotonin given a stimulation with number of pulses (p) and frequency (*f*), less the uptake that occurs over this time period. Lower panel: Concentration evoked by 50 pulse stimulation trains at 100, 20, and 10 Hz, as predicted by the model. Traces are representations of data based on Bunin et al. (1998).

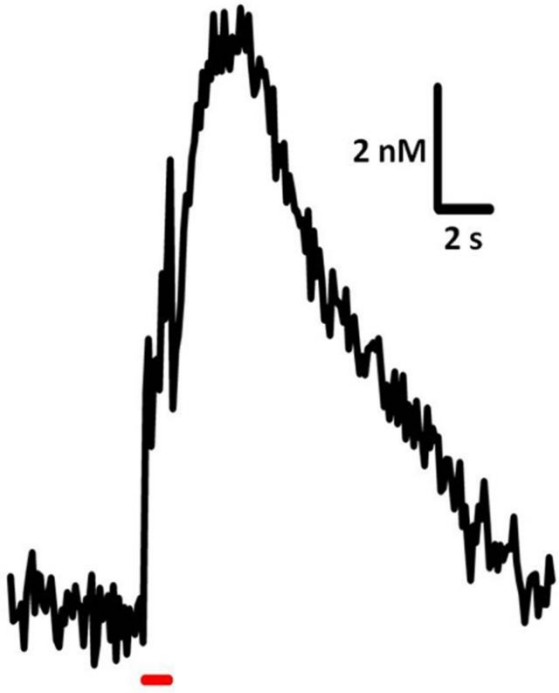

Figure 1.4 Sample trace of *in vivo* serotonin release and uptake. Release was elicited using 60 pulses, 60 Hz, 325 uA stimulation of the DRN and recorded in mouse SNr. Average of signals from 7 subjects.

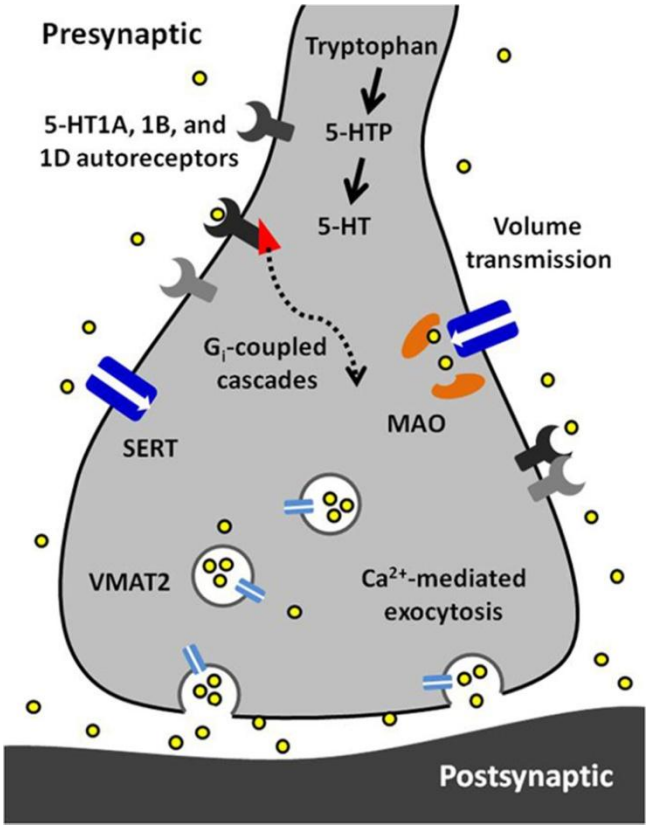

Figure 1.5 A synopsis of the findings presented in this article. Serotonin (5-HT) is synthesized from tryptophan in a two-step process requiring tryptophan hydroxylase and aromatic amino acid decarboxylase. Serotonin is packaged into vesicles by vesicular monoamine transporter 2 (VMAT2) and is released via calcium-dependent exocytosis. Released serotonin diffuses to extrasynaptic receptors and transporters via volume transmission. Its autoreceptors (5-HT1A, 1B, and 1D) are inhibitory and coupled to G_i proteins. The serotonin transporter (SERT) has high affinity and selectivity for uptake of extracellular serotonin. Inside the terminal, serotonin is primarily metabolized by monoamine oxidase (MAO).

CHAPTER 2: VOLTAMMETRIC DETECTION OF 5-HYDROXYTRYPTAMINE RELEASE IN THE RAT BRAIN [2]

Introduction

5-Hydroxytryptamine (5-HT), or serotonin, is an electroactive indole that acts as an important neurotransmitter in the brain. It has been the focus of considerable research efforts over the last 30 years. Despite its implication in several neurological disorders such as depression and anxiety (Aghajanian & Wang, 1978), for which serotonin-altering medications are widely prescribed, little is known about its dynamics in the brain. Limitations in analytical techniques for *in vivo* 5-HT detection come from a combination of low endogenous levels and rapid uptake of 5-HT from the extracellular space.

We have previously reported on the use of fast-scan cyclic voltammetry for *in vivo* dopamine monitoring (May, Kuhr, & Wightman, 1988; Stamford et al., 1984). Both dopamine and 5-HT undergo reversible 2-electron oxidations that yield characteristic and distinguishable cyclic voltammograms. However, unlike dopamine, the oxidative electrochemistry of 5-HT is complex, yielding many oxidation side-products which adsorb to the carbon surface on the conventional positive sweeping scan (Wrona & Dryhurst, 1990; Wrona, Lemordant, Lin, Blank, & Dryhurst, 1986). Even at the high scan rates (400 Vs^{-1}) used to detect dopamine with fast scan cyclic voltammetry, these oxidation side-products still

[2] This chapter previously appeared as an article in Analytical Chemistry. The original citation is as follows: Hashemi P, Dankoski EC, Petrovic J, Keithley RB, and Wightman RM. "Voltammetric detection of 5-Hydroxytryptamine release in the rat brain." *Anal. Chem.* 81:22 (Nov 2009) pp. 9462-71.

polymerize and produce films that quickly and irreversibly foul the carbon surface. This fouling has been reported to be minimized on diamond microelectrode surfaces since the diamond surface expresses significantly less oxygen groups when compared to the carbon surface.6 These microelectrodes have been used to provide real-time monitoring of 5-HT in guinea ileum where the endogenous 5-HT levels are relatively high (10-20 μM) (Bertrand, Hu, Mach, & Bertrand, 2008; Patel, Bian, Quaiserova-Mocko, Galligan, & Swain, 2007). Neurochemical measurements with diamond microelectrodes however, remain a challenge in part due to the relatively large size of the microelectrodes (~76 μm diameter) (Park et al., 2008). 76 μm is larger than inter-capillary distance in the rat brain (~30 μm); in brain tissue, such devices with dimensions larger than inter-capillary distance have been shown to cause tissue damage (Silvani et al., 2004). Even modest tissue damage caused by these microelectrodes may impede the measurements of synaptic 5-HT overflow that carbon fiber microelectrodes (~5 μm) are able to detect.

In previous work, we modified the electrochemical waveform that is routinely used for dopamine monitoring with carbon fiber microelectrodes to minimize the majority of side reactions using Nafion-modified carbon-fiber disc microelectrodes (Jackson et al., 1995). We showed the feasibility of this modification for *in vivo* use via a model described by Stamford et al. (1990), where striatal dopaminergic cells are forced to release high levels of 5-HT by arresting dopamine production and pre-loading dopamine neurons with a 5-HT precursor (5-HTP) (Bull et al., 1990). Although this was not a physiological situation, it demonstrated that fast-scan cyclic voltammetry can be applied to 5-HT measurements. This modified waveform also enables stable detection of 5-HT in tissue slice preparations in experiments that last up to 8 hours and in *D. melanogaster* (Borue et al., 2009; Bunin & Wightman, 1998; John &

Jones, 2007a). However, despite these studies, there remain no *in vivo* reports of the use of this approach for endogenous 5-HT detection.

A major physiological difference between tissue slice preparations and the intact brain is the concentration of extracellular metabolites such as 5-hydoxyindole acetic acid (5-HIAA). This metabolite is present at 200-1000 times the basal concentration of 5-HT in serotonin containing regions in the intact brain whereas in tissue slices, extracellular species such as ascorbic acid, and by the same reasoning 5-HIAA, wash out (Bell, McIlwain, & Thomas, 1956; Rice, 1999; Ross & Stenfors, 1997; Schenk, Miller, Gaddis, & Adams, 1982). 5-HIAA is an indole with electrochemical oxidation properties similar to 5-HT. Given the high and persistent baseline extracellular concentrations of 5-HIAA, we hypothesize that *in vivo* microelectrode implantation in a 5-HT rich brain region, even in the absence of 5-HT release, will lead to a quick and profound deterioration of the microelectrode due to electrode fouling by 5-HIAA.

Because 5-HIAA is negatively-charged in solution, cation exchange polymers such as Nafion can be deposited onto the microelectrode surface to limit its access. Carbon-fiber microelectrode discs can be dip-coated with Nafion in a straightforward process due to electrostatic properties of silica groups on the surface of the glass capillary (Baur, Kristensen, May, Wiedemann, & Wightman, 1988; Jackson et al., 1995). However, the small surface area of the discs makes them unsuitable for *in vivo* use: the microelectrode must have a larger surface area to sample enough release sites to record a substantial signal since these sites are not uniformly distributed throughout the tissue. Cylindrical carbon-fiber microelectrodes provide a large enough surface area to address this problem but uniform deposition of Nafion

onto cylindrical carbon-fiber microelectrodes is more challenging because the carbon fibers are inherently hydrophobic, and thus repel the negatively-charged polymer.

In this paper, we modify a technique described by Rice et al. to electrochemically deposit a thin, uniform layer of Nafion onto a cylindrical carbon-fiber microelectrode (Rice & Nicholson, 1989). Environmental scanning electron microscopy (ESEM) imaging displays the Nafion film on the carbon fiber surface and *in vitro* analyses confirm an attenuation of diffusible 5-HIAA to the microelectrode surface. Furthermore, the Nafion coating increases the sensitivity of the microelectrode to 5-HT. The cyclic voltammogram can easily be distinguished from other electroactive brain species, and common anionic species such as ascorbic acid are repelled. In previous work, we showed that microelectrodes with Nafion films of 340 nm still allowed rapid enough time responses to observe *in vivo* chemical dynamics (Kawagoe & Wightman, 1994). In this work, we modify the experimental deposition parameters to obtain a similar thickness. Using an *in vitro* dopamine step response and the diffusion coefficient of dopamine through Nafion, we calculate the thickness of the elecrodeposited Nafion film. Further, we back-calculate a diffusion coefficient for 5-HT through Nafion.

To validate this modified technique *in vivo*, we apply the microelectrodes to a rat model of 5-HT release in which we electrically stimulate 5-HT cell bodies in the dorsal raphe nucleus (DRN) and measure their terminal output in the substantia nigra reticulata (SNpr). The efficacy of the technique is verified by addressing previously described criteria for validation of microsensor selectivity *in vivo* (P. E. M. Phillips & Wightman, 2003). These include voltammetric identity, anatomical and physiological verification, chemical validation of 5-HT presence in release sites and pharmacological validation.

Experimental Methods

Carbon-fiber Microelectrodes

Carbon-fiber microelectrodes were constructed as described previously (Cahill et al., 1996). Cylindrical microelectrodes were made by vacuum aspiration of single a 2.5-μm-radius T-650 carbon fiber (Thornel, Amoco Co.) into a glass capillary of 0.6 mm external diameter and 0.4mm internal diameter (A-M Systems, Inc., Sequim, WA). A micropipette puller (Narashige, Tokyo, Japan) was used to taper the glass and form a carbon-glass seal. The exposed length of the carbon fiber was cut to approximately 100 μm.

Nafion Electrodeposition

The exposed length of carbon fiber from the glass tip of the microelectrode was soaked for 30 minutes in isopropyl alcohol (IPA) to clean the surface (Ranganathan, Kuo, & McCreery, 1999). The procedure for electrodeposition of Nafion was modified from work by Rice et al.(1989). The tip of microelectrode was lowered in Nafion solution (5 wt% 1100 EW NAFION ® in methanol, ION POWER, DE) and a constant potential of + 1.0 V vs. Ag/Ag Cl was applied to the microelectrode surface for 30 seconds. The microelectrode was dried in air for 10 seconds and then at 70º C for 10 minutes. The microelectrodes were stored dry prior to use.

Environmental Scanning Electron Microscopy

ESEM allows for imaging of low conductance or entirely non-conductive samples while eliminating the need for sputter coating. Control and Nafion-modified microelectrodes were imaged in low-vacuum (0.65 Torr) on a FEI Quanta 200 ESEM equipped with Schottky

field emission gun (accelerating voltage used in the studies was 10 kV); secondary electron images were obtained with a large field secondary electron detector.

Data Acquisition

In most experiments, a 5-HT specific waveform was used as described elsewhere (Jackson et al., 1995). Briefly, this waveform was applied with a scan rate of 1000 V s^{-1} with a resting potential of 0.2 V versus Ag/AgCl. The potential is ramped up to 1.0 V, then down to -0.1 V and back to resting potential of 0.2 V. In one experiment, the conventional dopamine waveform was used as described by Heien et al. (Heien, Phillips, Stuber, Seipel, & Wightman, 2003). In brief, this triangular waveform was applied at 400 V s^{-1} with a resting potential of -0.4V. The potential is then ramped up to 1.3V and back to the resting potential of -0.4 V. In both cases, scans were repeated every 100 ms. A customized version of TH-1 software (ESA, Chelmsford, MA) written in LABVIEW (National Instruments, Austin, TX) was used for waveform output and data acquisition. The software allowed output of waveforms with a DAC/ADC card (NI 6251 M). The second card (NI 6711) was used for triggering the DACs and ADCs as well as for synchronization of the electrochemical experiment with flow injection of the analytes. A custom-built instrument for potential application to the electrochemical cell and current transduction (University of North Carolina at Chapel Hill, Department of Chemistry Electronics Facility) was employed. Signal processing (background subtraction, signal averaging, and digital filtering (4-pole Bessel Filter, 5 kHz)) was software-controlled.

Chemicals

5-HT, 5-HIAA, dopamine, norepinephrine, epinephrine, DOPAC (3,4-dihydroxyphenylacetic acid), ascorbic acid, citalopram and GBR 12909 were purchased and used as received from Sigma−Aldrich. A physiological buffer solution (15 mM Tris, 126 mM NaCl, 2.5 mM KCl, 25 mM NaHCO3, 2.4 mM CaCl2, 1.2 mM NaH2PO4, 1.2 mM MgCl2, 2.0 mM Na2SO4) at pH 7.4 was used in all flow injection analysis experiments. All aqueous solutions were made using doubly distilled deionized water (Megapure System, Corning model D2).

Flow Injection Apparatus

The flow injection analysis apparatus has been described elsewhere (E. W. Kristensen, Wilson, & Wightman, 1986a). Briefly, the carbon-fiber microelectrode was affixed in the output of a flow-injection apparatus that consisted of a six-port HPLC loop injector mounted on a two-position actuator (Rheodyne model 7010 valve and 5701 actuator) that was operated with a 12 V DC solenoid valve kit (Rheodyne, Rohnert Park, CA). The apparatus allowed for the introduction of a rectangular pulse of analyte to the microelectrode surface by a syringe infusion pump (Harvard Apparatus model 940, Hollison, MA) at a flow rate of 2 mL min^{-1}.

Modeling of Film Thickness and Diffusion Coefficients

A procedure from Kawagoe and Wightman was modified in order to determine both the thickness of the Nafion film, lp, and the diffusion coefficient of 5-HT inside the Nafion film, D5-HT (Kawagoe & Wightman, 1994). The response to a step concentration of dopamine (10 μM) was measured on a Nafion-coated carbon-fiber microelectrode using the modified 5-HT waveform in the flow injection system. The process was repeated with the

same microelectrode for a step concentration of 5-HT (1 μM). Each peak current vs. time trace was extracted, corrected to zero background, and normalized to a maximum of 1. The normalized dopamine trace was fit to the equation:

$$\frac{C(t)}{C_0} = 1 - \frac{4}{\pi}\sum_{n=0}^{\infty}\frac{(-1)^n}{(2n+1)}\exp\left(-\frac{D\pi^2(2n+1)^2 t}{4l_p^2}\right) \quad \text{(Eq. 1)}$$

where C(t) is the concentration at the microelectrode surface, C0 is the concentration in bulk solution outside the Nafion film, D is the diffusion coefficient of the analyte inside of the Nafion film, and t is the time from the initial exposure to the concentration bolus. lp was allowed to vary between 1 and 1000 nm in 1 nm increments. A value of 1 x 10-9 cm^2s^{-1} (from previous work) was used for the diffusion coefficient for dopamine inside the Nafion film, DDA, this value closely resembles the reported values through thick Nafion films (Kawagoe & Wightman, 1994; Rocha & Carapuca, 2006). The value of lp that gave the best least-squares fit between the model and the step concentration of dopamine was used as an initial estimate for the thickness of the Nafion film. This thickness was used in Equation 1 to fit the normalized response to the 5-HT concentration step where D5-HT was allowed to vary between 0.1 x 10-10 cm^2s^{-1} and 1.0 x 10-8 cm^2s^{-1} in 0.1 x 10-10 cm^2s^{-1} steps. The value of D5-HT that gave the best least-squares fit between the model and the step concentration of 5-HT was used to generate an improved estimate for lp which was then used to obtain an improved estimate for D5-HT and the process was repeated iteratively until the solutions for lp and D5-HT converged.

Surgery

Male Sprague-Dawley rats weighing between 350-425 grams were anaesthetized with urethane (1.5 g/kg rat weight) and positioned into a stereotaxic frame. Holes were drilled in the skull according to stereotaxic coordinates referenced to bregma and taken from a stereotaxic atlas (Paxinos & Watson, 2007). Placement of the carbon-fiber microelectrode was in the SNpr (stereotaxic coordinates AP, -5.2; ML, +2.0; DV, −8.5 mm) and the bipolar stimulating electrode in the DRN (AP −8.0; ML, 0.0; DV, −6.0 mm). The Ag/AgCl wire that served as the reference electrode was implanted into the contralateral hemisphere. Biphasic stimulating pulses, 2 ms each phase, 300 μA each phase, were applied at 60 Hz for two seconds to evoke 5-HT release. Stimulation-evoked release was recorded during and after the stimulation, and selectivity for 5-HT was verified pharmacologically. Clearance of 5-HT from the extra-cellular fluid depends largely upon selective re-uptake through serotonin uptake transporters (SERTs), and these transporters can be blocked by selective serotonin reuptake inhibitors (SSRIs) (Hyttel, 1982). To pharmacologically verify our signal, we administered the SSRI citalopram (10 mg kg^{-1}) (Hyttel, 1982). Similarly, clearance of dopamine can be selectively blocked by administration of a dopamine transporter (DAT) inhibitor, GBR 12909 (Andersen, 1989); we administered GBR 12909 (15 mg kg^{-1}) to ascertain contribution of dopamine to the signal (May et al., 1988).

Results and Discussion

Characterization of Cylindrical Microelectrodes with the 5-HT Modified Waveform

We have characterized 5-HT detection with the waveform employed by Jackson et al. (1995) but with cylindrical carbon-fiber microelectrodes without Nafion coatings. Figure 2.1

shows *in vitro* comparisons between a single injection of either dopamine (1 and 2) or 5-HT (3 and 4) onto clean microelectrodes with (A) the conventional waveform used for detection of dopamine at 400 Vs^{-1} and (B) the modified Jackson waveform at 1000 Vs^{-1}. The color plots are a 2-dimensional representation of the cyclic voltammograms with current changes detected upon injection of the sample shown in false color (D. J. Michael, Joseph, Kilpatrick, Travis, & Wightman, 1999). Individual cyclic voltammograms recorded at three time points during the injection (1, 3 and 5 s) are displayed under each color plot. With the conventional waveform (A), a typical dopamine response (1) shows the cyclic voltammograms are stable throughout the injection. In contrast, a 5-HT injection using this waveform (Chazal & Ralston) yields a cyclic voltammogram that changes at each time point, gaining extra peaks both on the forward and backward parts of the scan. This is indicative of the adsorption of products formed during the electrooxidation. This problem does not occur with the modified waveform for 5-HT (4), in which the cyclic voltammograms retain their shape throughout the injection as previously reported.11 This is predominantly due to two characteristics of the modified waveform. First, when scanning at 1000 Vs^{-1} compared to 400 Vs^{-1}, more of the side reactions are outrun. Second, by holding the rest potential of the microelectrode at 0.2 V, the major adsorbed product is oxidized and its contribution to the current during the scan is minimized. A further point of interest is that the modified waveform does not show as good sensitivity towards dopamine (2), yielding approximately 8 nA for a 10 μM dopamine injection compared to 20 nA for a 1 μM 5-HT injection. Further, the cyclic voltammogram for dopamine can be easily distinguished from 5-HT by its reduction peak, which occurs on the positive scanning part of the wave (shown in red arrows). Dopamine reduction ordinarily occurs at -0.2V, which is beyond the negative sweep of the modified waveform. The

reduction peak on the forward part of the negative scan is most likely due to the reduction of the quinone group on dopamine-o-quinone, a reaction that at 1000 Vs^{-1} is kinetically sluggish.

Microelectrode Fouling by 5-HIAA

Despite the fact that the modified 5-HT waveform has previously been implemented for recordings in *D. melanogaster* (Borue et al., 2009), tissue slice preparations (Bunin & Wightman, 1998; John & Jones, 2007a), and *in vivo* models with preloaded dopaminergic cells (Jackson et al., 1995), we found that the electrochemical signal deteriorated during *in vivo* endogenous 5-HT monitoring. In preliminary *in vivo* investigations with the 5-HT waveform, we stimulated 5-HT release by DRN stimulation and measured in the SNpr. In contrast to the Jackson study where 5-HT release was evoked artificially in a brain region that is physiologically dopaminergic, the SNpr has high 5-HT content. In the SNpr, the electrochemical responses were very low in amplitude and the cyclic voltammograms were irreproducible. The oxidation and reduction peaks observed on an *in vivo* cyclic voltammogram show little similarity to the *in vitro* chemical signature for 5-HT shown in Figure 2.1-4. *In vivo*, a small oxidation peak is recorded on the initial positive scan, but a larger peak occurs on the subsequent negative scan. Additionally, the *in vitro* signal has a reduction peak at 0 V on the negative scan, whereas the *in vivo* cyclic voltammogram has this peak on the forward part of the negative scan (Figure 2.2A). The appearance of peaks on the reverse scans of *in vivo* signals indicates filming at the carbon fiber surface, which slows oxidative and reductive processes.

The results shown in Figure 2.1-4 indicate that the filming is not due to 5-HT oxidation, since it does not occur with 5-HT alone in solution. The major metabolite of 5-HT in the brain, 5-HIAA, may contribute to this filming. It is present in the extracellular fluid in concentrations that are approximately 200-1000 times that of 5-HT (Ross & Stenfors, 1997). These two indoles are very similar in structure and may consequently have similar filming electrochemistry. Therefore, we added 5-HIAA (10 μM) to the flow injection buffer and the solutions of 5-HT. In this experiment, the microelectrode was cycled in the 5-HIAA containing buffer for two hours before injection. Cyclic voltammograms of 5-HT obtained under these conditions resemble those obtained *in vivo* (Figure 2B). Note that this fouling has not been observed in rat brain slices, wherein reproducible cyclic voltammograms can be obtained for up to 8 hours (Bunin & Wightman, 1998; John & Jones, 2007a). However, in slices, the tissue is continually perfused, allowing for washout of extracellular substances. For example ascorbate is rapidly lost from the perfused slices for this reason, and the same appears true for 5-HIAA (Bell et al., 1956; Rice & Nicholson, 1989; Schenk et al., 1982). This filming was not an issue in the Jackson et al. study, in which we recorded super-physiological concentrations of 5-HT release with a Nafion-modified microelectrode disc (Jackson et al., 1995). Interestingly, monoamine oxidase (MAO), the enzyme responsible for 5-HIAA formation is profoundly less active in *D. melanogaster* than in mammalian nervous tissue, which minimizes the problem of 5-HIAA fouling in the fruit fly model (Dewhurst, Croker, Ikeda, & McCaman, 1972). We conclude that it is not feasible to obtain *in vivo* cyclic voltammograms that have the shape found *in vitro* in brain regions with high levels of 5-HT because of fouling of the microelectrode by 5-HIAA.

Exclusion of 5-HIAA from the Microelectrode Surface

5-HIAA is an anion at physiological pH. To exclude anions from carbon microelectrodes a cation exchange polymer is a popular choice (Baur et al., 1988; Brazell et al., 1987; G. A. Gerhardt, A. F. Oke, G. Nagy, B. Moghaddam, & R. N. Adams, 1984). Our own work has employed carbon-fiber microelectrode discs that can be coated with a thin layer (~300 nm) of Nafion by a dip-coating procedure (Cahill et al., 1996; Jackson et al., 1995; Kawagoe & Wightman, 1994; May et al., 1988; Wiedemann, Basse-Tomusk, Wilson, Rebec, & Wightman, 1990). Nafion adsorbs readily to the silica groups of the glass barrel in which the microelectrode is housed. However, with a cylindrical microelectrode, the hydrophobic carbon fiber extends 75 – 100 μm beyond the glass barrel and is thus not proximate to these silica groups. Further, the dip-coating procedure does not uniformly coat the surface of the microelectrode. Because of its negative charge, Nafion® can be electrostatically deposited onto cylinders (Brazell et al., 1987; Rice & Nicholson, 1989). We applied +1.0 V vs. Ag/Ag Cl to the cylindrical microelectrode while immersed in a 5% Nafion solution in methanol. These parameters were chosen to provide protection against 5-HIAA while still maintaining a film sufficiently thin that the response time is not greatly increased. Figure 2.3i shows ESEM images comparing (A) a bare cylinder to (B) a Nafion-modified cylinder. The resolution of the instrument allows us to observe individual striations on the surface of the bare carbon-fiber microelectrode; however, because of electroformation of a film, these striations are indistinguishable on the Nafion-modified carbon fiber. Also apparent is the excess extension of this film beyond the tip of the carbon fiber on the Nafion-modified microelectrode.

Figure 2.3ii shows a comparison between (A) a bare microelectrode to (B) a Nafion-modified microelectrode in their responses to 1 μm 5-HT (dashed line) and 10 μM 5-HIAA (solid line). Both microelectrodes measured approximately 100 μm in length. Before Nafion coating, the sensitivity to 5-HT is about 30 times greater than for 5-HIAA. This is a result of the greater adsorption of 5-HT. Nafion deposition reduces the 5-HIAA response at the microelectrode surface: in the displayed example, a bare microelectrode yields 10.7 nA in response to a 10 μM 5-HIAA injection, whereas a Nafion-modified microelectrode yields a 3.3 nA response. Moreover, in this example, the Nafion-modified microelectrode displays increased sensitivity to a 1 μM 5-HT injection, yielding 36.5 nA compared to the bare microelectrode response, 26.5 nA. On average, Nafion-modified microelectrodes yield 49.5 ± 10.24 nA to a 1 μM 5-HT injection compared with 20.8 ± 1.84 nA for a bare electrode (n=4 ± SEM) (Table 2.1).

Exclusion of Electronegative Species and Survey of Other Endogenous Electroactive Neurotransmitters

Averaged responses (n=4) to common anionic and cationic species on a bare microelectrode compared to a Nafion electrodeposited microelectrode are presented in Table 2.1. We observe enhanced sensitivity to 5-HT and dopamine, sensitivity to norepinephrine and epinephrine remained approximately unchanged, and decreased sensitivity to the anions ascorbic acid, DOPAC, and 5-HIAA. These differences arise from the partition of the species between the Nafion film and the solution. Importantly, the 5-HT molecule pre-concentrates in the Nafion membrane and results in the observed sensitivity enhancement, a phenomenon that has previously been reported to be advantageous for chemical sensors. The increased sensitivity of Nafion-modified microelectrodes is also evident in the averaged 5-HT

calibrations for these two microelectrodes in a flow-through buffer that contains physiological levels of 5-HIAA (Figure 2.3iii), where the fouling species are repelled. After Nafion electrodeposition, the microelectrode is almost 200 times more sensitive to 5-HT than to 5-HIAA.

To confirm exclusion of other electroactive anions, we compared responses of bare and Nafion-modified microelectrodes to other endogenous species. Figure 2.4 compares the responses of bare (grey) to Nafion-modified (black) microelectrodes to (i) ascorbic acid (400 μM), (ii) DOPAC (20 μM), and (iii) 5-HIAA (10 μM). A shows the averaged responses to these species (n=4 ± SEM) while B shows a single example of the corresponding cyclic voltammograms for bare (grey, dashed) and Nafion-modified (black, solid). The concentration ratios chosen are in the physiological range (Miele & Fillenz, 1996; Smith, Olson, & Justice, 1992). It is evident that Nafion-modified microelectrodes exclude the negatively-charged specie compared to bare microelectrodes. The ascorbic acid response is reduced from 50.6 ± 15.6 nA to 20.0 ± 4.7 nA. The DOPAC response is reduced from 4.9 ± 1.2 nA to 1.6 ± 0.2 nA. Finally, the 5-HIAA response is reduced from 13.8 ± 1.6 nA to 2.9 ± 0.9 nA. Thus, Nafion electrodeposition enhances specificity for 5-HT by excluding anions.

Diffusion of 5-HT through a thin Nafion Film

In previous work, we modeled a dopamine step concentration response and calculated the thickness of a Nafion dip-coated microelectrode disc to be 340 nm (Kawagoe & Wightman, 1994). This thickness, despite slowing response time, still allows for observations of dynamic chemical changes associated with release and uptake of dopamine. We chose our electrodeposition parameters to attain this magnitude of thickness on our electrodeposited

microelectrodes. Figure 2.5 shows a representative example application of Equation 1 in modeling step concentrations of dopamine and 5-HT in a flow injection system to determine lp and D5-HT. A shows simulations for various values of lp to a normalized step concentration of dopamine, assuming a value of 1.0 x 10-9 cm^2s^{-1} for DDA (from previous work), which is very close to the value reported for thick films (1.5 x 10-9 cm^2s^{-1}) (Kawagoe & Wightman, 1994; Rocha & Carapuca, 2006). For the microelectrode shown in Figure 2.5, lp is approximately 300 nm. Figure 2.5B shows simulations for various values of D5-HT to a normalized step concentration of 5-HT, using lp from the best fit model to the step in dopamine concentration. A value for D5-HT of approximately 5.0 x 10-10 $cm^2 s^{-1}$ best fits the experimental step in 5-HT concentration for this microelectrode. The value of D5-HT was used to improve the solution for lp, which was used to improve the solution to D5-HT and the process was repeated until values for lp and D5-HT converged. Values for lp and D5-HT were determined to be 340 + 8 nm and 7.6 + 0.8 x 10^{-10} cm^2s^{-1}, respectively (average + SEM, n=5). The value of lp is consistent with values obtained by dip coating carbon-fiber microelectrode discs (Kawagoe & Wightman, 1994). As expected, D5-HT and DDA are both several orders of magnitude smaller than conventional values for diffusion coefficients in bulk solution because these molecules are diffusing through a denser polymer network. In addition, D5-HT is smaller than that of DDA, which is consistent with values obtained previously in bulk solution (Gerhardt & Adams, 1982).

In Vivo Electrochemical Identification

To validate the *in vivo* signal, we address previously described criteria for characterization of a novel electrochemical signal (P. E. M. Phillips & Wightman, 2003).

Figure 2.6i compares the normalized cyclic voltammograms of 50 nM 5-HT *in vitro* to that obtained in SNR *in vivo*. Close similarity between the shapes of the cyclic voltammograms confirms identification of 5-HT *in vivo* ($r^2 = 0.94$). Figure 2.6ii is the corresponding color plot from which this cyclic voltammogram is taken at the time indicated by the dashed white line.

In vivo microdialysis coupled to HPLC in the SNpr confirms the release of 5-HT in the SNpr brain region (Bergquist, Shahabi, & Nissbrandt, 2003; Hewton, Salem, & Irvine, 2007; Thorre, Sarre, Ebinger, & Michotte, 1997). Tissue content analysis in the SNpr confirms the presence of endogenous 5-HT at high levels (Palkovits, Brownstein, & Saavedra, 1974; Reubi & Emson, 1978).

In vivo investigations of DRN electrical stimulation have shown that stimulations even lower than 60 Hz are sufficient for evoking serotonin release (Hajos-Korcsok & Sharp, 2002). Autoradiographic tracing studies report on the existence of a serotonergic pathway from the DRN to the SNpr (Azmitia & Segal, 1978; Halaris, Jones, & Moore, 1976; Moore, Halaris, & Jones, 1978a; Wirtshafter, Stratford, & Asin, 1987). While there are no reports of a dopaminergic projection from the DRN to the SNpr (Stratford & Wirtshafter, 1990), the target location of the microelectrode is proximal to dopamine terminals in a region just above the SNpr, the substantia nigra pars compacta (SNpc), which could theoretically contribute erroneously to the signal. Figure 2.6ii demonstrates stimulation-evoked 5-HT release in the target area (8.5 mm ventral to the top of the skull) of the SNpr. Figure 6iii demonstrates that little release is measured 1.5 mm above the SNpr (7 mm ventral to the top of the skull), confirming specificity of the anatomical placement of the microelectrode.

Lastly, although we have shown that the modified microelectrode displays almost 50 times more sensitivity to 5-HT than to dopamine *in vitro*, we verify pharmacologically that dopamine does not contribute to the *in vivo* signal. We administered GBR 12909 (15 mg kg^{-1}) and citalopram, (10 mg kg^{-1}) pharmaceutical agents that respectively inhibit re-uptake of dopamine by DAT or 5-HT by SERT (Andersen, 1989; Hyttel, 1982). If the transporter specific to the analyte is blocked, clearance time of the released specie will increase. Figure 2.7 shows stimulated release of 5-HT upon (A) control, (B) GBR 12909, and (C) citalopram treatments in the same anaesthetized rat displayed as current in 2-dimensional false color (i) and concentration vs. time traces (ii). GBR 12909 has no significant effect on analyte amplitude or clearance, whereas citalopram significantly increases release amplitude and more importantly, clearance time, providing pharmacological identification of the released specie as 5-HT.

As we have confirmed the identity of the released analyte according to the criteria of Phillips and Wightman (2003), we report that the presented technique enables the first quantitative, *in vivo* sub-second recording of 5-HT release and uptake.

Conclusion

FSCV of *in vivo* 5-HT is challenging due to the electrochemically fouling side-products produced when 5-HT is oxidized. The electrochemical modifications that allow 5-HT to be monitored in tissue slice preparations and in *D. melanogaster* are not sufficient for *in vivo* monitoring where there are persistent and high levels of fouling 5-HT metabolites such as 5-HIAA. By electrodepositing Nafion onto cylindrical carbon-fiber microelectrodes, we have shown that 5-HIAA can be excluded from the microelectrode surface; moreover, due to pre-concentration of the positively-charged 5-HT ions in solution, the microelectrodes

are 50 – 100% more sensitive to 5-HT. Having reproduced the dip-coated thickness of the Nafion film (~300 nm) described by our own previous work (Kawagoe & Wightman, 1994), we back-calculated a diffusion coefficient for 5-HT through a Nafion film on a cylindrical carbon-fiber microelectrode. The Nafion-modified cylinders significantly exclude contributions from common brain anions. Validation of the *in vivo* signal meets previously established criteria for identification of a novel analyte with a microsensor: we have demonstrated electrochemical validation, established independent chemical analyses, verified anatomical and physiological feasibility as well as pharmacological characterization of the signal.

We have used this technology to present the first measurement of 5-HT release and uptake *in vivo*. We plan to apply this method to answer long-anticipated questions regarding the dynamics, characteristics, and pharmaceutical effects of 5-HT *in vivo*.

Support

The authors would like to thank Julie Gras-Najjar, Ellen Ambrose, Folabomi Oladosu, Rachel Clark, Brendan Macquellon and Ronny Gentry for their experimental help. The University of North Carolina Department of Chemistry Electronics Facility designed and fabricated the instrumentation for these experiments. This research was supported by NIH (NS15841 to RMW). Richard B. Keithley is supported by a National Defense Science & Engineering Graduate Fellowship.

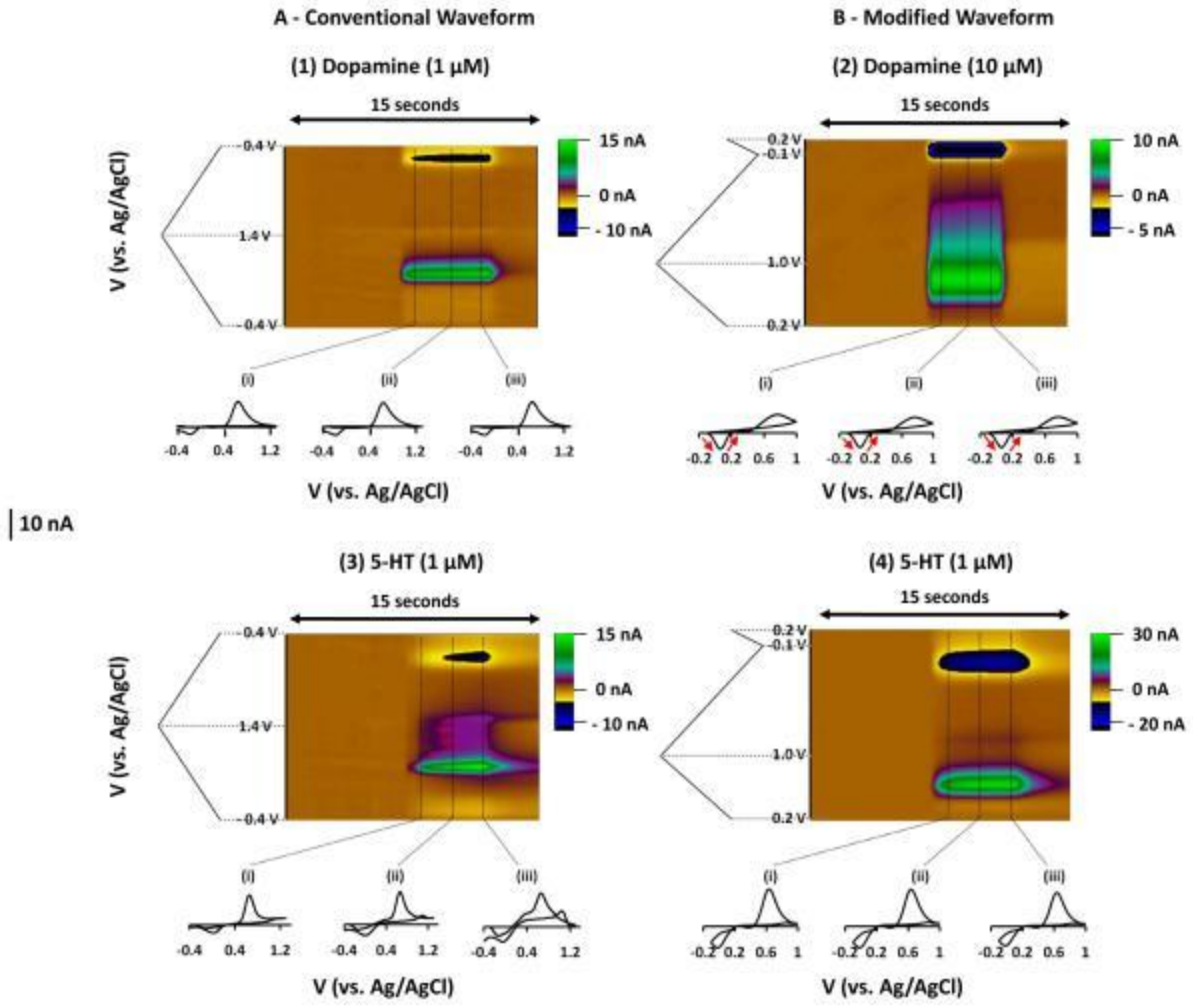

Figure 2.1 Comparison of waveforms for detection of dopamine and serotonin. Signals shown were obtained following introduction of dopamine (1 and 10 µM) (top) and 5-HT (1 µM) (bottom) into a flow injection system. employing both the traditional (A) and modified (B) waveforms. The current response is represented in false color. Representative cyclic voltammograms (vs. Ag/Ag Cl) at time points (i), (ii) and (iii) are single scans recorded at 1, 3, and 5 s post sample injection, respectively.

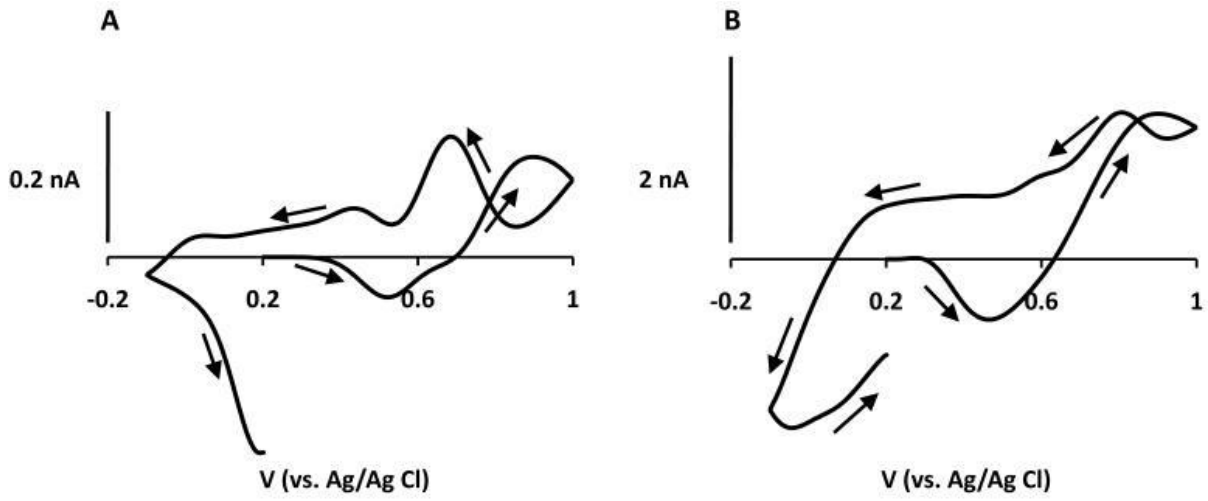

Figure 2.2 Comparison of cyclic voltammograms obtained *in vivo* vs. *in vitro*. Cyclic voltammograms (vs. Ag/Ag Cl) for (A) the signal obtained *in vivo* with DRN stimulation and SNpr measurement and (B) *in vitro* signal obtained via 1 μM 5-HT injection onto the microelectrode after it had cycled for 2 hours in a buffer containing physiological levels of 5-HIAA (10 μm).

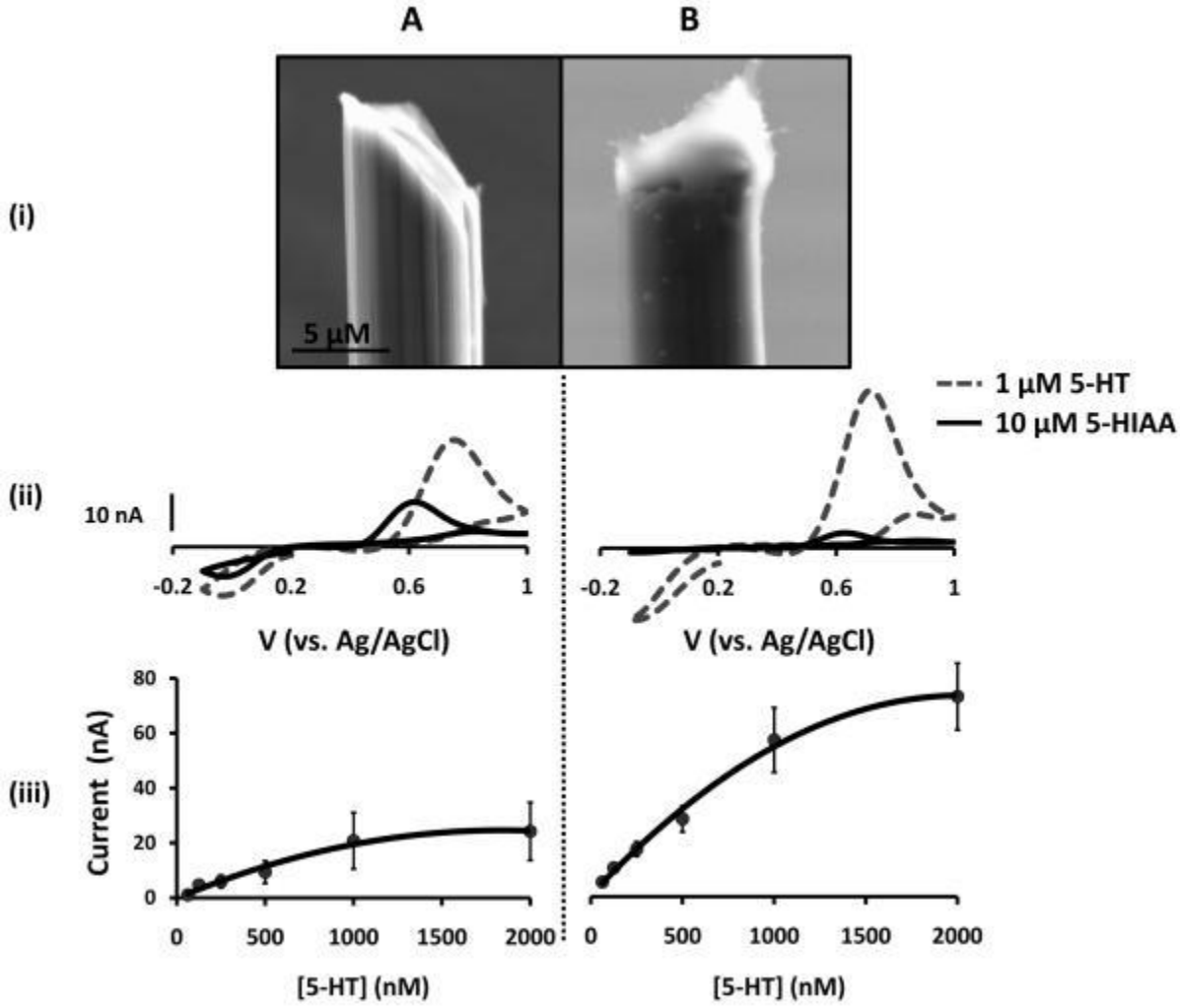

Figure 2.3 Nafion-modified microelectrodes are more sensitive to 5-HT. Top panel (i) shows ESEM images for (A) bare microelectrode and (B) Nafion-modified microelectrode. Panel (ii) shows cyclic voltammograms (vs. Ag/Ag Cl) for (A) a bare microelectrode compared to a (B) Nafion-modified microelectrode and their responses to 10 µM 5-HIAA (black line) and 1 µM 5-HT (grey dashed line). Bottom panel (ii) shows the respective concentration vs. current calibrations of (A) a bare microelectrode and (B) a Nafion-modified microelectrode in a buffer containing physiological levels of 5-HIAA (10 µM). The values are averages (n=4) ± SEM. The data is plotted with a polynomial line of best fit.

Species	**Average Response**		
	Bare Electrode (nA ± SEM)	**Nafion Electrode (nA ± SEM)**	**Nafion / Bare**
5-HT (1 µM)	20.8 ± 1.83	49.50 ± 10.24	2.38
Dopamine (10 µM)	8.50 ± 1.33	12.07 ± 2.61	1.42
Norepinephrine (10 µM)	8.30 ± 3.50	7.45 ± 1.42	0.90
Epinephrine (10 µM)	6.63 ± 3.80	6.32 ± 0.70	0.95
Ascorbic Acid (400 µM)	50.62 ± 15.63	20.02 ± 4.73	0.40
DOPAC (20 µM)	4.90 ± 1.17	1.55 ± 0.24	0.32
5-HIAA (10 µM)	13.78 ± 1.63	2.85 ± 0.90	0.21

Table 2.1 Comparison of Responses of Bare vs. Nafion-Modified Microelectrodes to Common Brain Species. Averaged *in vitro* responses obtained from four electrodes for common electroactive brain species on bare and Nafion®-modified microelectrodes. The values are an average (n=4 ± SEM).

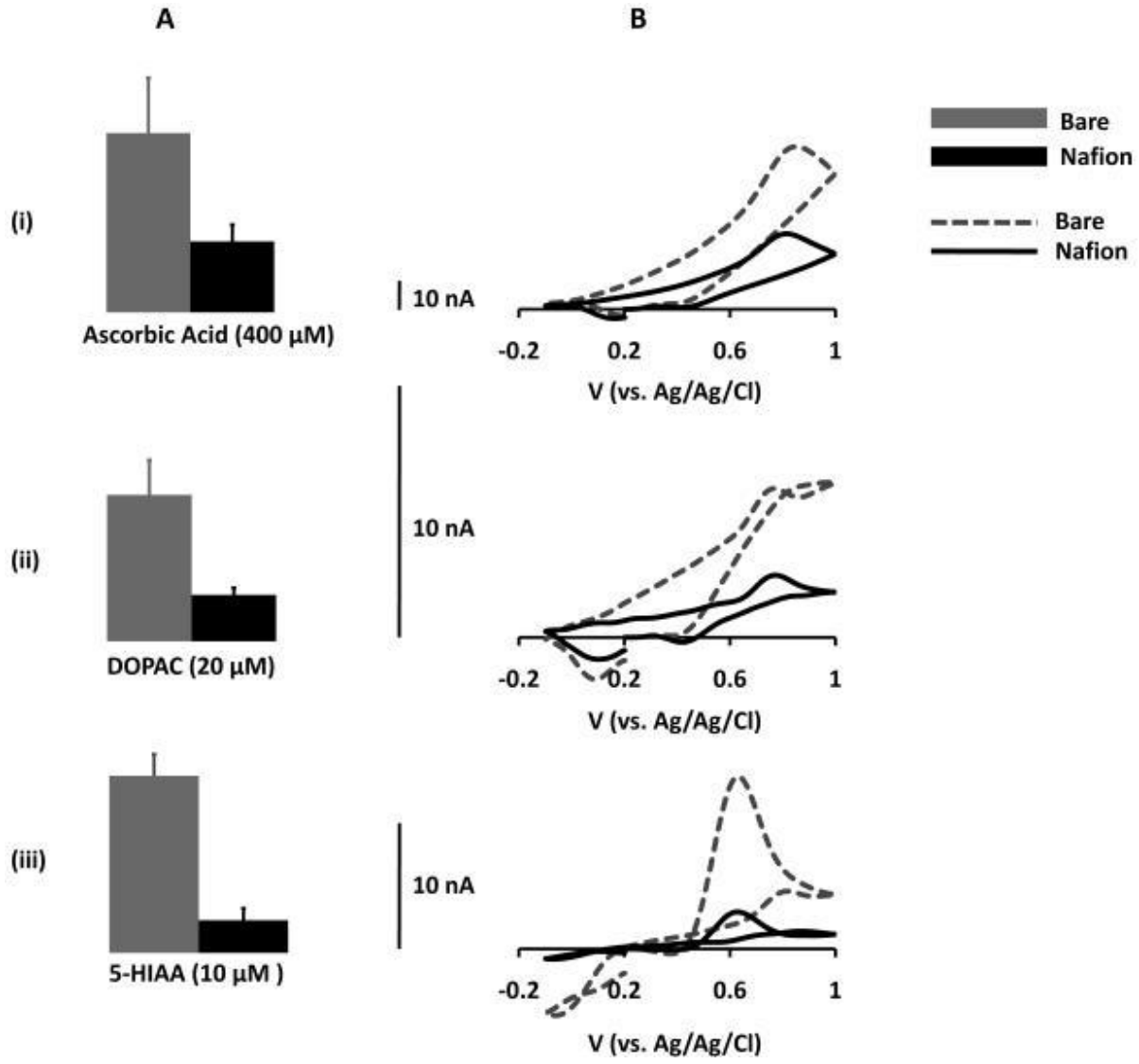

Figure 2.4 Response of bare and Nafion-modified electrodes to common electronegative species. Comparison of the responses of bare (grey) and Nafion-modified (black) microelectrodes to electronegative species (i) ascorbic acid, (ii) DOPAC and (iii) 5-HIAA *in vitro*. The values are averages (n=4) ± SEM. (B) shows single examples of the cyclic voltammograms (vs. Ag/Ag Cl) for bare (dashed grey line) and Nafion®-modified (black solid line) for (i) ascorbic acid, (ii) DOPAC and (iii) 5-HIAA.

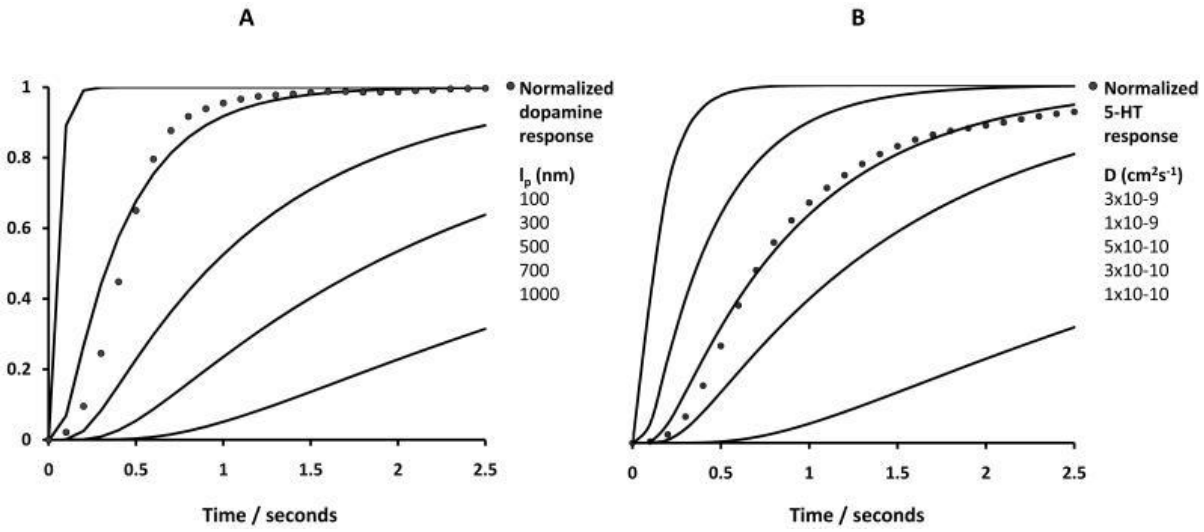

Figure 2.5 Determination of lp and D5-HT for a Nafion-coated carbon-fiber microelectrode using flow injection analysis. Panel A shows a normalized peak current response (grey dashed) towards a step concentration in dopamine (10 μM) fitted with equation 1 using various example values of lp, assuming a value of DDA of 1 x 10-9 cm2s-1 (solid black lines). Panel B shows a normalized peak current response towards a step concentration of 5-HT (1 μM) fitted with equation 1 using various example values of D5-HT and a value of lp obtained from the best fit to the dopamine step concentration.

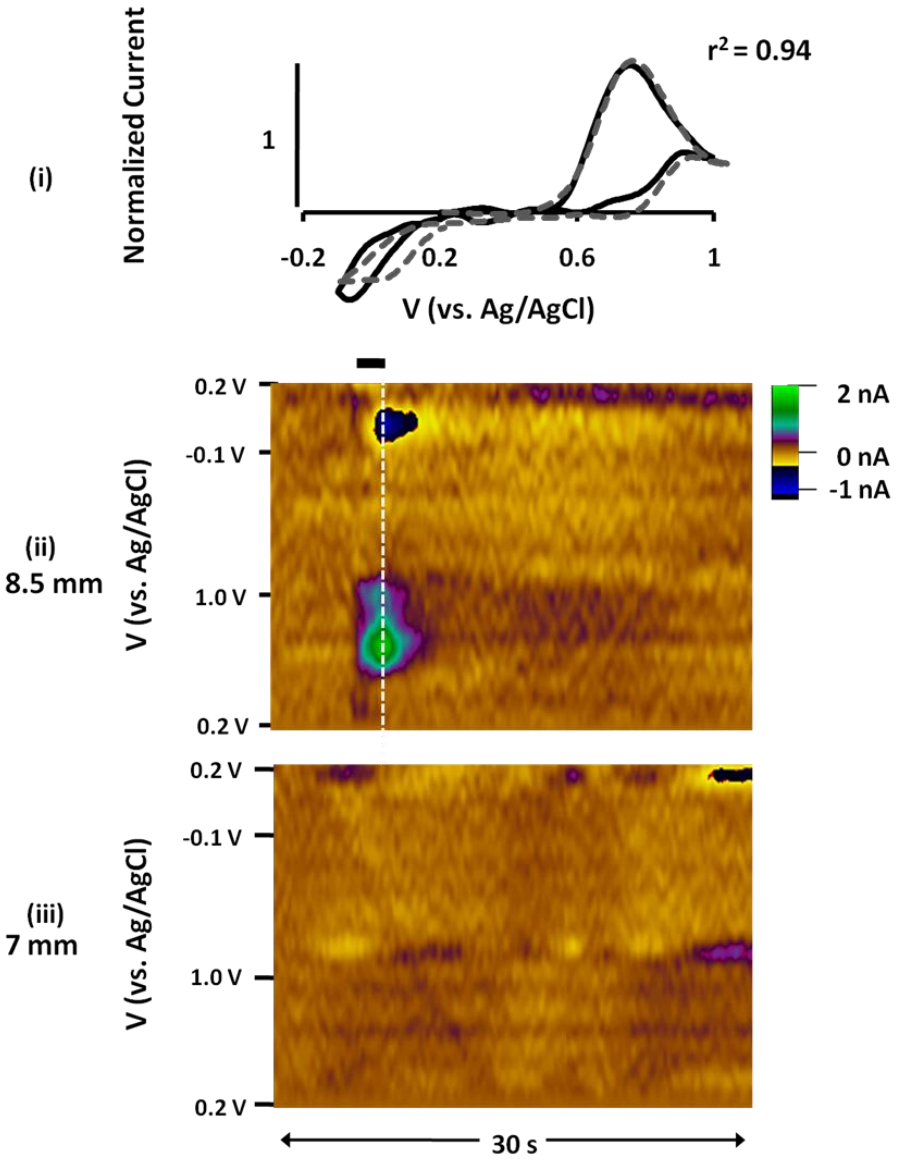

Figure 2.6 Electrochemical and anatomical validation of 5-HT detection. Panel (i) shows a normalized comparison of an *in vivo* signal (black solid) to an *in vitro* 5-HT (100 nM) measurement. Panel (ii) is the corresponding *in vivo* color plot with potential on y-axis plotted against time on the x-axis at 8.5 mm ventral to the surface of the skull, the white dash line signifies the time section at which the cyclic voltammogram is taken. The current response is represented in false color, the black line horizontal to the x-axis is the duration of the stimulation. Panel (iii) is the *in vivo* color plot with potential on y-axis plotted against time on the x-axis at 7 mm ventral to the surface of the skull.

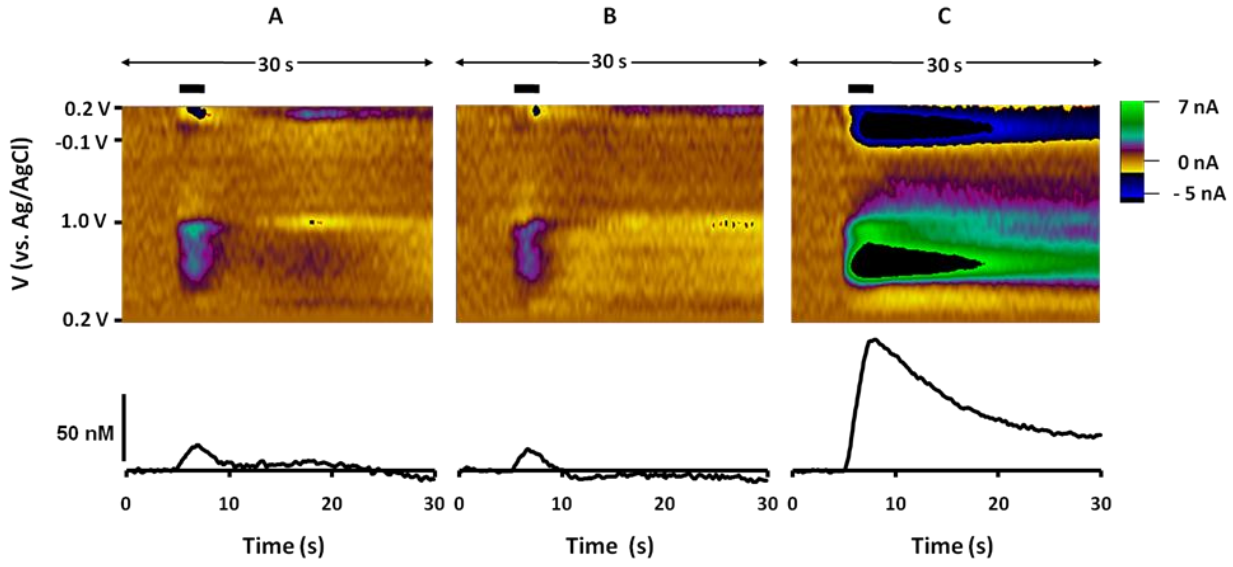

Figure 2.7 Pharmacological validation of 5-HT signal with GBR 12909 and citalopram. The top panel shows the potential on y-axis plotted against time on the x-axis, the current response is represented in false color. The black blocks horizontal to the x-axis are the durations of the stimulations. The bottom traces show concentration vs. time. These responses are for (A) stimulation-evoked control response, (B) 40 minutes after systemic administration of GBR 12909 (15 mg kg^{-1}) and (C) 40 minutes after systemic administration of citalopram (10 mg kg^{-1}).

CHAPTER 3: SIMULTANEOUS SEROTONIN AND HISTAMINE RELEASE FOLLOWING MEDIAL FOREBRAIN BUNDLE STIMULATION [3]

Introduction

5-HT is an important neuromodulator and dysfunctions of the 5-HT system are particularly well-documented in neurological disorders such as anxiety and depression (Petty, Davis, Kabel, & Kramer, 1996). *In vivo* neurochemical measurements of 5-HT are necessary for furthering our understanding of the mechanisms that govern these disorders, and will improve their diagnosis and treatment. Microdialysis studies have correlated *in vivo* basal level 5-HT changes to behavioral and pharmacological manipulations (Barnes & Sharp, 1999; Rueter, Fornal, & Jacobs, 1997). Basal 5-HT levels are determined by numerous individual neurotransmission events that are averaged in one microdialysis reading (Robinson & Wightman, 2007) and to fully understand the mechanisms that underlie these slow changes requires quantitative, sub-second endogenous 5-HT detection. This has traditionally been accomplished with fast-scan cyclic voltammetry (FSCV) in tissue slice preparations (Bunin & Wightman, 1998; John et al., 2006; O'Connor & Kruk, 1991a; Rice et al., 1994). These studies have provided a solid understanding of 5-HT release and uptake kinetics (Bunin et al., 1998), 5-HT receptor pharmacology (Davidson & Stamford, 1996; Threlfell et al., 2010), and 5-HT metabolism by monoamine oxidase (John & Jones, 2007b). Recently, FSCV has been used to perform similar characterizations in *D. melanogaster*

[3] This chapter previously appeared as an article in Journal of Neurochemistry. The original citation is as follows: Hashemi P, Dankoski EC, Wood KM, Ambrose RE, and Wightman RM. "*In vivo* electrochemical evidence for simultaneous 5-HT and histamine release in the rat substantia nigra pars reticulata following medial forebrain bundle stimulation." *J. Neurochem.* 118, 5 (Sep 2011) pp. 749-59.

(Borue et al., 2010; Borue et al., 2009). While these types of studies are essential to describe basic 5-HT mechanisms, *in vivo* measurements in a mammalian brain are necessary to understand how 5-HT dynamics are modulated in the complex entity of the intact nervous system. Recently we described a FSCV technique in which carbon-fiber microelectrodes were coated with Nafion to monitor 5-HT *in vivo* (Hashemi et al., 2009). The Nafion modification reduces electrode fouling while increasing its sensitivity to 5-HT. This is the first technique capable of monitoring endogenous, *in vivo* 5-HT release and uptake on a sub-second time scale. In this previous work, we established a physiological model where we evoked 5-HT release with a bipolar stimulating electrode in the dorsal raphe nucleus (DRN), the location of 5-HT cell bodies, and recorded terminal 5-HT release and uptake in the substantia nigra pars reticulata (SNpr) (Hashemi et al., 2009).

In this paper, we explore an alternative method of evoking 5-HT release in the SNpr. Using the well-documented efferent circuitry of the DRN (Azmitia & Segal, 1978; Imai, Steindler, & Kitai, 1986; Moore, Halaris, & Jones, 1978b; Parent, Descarries, & Beaudet, 1981), we exploit a branched 5-HT projection to both the SNpr and the striatum (Imai et al., 1986; van der Kooy & Hattori, 1980) that is located in the medial forebrain bundle (MFB). We previously showed that electrical stimulation of the MFB released an unidentified substance in the red nucleus of the rat, that we suspected was 5-HT (Kita, Kile, Parker, & Wightman, 2009). This suggested that MFB stimulation could evoke 5-HT release in targets posterior to the stimulating electrode. Here, we confirm this expectation by demonstrating that branched 5-HT fibers can be retrogradely activated, allowing the experimenter to avoid targeting the DRN, an anatomically challenging surgical technique. However, we find that MFB stimulation elicits release of an additional species in the SNpr. With electrochemical

and pharmacological data, in addition to literature well documenting histamine's physiological, anatomical and independent chemical verification in the SNpr (Brown, Stevens, & Haas, 2001), we identify this substrate as histamine. Threllfel *et al.* have previously shown that pharmacological activation of H-3 receptors inhibits 5-HT release (Threlfell et al., 2004). In accord with this, we find significant decreases in 5-HT release upon administration of SKF 91488, an agent that prolongs histamine lifetime in the synapse. With no drug present, we compare the 5-HT concentration release and uptake profiles between DRN and MFB stimulations and find that histamine release does not interfere with the quantification of the 5-HT signal. We thereby present a novel and robust method for studying 5-HT and histamine neurotransmission in the SNpr.

Materials and Methods

Animals

Male Sprague–Dawley rats, 8–12 weeks old, weighing 250–350 g, were purchased from Charles River Labs (Raleigh, NC, USA). Rats were housed under 12h/12h light cycles with controlled temperature and humidity. Food and water were available *ad libitum*. All animal care was in accordance with the Guide for the Care and Use of Laboratory Animals and was approved by the Institutional Animal Care and Use Committees of the University of North Carolina.

Surgery

Rats were anesthetized with urethane (1.5 g kg^{-1} rat weight) and positioned into a stereotaxic frame (David Kopf Instruments, Tujunga, CA, USA). Holes were drilled in the skull according to stereotaxic coordinates referenced from bregma and taken from Paxinos

and Watson's Rat Brain Atlas (Paxinos & Watson, 2007). Nafion-modified carbon-fiber microelectrodes were implanted in the SNpr (stereotaxic coordinates AP -4.8 to -5.2; ML +2.0; DV -8.5). A bipolar stainless steel stimulating electrode, insulated to the tip (0.2 mm diameter, Plastics One, Roanoke, VA, USA) was implanted into the MFB (AP -2.5 to -2.8; ML 1.7; DV -8.0) or DRN as described previously (Hashemi et al., 2009). An Ag/Ag Cl wire serving as a reference electrode was implanted into the contralateral hemisphere. Computer-generated biphasic pulse trains were applied through constant current stimulators (NL 800A, Neurolog, Medical Systems Corp., Great Neck, NY, USA), 2 ms in width and 350 µA each phase (unless otherwise noted), at 60 Hz for 2 s to evoke 5-HT release.

Voltammetric Procedures

Cylindrical carbon-fiber microelectrodes were constructed by aspiration of a single 2.5-µm radius carbon fiber (T-650, Thornel, Amoco Co.) into a glass capillary of 0.6 mm external diameter and 0.4 mm internal diameter (A-M Systems, Inc., Sequim, WA). A micropipette puller (Narishige, Tokyo, Japan) was used to taper the glass and form a carbon-glass seal. The exposed carbon fiber was cut to approximately 100 µm in length and was soaked for 30 minutes in isopropyl alcohol (IPA) to clean the surface. The procedure for electrodeposition of Nafion was described previously (Hashemi et al., 2009). Dopamine and 5-HT specific electrochemical detection waveforms were used as described elsewhere (Heien et al., 2003; Jackson et al., 1995). A customized version of TH-1 software (ESA, Chelmsford, MA) written in LABVIEW (National Instruments, Austin, TX) was used for waveform generation and data acquisition. A custom-built UEI potentiostat (University of North Carolina at Chapel Hill, Department of Chemistry Electronics Facility) was employed. All potentials are reported versus an Ag/Ag Cl reference electrode. Signal processing

(background subtraction, signal averaging, and digital filtering (4-pole Bessel Filter, 5 kHz)) was also done in TH-1 software. Voltammetric data are visualized as color plots that show multiple background-subtracted cyclic voltammograms that were consecutively collected. The abscissa is time and the current is encoded as false color (D. Michael, Travis, & Wightman, 1998). For most of the work in this paper, the ordinate is the voltage axis that peaks at 1.0 V, scans back to -0.1 V and returns to 0.2 V, the rest potential. The sensitivity with this waveform on Nafion modified microelectrodes to 5-HT is 49.5 nA μM^{-1} and 0.4 nA μM^{-1} to histamine.

Histology

To verify the spatial placement of the electrodes *in vivo*, the carbon-fiber microelectrode that acquired data was used to create a small, specific lesion in the recording site by a applying constant voltage (20 V for 10 s) (Park, Kile, & Wightman, 2009). Following the experiment, rats were sacrificed and perfused with 10% formalin solution. Brains were then removed from the skull and stored in 10% formalin. After at least 3 days, the brains were flash-frozen, sectioned into 40 µm slices in a cryostat, mounted on glass slides, and stained with 0.2% thionine. The brains were visualized and photographed with an optical microscope.

Drugs and Reagents

Serotonin hydrochloride, histamine dihydrochloride and thioperamide maleate were obtained from Sigma-Aldrich (St. Louis, MO, USA) at reagent quality and used without purification. SKF 91488 dihydrochloride was obtained from Tocris Biosience (Ellisville, MO, USA) and was delivered at a high dose to ensure permeation across blood brain barrier

and cause robust *in vivo* effects (50 mg kg^{-1}). Drugs were dissolved in saline and were injected intraperitoneally at a volume of 0.6 ml kg^{-1}.

Data Analysis

Kinetic characterization of 5-HT release and uptake was adapted from techniques previously used to describe kinetics of release and uptake of the dopamine system (P. A. Garris & Wightman, 1994) . Release was described as $[5\text{-HT}]_p * f$, where $[5\text{-HT}]_p$ is the amount of 5-HT released per stimulation pulse, and f is the frequency of stimulation pulses. The rate of change during stimulation is:

$$\frac{d[5-HT]}{dt} = \left([5-HT]_p * f\right) - \left\{\frac{d[5-HT]}{dt}\right\}_{uptake} \quad (1)$$

in which the duration of the release term is determined by the number of pulses in the stimulation. Only the uptake term dominates after the stimulation terminates. The uptake rate of 5-HT from the extra-cellular space (v) following electrically stimulated release was assumed to follow the Michaelis-Menten equation:

$$v = \left\{\frac{d[5-HT]}{dt}\right\}_{uptake} = \frac{V_{max}}{\frac{K_m}{[5-HT]}+1} \quad (2)$$

V_{max} is the maximal rate of uptake, and K_m is the Michaelis-Menten constant that describes the affinity of the 5-HT transporter for the 5-HT molecule. It was taken to be 170 nM, a value found in rat brain synaptosomes (Mosko, Haubrich, & Jacobs, 1977; Shaskan & Snyder, 1970).

In all simulations, analyte diffusion through a thin layer (300 nm) of Nafion was accounted for (E.W. Kristensen, Kuhr, & Wightman, 1987). The amount of 5-HT released

per stimulation pulse ($[5\text{-HT}]_p$) and K_m and V_{max} were determined by fitting the model to the experimental data. In experiments involving transport inhibition, V_{max} was fixed to values determined in pre-drug models.

Student's t-tests were performed on paired data sets, $p<0.05$ was taken as significant.

Flow Injection Analysis

For experiments characterizing histamine and 5-HT *in vitro*, flow injection analysis was used (E. W. Kristensen, Wilson, & Wightman, 1986b). The carbon-fiber microelectrode was placed in the output of a six-port HPLC loop injector mounted on a two-position actuator (Rheodyne model 7010 valve and 5701 actuator), operated by a 12 V DC solenoid valve kit (Rheodyne, Rohnert Park, CA). The apparatus enabled the introduction of a rectangular pulse of analyte to the microelectrode surface using a syringe infusion pump (Harvard Apparatus model 940, Hollison, MA) at a flow rate of 2 ml min^{-1}.

For *in vivo* experiments, the recording electrode was used to make a lesion in the tissue at the end of all experiments to verify its placement histologically. The high voltage across the working electrode used to achieve this necessarily over-oxidizes the carbon surface altering its sensitivity. Therefore, post-calibrations would not be a reliable measure of the electrode response. Rather, pre-calibrations were used to obtain a calibration curve, as described previously (Hashemi et al., 2009).

Results

Comparison of 5-HT following DRN or MFB stimulation

Histology verified the location of the stimulating and carbon-fiber microelectrodes in coronal slices of brains used in *in vivo* experiments (Figure 3.1). The stimulating electrode was in the MFB and the carbon-microelectrode was in the SNpr as indicated by the small lesions.

We have previously shown that electrical stimulation of the DRN releases 5-HT in the SNpr (Hashemi et al., 2009). In Figure 3.2, we compare this type of electrically stimulated 5-HT release (Figure 3.2A) to 5-HT release elicited via MFB stimulation (Figure 3.2B). The horizontal dashed lines in panel Figure 3.2A(iii) are at the peak potential for 5-HT oxidation (0.65 V) (1) and oxidation of an additional substrate (0.85 V) (2). The currents at these potentials were converted to concentrations and are plotted directly above this ((i) 5-HT, (ii) additional substrate). In (i) the current begins to rise at stimulus initiation and peaks within 0.5 seconds of the stimulation termination. In Figure 3.2A(ii), there is a small increase in current in response to the stimulation. The vertical dashed line in the color plot (iii) at the end of the stimulation and the current at this time were used to construct the cyclic voltammogram (inset). This cyclic voltammogram is identical to those obtained *in vitro* for 5-HT where the presence of the reverse wave is characteristic of 5-HT. Similar results were obtained with MFB stimulation (Figure 3.2B). In Figure 3.2B(i), the 5-HT current profile closely matches the 5-HT current profile in Figure 3.2A(i), however the current obtained upon stimulation in Figure 3.2B(ii) is 3-fold greater with MFB stimulation that with DRN

stimulation. The cyclic voltammogram (inset α) is taken at the vertical dashed line at the end of the stimulation. An additional vertical dashed line (β) is taken two seconds after the stimulus termination, the current at this time was used to construct the cyclic voltammogram in inset β. Panel C shows the averaged maximal release amplitudes of (1) 5-HT and (2) the additional substrate as the stimulating electrode is lowered down the dorsal/ventral tract above the MFB (n=6 ± SEM). For each line, the data are normalized to the maximal signal along the stimulation track. When two points are statistically different, the p value is added.

The concentration changes extracted from the current at 0.65 V exhibit a time-course in the SNpr very similar to the DRN stimulation. DRN and MFB averaged maximal concentrations in the SNpr are statistically identical: 12.7 ± 1.6 nM (n=6 ± SEM) 5-HT with DRN stimulation (Hashemi et al., 2009) and 12.8 ± 1.0 nM (n=6 ± SEM) with MFB (p=0.29). Similarly, the time for 5-HT to be cleared to one half of its maximal value ($t_{1/2}$) is 1.7 ± 0.3 s with DRN stimulation (n=6 ± SEM) and 1.8 ± 0.2 s with MFB stimulation (n=6 ± SEM) (p=0.45).

Examination of the color plot reveals additional features around the time of the stimulation. An oxidation process at 0.85 V on the reverse scan accompanied by a reduction process at 0.1 V are simultaneous with the 5-HT signal. Because these processes disappear rapidly after the stimulation, a cyclic voltammogram collected at 2 s after the stimulation (inset β) has the characteristic 5-HT cyclic voltammogram. However, when it is recorded at the end of the stimulation (inset α), it has additional features. Because 5-HT is oxidized at a potential that is reached before the additional species, the presence of the second species does not distort the time-course of 5-HT detection.

Characterization of Histamine Cyclic Voltammetry

The additional oxidation and reduction occur on the backwards oxidation scan and forwards reduction scan. This indicates a kinetically limited reaction that is dependent on the initial sweep that regenerates the electrode's carbon surface (Takmakov et al., 2010). The SNpr is populated with histaminergic terminals (Panula, Pirvola, Auvinen, & Airaksinen, 1989) and histamine displays this type of kinetically limited electrochemistry as demonstrated by following the direction of the potential sweep with the arrows in Figure 3.3. This figure compares *in vitro* responses at a carbon-fiber microelectrode, using the 5-HT waveform (see above) of (A) 5-HT (500 nM), (B) histamine (20 µM), (C) 5-HT + histamine (500 nM + 20 µM, respectively) to (D) the *in vivo* response in the SNpr during MFB stimulation. Panel (i) shows the color plots and panel (ii) shows the cyclic voltammograms taken at the white dashed vertical lines. The microelectrode's response to histamine (20 µM) injected alone is 7.9 ± 0.9 nA (n=4 ± SEM) and to histamine (20 µM) injected with 5-HT is 7.5 ± 0.7 nA (n=4 ± SEM)(p=0.6). The features of the *in vivo* response (D) are clearly electrochemically reproduced via a 5-HT + histamine mixture (C).

Figure 3.4 shows how the histamine signal changes with the applied waveform. Figure 3.4A shows a log-log trace of the current response (n=5 ± SEM) *in vitro* to flow injections of histamine (20 µM) as a function of increasing the scan rate of the detection waveform. It can be seen that the histamine response is proportional to the scan rate; the slope of the log-log plot is 0.56 indicating diffusion-driven electrochemistry. In Figure 3.4B, the peak amplitude for histamine oxidation is shown as a function of increasing the positive limit of the applied voltage. Increasing the potential window of the detection waveform causes an increase in the histamine response from 6.6 ± 2.2 nA (n=5 ± SEM) at 1.2 V to 13.4

± 3.7 nA (n=5 ± SEM) at 1.3 V (p=0.01). This behavior has been seen previously for dopamine (Hafizi, Kruk, & Stamford, 1990). At the same time, the peak on the reverse scan occurs at more positive potentials as the scan limit is increased, shown by the inset cyclic voltammograms.

Responses to Inhibition of Histamine N-methyltransferase

Unlike most biogenic amine neurotransmitters, histamine is not thought to be inactivated by a specific transporter (Brown et al., 2001). Instead, it is primarily inactivated by methylation, a process that is catalyzed by histamine N-methyltransferase. To pharmacologically verify the species detected at more positive potentials as histamine, an inhibitor of histamine N-methyltransferase, SKF 91488 (50 mg kg^{-1}) was administered. SKF 91488 is a potent, non-competitive inhibitor of histamine N-methyl transferase that is inactive at histamine receptors (Beaven & Shaff, 1979). Panel (i) of Figure 3.5 displays the effects of this agent in one rat. Figure 3.5A shows the average color plot of 5 control stimulations, taken 10 minutes apart. Figure 3.5B shows the average color plot of 5 stimulations one hour after drug administration, taken 10 minutes apart. Horizontal white dashed lines α and β were used to construct concentration vs. time plots of histamine (α) and 5-HT (β) which were then averaged for 5 animals and displayed in panel (ii) (n=5 ± SEM). The control responses are shown in blue and the drug responses are shown in black. Electrically stimulated histamine release was 2.8 ± 1.3 µM (n=5 ± SEM). After drug administration, the $t_{1/2}$ for histamine was significantly increased from 4.1 ± 0.9 s to 10.4 ± 2.1 s (p=0.03) with no change in amplitude. The maximal evoked concentration of 5-HT decreased from 9.3 ± 1.0 nM to 4.6 ± 0.4 nM (p=0.01) without a change in its $t_{1/2}$ value. Figure 3.5iii shows the effects of SKF 91488 on 5-HT release amplitude in control rats (A)

(n=5 ± SEM) and in rats pre-treated with thioperamide (10 mg kg^{-1}) (n=6 ± SEM), a selective H-3 receptor antagonist (B). In rats pre-treated with thioperamide, 5-HT release is not significantly affected after SKF 91488 administration; the control response was 10.2 ± 1.3 nM and 10.4 ± 1.5 nM after SKF 91488 administration (p=0.76).

Modeling 5-HT Release and Uptake

Figure 3.6 compares experimental and modeled 5-HT data between the two stimulations. The experimental data (blue dots) are superimposed on the model (black line). The model is a composite of linear release and uptake governed by Michaelis-Menten kinetics (R.M. Wightman et al., 1988). The concentration of 5-HT released per stimulation pulse, $[5\text{-HT}]_p$, and the maximal uptake velocity, V_{max}, were adjusted for the best fit while the value of the K_m for uptake was fixed at 170 nM. During DRN stimulation, the model yields $[5\text{-HT}]_p$ of 1.5 nM and a V_{max} of 0.63 µM s^{-1}, and during MFB stimulation, the model yields $[5\text{-HT}]_p$ of 1.1 nM, with a V_{max} of 0.67 µM s^{-1}.

Discussion

Electrical MFB stimulation evokes 5-HT Release in the SNpr

The efferent circuitry of the DRN to the SNpr is well-documented (Corvaja, Doucet, & Bolam, 1993; Dray, Gonye, Oakley, & Tanner, 1976; Fibiger & Miller, 1977; Wirtshafter et al., 1987), as are its projections to the striatum (Miller, Richardson, Fibiger, & McLennan, 1975; Steinbusch, Nieuwenhuys, Verhofstad, & Van der Kooy, 1981; Steinbusch, van der Kooy, Verhofstad, & Pellegrino, 1980). Some studies, including a retrograde labeling study by Van der Kooy *et al.,* show that the same 5-HT projection branches to both the SNpr and the striatum (Imai et al., 1986; van der Kooy & Hattori, 1980). Striatal bound 5-HT fibers

travel within the MFB (Miller et al., 1975). If axonal stimulation in the MFB could be used in place of DRN stimulation, certain experimental challenges associated with DRN stimulation can be avoided. These challenges arise primarily from the small size, inaccessible location and complicated topography of the DRN (Dib, 1994; Whishaw, Cioe, Previsich, & Kolb, 1977). However, before this work, it had not been established whether electrical stimulation of the MFB at a location anterior to the terminal site (SNpr) would release 5-HT. We had previously reported a similar phenomenon: the release of an unidentified substance in the red nucleus terminals upon anterior stimulation of the MFB (Kita et al., 2009). We suspected this substance was 5-HT, but since we had not yet optimized our electrochemical detection method with Nafion, we were unable to electrochemically verify this. Due to our recent technological advances for *in vivo* 5-HT detection (Hashemi et al., 2009), we are able to study whether this phenomenon applies to 5-HT release in the SNpr with MFB stimulation.

In Figure 3.2, we compare the terminal output in the SNpr upon DRN and MFB stimulation. Comparison of the inset cyclic voltammograms electrochemically confirms that 5-HT is released upon MFB stimulation. However another substrate is present in the MFB cyclic voltammogram in Figure 2.2B. The main reductive process of 5-HT is delayed with both DRN and MFB stimulation and indeed in *in vitro* (inset β). However, the reduction associated with the other substrate occurs simultaneously with the oxidation (inset α) showing this substrate is electrochemically independent from 5-HT. While the second substrate overlaps with the voltammograms for 5-HT, it does not interfere with the concentration of 5-HT obtained at 0.65 V because its electrolysis peaks occur later in the cyclic voltammogram. We have previously found somatodendritic dopamine release in the VTA upon MFB stimulation (Kita et al., 2009), however due to the low levels of dopamine

in the SNpr (Heeringa & Abercrombie, 1995) and the low sensitivity of the 5-HT specific waveform to dopamine (Hashemi et al., 2009), it is unlikely that there is a significant contribution from dopamine to this signal. Moreover, we had previously shown that the signal in the SNpr is unresponsive to pharmacological manipulations by GBR 12909 when we stimulate the DRN (Hashemi et al., 2009). We also confirmed this to be true for MFB stimulation (data not shown).

Histamine is Simultaneously Released with 5-HT in the SNpr *during MFB Stimulation*

The oxidation and reduction peaks of the additional substrate occur on the backward sweep of the oxidation scan and the forward sweep of the reduction scan. Such features have been previously seen in fast-scan cyclic voltammetry (Pihel, Hsieh, Jorgenson, & Wightman, 1995), and they are indicative of an electrochemical process that requires electrochemical cleaning of the electrode prior to its oxidation. Possible candidates based on these electrochemical characteristics are histamine, adenosine, or hydrogen peroxide (Cechova & Venton, 2008; Pihel, Hsieh, Jorgenson, & Wightman, 1998; Sanford et al., 2010). All three of these compounds are oxidized at very positive potentials and could be released by electrical stimulation of the medial forebrain bundle. We have previously shown that 5-HT itself can have distorted peaks when the electrode surface is fouled, but Nafion electrodeposition employed in our technique minimized this effect (Hashemi et al., 2009). Additionally, some groups have found 'switching' artifacts that occur at the switching potential of the waveform (Bull et al., 1990). The small current obtained at 0.85V in Figure 3.2A(ii) may have contributions by such a switching artifact at around 1 V, however, the equivalent MFB stimulation causes a much larger current at 0.85 V (Figure 3.2B(ii)).

Collectively, the evidence presented in this paper indicates that histamine is the substance detected along with 5-HT. Histaminergic projections originate from the tuberomammillary nucleus (TM), located immediately ventral to the MFB, and traverse the MFB (Garbarg, Barbin, Bischoff, Pollard, & Schwartz, 1976; Garbarg, Barbin, Feger, & Schwartz, 1974; Kohler, Swanson, Haglund, & Wu, 1985; Panula et al., 1989). One of the target regions is the SNpr where dense populations of histamine containing nerve terminals and histaminergic receptors are found (Panula et al., 1989; Schwartz, Arrang, Garbarg, Pollard, & Ruat, 1991). High amounts of histamine and histidine decarboxylase, the enzyme responsible for histamine synthesis from histidine, have been chemically verified in the SNpr using microenzymatic methods (Pollard, Llorens-Cortes, Barbin, Garbarg, & Schwartz, 1978). Furthermore, the H-3 receptors present in the SNpr (Anichtchik et al., 2000; Cumming, Shaw, & Vincent, 1991; Pollard, Moreau, Arrang, & Schwartz, 1993) have been shown to modulate GABA and 5-HT dynamics (Garcia, Floran, Arias-Montano, Young, & Aceves, 1997; Korotkova, Haas, & Brown, 2002; Threlfell et al., 2004). Thus, histamine release in the SNpr following MFB stimulation is an anticipated result. Given the close locality of these two locations (MFB and TM), it is not possible to selectively stimulate the TM without activating the MFB. Thus, to gain more insight into the nature of the stimulation, we recorded maximal 5-HT and histamine release in the SNpr while we lowered the stimulating electrode down the dorsal/ventral tract above our MFB coordinates in 0.5mm intervals from 5.5 – 10mm. Figure 3.2C shows that the maximal response for both 5-HT and histamine are at D/V 8.5 mm (n=6 ± SEM) which is not surprising since this is the dorsal/ventral location of the MFB. However, the histamine response significantly peaks earlier than the 5-HT response dorsal to this location. This implies that the histaminergic

fibers have a broader and independent fiber distribution through the MFB than the 5-HT fibers. In contrast to the MFB, the DRN has very little histaminergic innervation (Panula et al., 1989), explaining why stimulation of this region causes 5-HT release in the SNpr with little or no histamine release.

Further evidence that the additional species is histamine comes from our electrochemical and pharmacological experiments. First, as shown in Figure 3.3, the cyclic voltammetry of the unknown species closely resembles that for histamine in pH 7.4 solution. Second, administration of the highly selective ligand, SKF 91488, which potently inhibits histamine N-methyltransferase (Beaven & Shaff, 1979), significantly increased the clearance time of the signal in comparison to the control with no effect on the signal amplitude (Figure 3.5ii(α)). This drug also caused a significant decrease in the release amplitude of 5-HT after drug administration (β). Prior work has shown that activation of H-3 receptors inhibits 5-HT release (Threlfell et al., 2004). Since SKF 91488 prolongs histamine's half-life in the extracellular space, this would result in increased activation of H-3 receptors and suppression of 5-HT release. We confirm this by pre-treating rats with thioperamide (10 mg kg^{-1}), a highly selective H-3 receptor antagonist (Arrang et al., 1987) prior to SKF 91488 administration. Figure 3.5iii shows that thioperamide pre-treatment significantly arrests the SKF 91488 mediated inhibition of 5-HT release (n=6 ± SEM).

Thus, on the basis of electrochemical, anatomical, physiological, and pharmacological evidence, we assign the second signal simultaneously released upon MFB stimulation to histamine.

The Dynamic Rate of Electrically Stimulated 5-HT Release is Independent of DRN or MFB Stimulation

To confirm that MFB and DRN stimulations evoke release from a similar population of terminals in the SNpr, we compared 5-HT signals obtained with each stimulation and compared kinetic parameters based on a model previously used to characterize 5-HT release in brain slices containing the SNpr (Bunin & Wightman, 1998). Figure 3.6 illustrates that there are no significant differences in $[5\text{-HT}]_p$ or V_{max} in the SNpr with stimulation of the DRN or MFB. Furthermore, the calculated values of V_{max} in the SNpr with both types of stimulation (0.63 and 0.67 μM s^{-1}, respectively) agree with ones previously established in tissue slice preparations (0.57 μM s^{-1}) (Bunin et al., 1998). Since V_{max} is a function of the number of active transporters, this term is expected to be the same in slices and *in vivo*. Thus, our finding of similar maximal uptake rates for 5-HT is consistent with removal of 5-HT by a transporter in each preparation.

However, these quantitative modeling studies reveal that 5-HT release evoked *in vivo* is much smaller than evoked in tissue slice preparations ($[5\text{-HT}]_p$ = 55 nM in slices containing the SNpr (Bunin et al., 1998) but 1.5 nM *in vivo* with MFB stimulation). This large difference in release amplitude may have contributed to the previous physical and analytical challenges of *in vivo* 5-HT voltammetric detection. It would appear that the local stimulations that were employed in the tissue slice preparation, bypassed the regulatory mechanisms that tightly control 5-HT release *in vivo*. This suggests that intact *in vivo* physiological mechanisms, combining both cell body and terminal feedback, may profoundly regulate 5-HT release. This regulation may be at the level of 5-HT autoreceptors (Blier, Pineyro, el Mansari, Bergeron, & de Montigny, 1998; Daws, Gould, Teicher, Gerhardt, &

Frazer, 2000), release of different vesicular pools (Pellegrino de Iraldi, 1992), or activation of other inhibitory mechanisms (R. W. Invernizzi et al., 2007). These regulatory mechanisms, in combination with the fact that there is no known transporter for histamine, may also explain why the magnitude of histamine release is far greater than 5-HT release. These mechanisms are the focus of our ongoing studies.

In conclusion, this work shows that 5-HT release can be evoked by stimulating a collateral 5-HT projection in the MFB that branches to both the SNpr and the striatum. We verified electrochemically, anatomically, physiologically and chemically that the additional species present upon MFB is histamine. We confirmed that MFB stimulation evokes 5-HT release that is quantitatively equivalent to that evoked by DRN stimulation; however, in both models, release is profoundly less than in tissue slice culture experiments. This highlights the importance of *in vivo* methods in exploring the mechanisms of 5-HT dynamics.

Support

The authors thank Jessica Briley, Julie Gras-Najjar and Rinchen Lama for their experimental assistance. Department of Chemistry Electronics Facility designed and fabricated the instrumentation for these experiments. This research was supported by NIH (Grant NS15841 to R.M.W.).

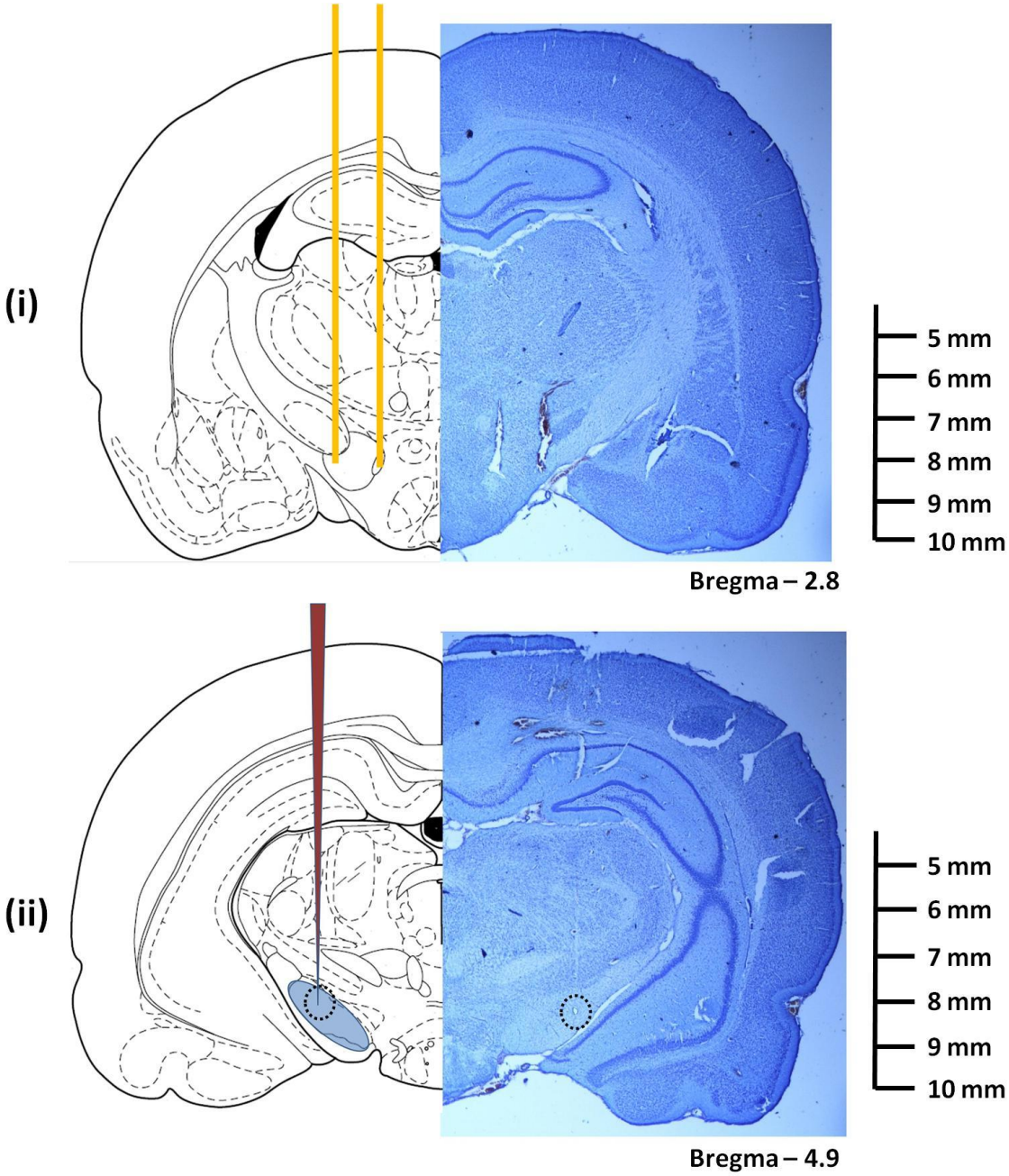

Figure 3.1 Histology of Stimulating and Carbon-Fiber Electrode Placements in the MFB and SNpr. Left hemisphere is a diagram showing intended placement of (i) stimulation electrode in the MFB or (ii) carbon fiber microelectrode in the SNpr at coordinates described in the methods section. Right hemisphere shows actual placement in a representative brain.

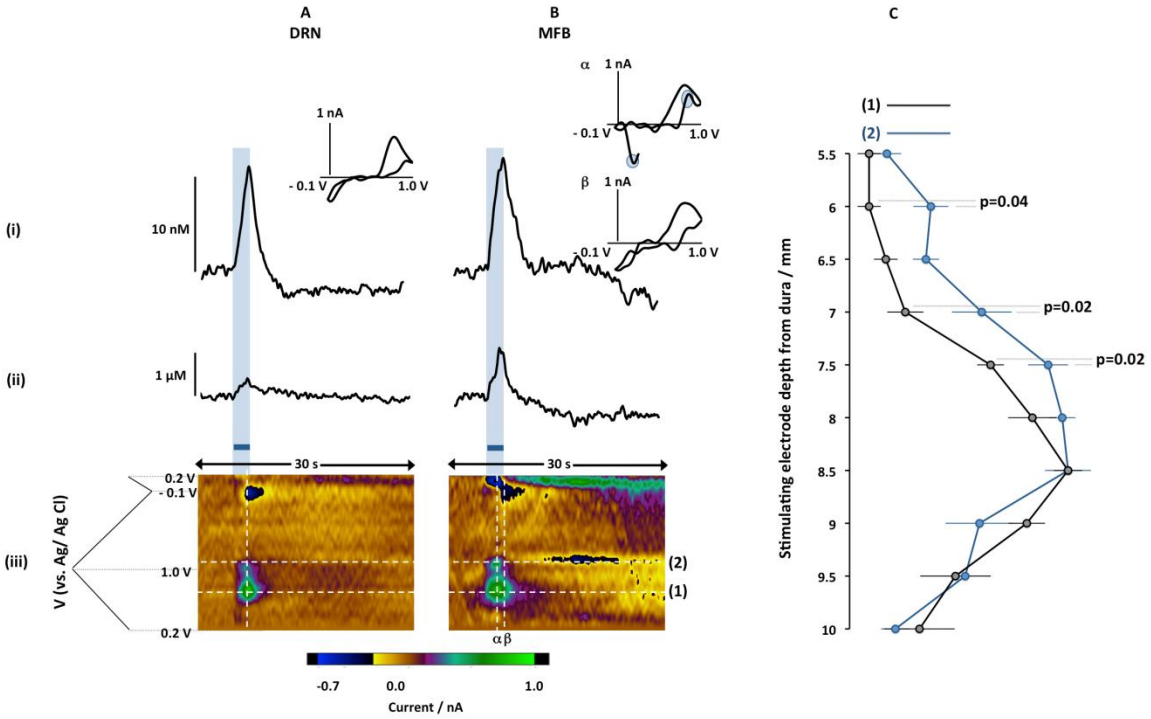

Figure 3.2 5-HT Color Plot, CV and Time Profile of Response in SNpr with DRN and MFB Stimulation. (A) and (B) - Comparison of signals obtained in SNpr obtained following DRN and MFB electrical stimulation respectively. Concentrations vs. time taken at the horizontal white dashed lines are shown above the color plots in panels (i) and (ii), and representative cyclic voltammograms (vs. Ag/ Ag Cl) taken at the vertical white dashed lines are inset. Bipolar stimulation onset at 5 seconds is 350 µA, 60 Hz and 120 pulses, represented by blue bar. (C) shows averaged, normalized maximal release amplitude of 5-HT (1) and the additional substrate (2) at 0.5 mm dorsal/ventral intervals of the stimulating electrode (n=6 ± SEM). Where the two values are statistically different, the p value is added.

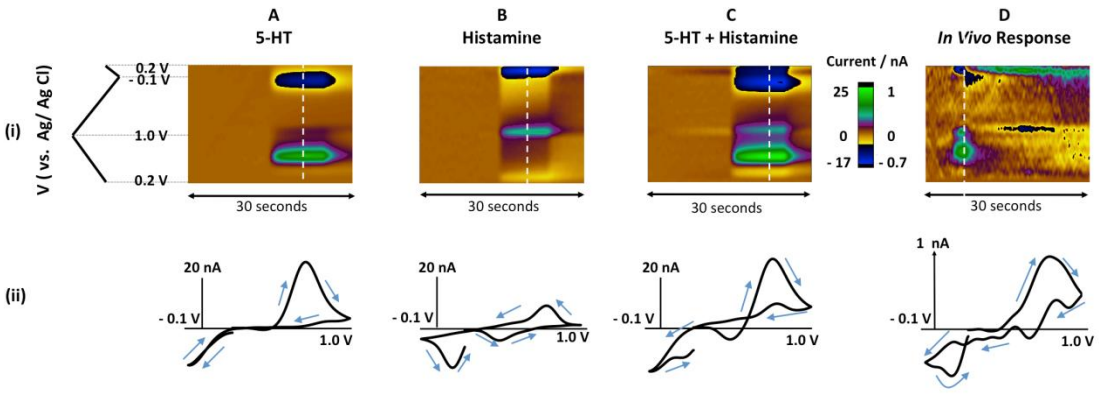

Figure 3.3 Comparison of *In vivo* Signal to a Mixed *In vitro* 5-HT and Histamine Signal. *In vitro* injections of (A) 5-HT (500 nM), (B) histamine (20 µM), or (C) 5-HT (500 nM) + Histamine (20 µM), and (D*) in vivo* response shown in (i) color plot format and (ii) cyclic voltammograms. Current is represented in false color and is a dual scale (left for *in vitro* and right for *in vivo*). Representative cyclic voltammograms were taken at the white dashed lines; in (D), the cyclic voltammogram was taken at 0.5 s after stimulation duration, indicated by the white dashed line. This position best captures both substrates.

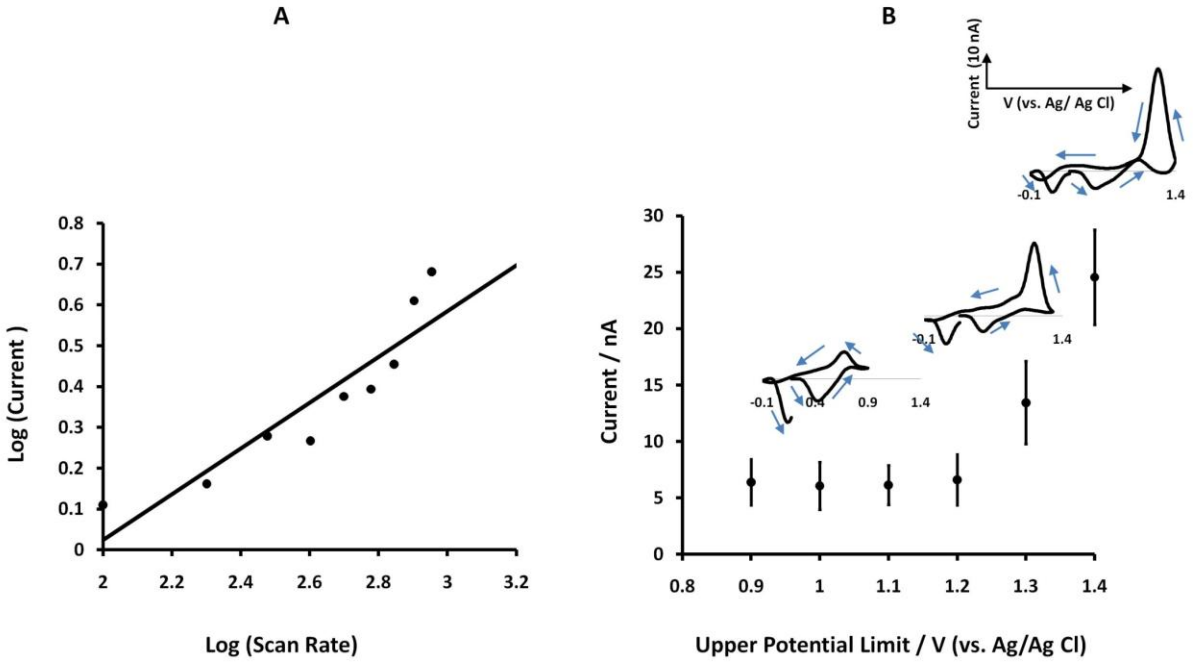

Figure 3.4 Effect of Varying Scan Rate and Upper Potential Limit on Histamine Response *In vitro.* (A) Log-log current response to *in vitro* injections of histamine (20 µM) as the waveform scan rate is increased from 100 V s^{-1} to 2000 V s^{-1} with conventional 5-HT waveform (-0.2 – 1.0 V) (n=5 ± SEM), where the line of best fit is a linear regression. (B) Current response to *in vitro* injections of histamine (20 µM) as the upper potential window is increased from 0.9 V to 1.4 V (n=5 ± SEM) vs. Ag / Ag Cl. Representative cyclic voltammograms are inset at 1.0, 1.3 and 1.4 V.

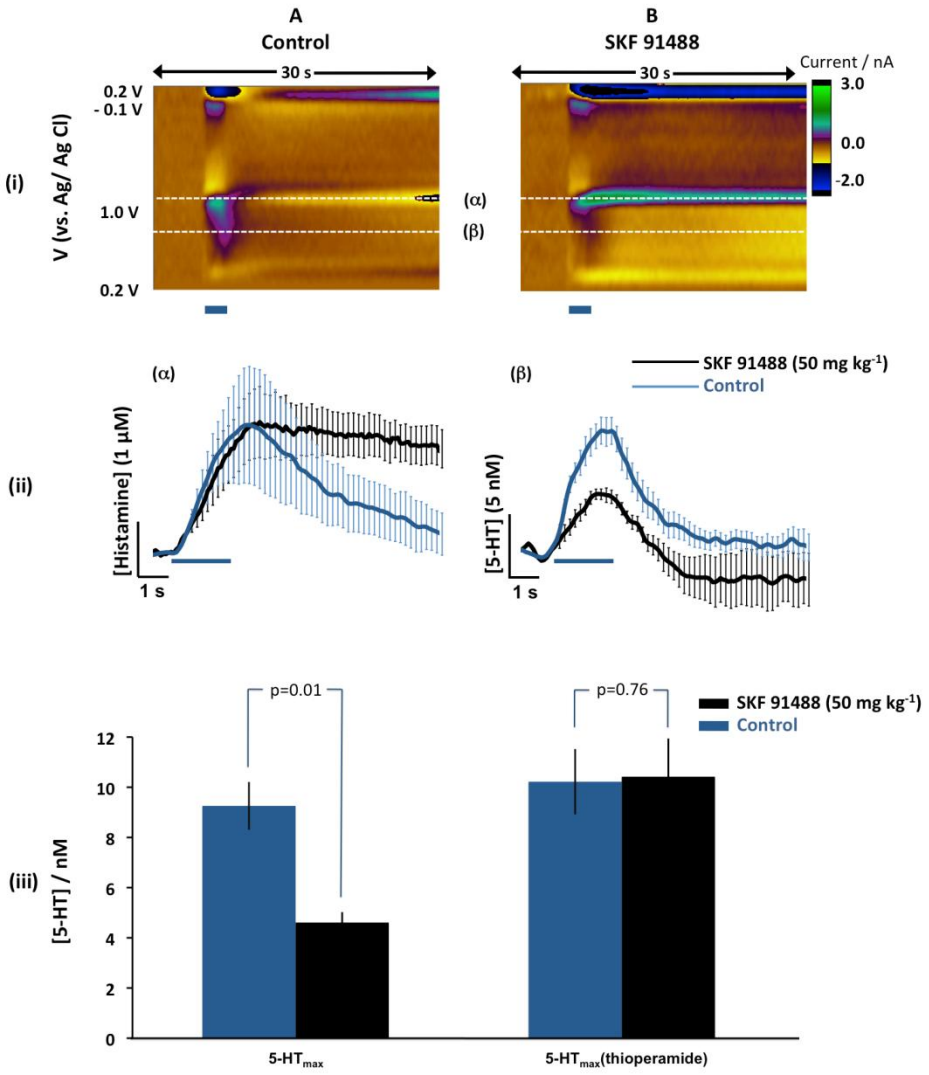

Figure 3.5 Pharmacological Characterization of Histamine with SKF 91488. (i) Color plots showing electrically stimulated response in the SNpr in (A) control and (B) 1 hour after intra-peritoneal SKF 91488 (50 mg kg^{-1}) administration. (ii)(α) Averaged concentration vs. time responses taken at oxidation potential α in control (blue) and 1 hour after intra-peritoneal SKF 91488 (50 mg kg^{-1}) administration (black) (n=5 ± SEM). (ii)(β) Averaged concentration vs. time responses taken at oxidation potential β in control (blue) and 1 hour after intra-peritoneal SKF 91488 (50 mg kg^{-1}) administration (black) (n=5 ± SEM). The blue bars represent the durations of the stimulus (350 µA, 60 Hz and 120 pulses) and error bars are SEM. (iii) Averaged maximal 5-HT release concentraion in control rats (A) and rats pre-treated with thioperamide (10mg kg^{-1}) (B). The bars are averages of the maximal 5-HT release in control stimulations (blue) and after SKF 91488 (50 mg kg^{-1}) administration (n=6 ± SEM).

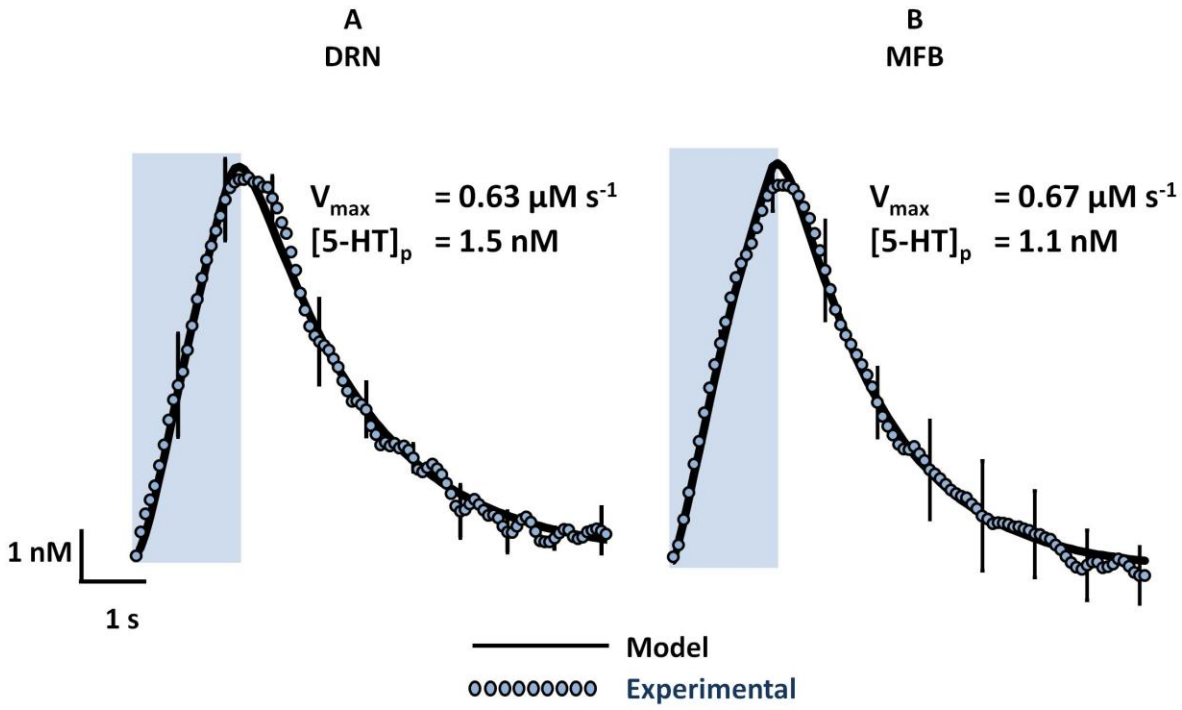

Figure 3.6 A Comparison of 5-HT Experimental Data and Kinetic Analysis Between DRN and MFB Stimulation. Averaged, normalized experimental data evoked by a 350 µA, 60 Hz and 120 pulse stimulation of the DRN (A) and the MFB (B) (blue dots, n=6 ± SEM). Kinetically modeled data (black line) is superimposed and kinetic parameters V_{max} and $[5\text{-HT}]_p$ are inset when K_m is fixed at 170 nM. Blue box indicates duration of stimulation and error bars are SEM.

CHAPTER 4: DIFFERENTIAL MECHANISMS IN THE REGULATION OF IN VIVO DOPAMINE AND SEROTONIN RELEASE [4]

Introduction

Dopamine and serotonin (5-hydroxytryptamine or 5-HT) are neurotransmitters with important, conserved roles in the vertebrate nervous system. Dopamine is important in neuronal circuitry that controls reward and in brain regions that regulate movement (Haber & Knutson, 2010). Assigning a specific functional role to 5-HT has proven more difficult because electrophysiological recordings of 5-HT neurons reveal unchanged firing in response to most stimuli (Jacobs & Fornal, 1999). Competing roles have been suggested for dopamine and 5-HT in reward circuitry, with dopamine signals predicting positive stimuli and 5-HT signals predicting negative consequences (Boureau & Dayan, 2011; Daw, Kakade, & Dayan, 2002). Biochemically, their regulation is quite similar, with similar proteins regulating synthesis, storage, release, uptake, and metabolism. To compare functional dopamine and 5-HT regulation in the brain, methods have been developed to monitor dynamic changes in their concentrations in the extracellular space.

Transient fluctuations of dopamine concentrations in the extracellular space of the nucleus accumbens core (Monachon, Burkard, Jalfre, & Haefely) can be evoked by electrical stimulation of the medial forebrain bundle (MFB) and have been characterized in the rat using *in vivo* voltammetric methods (Gonon & Buda, 1985; Millar et al., 1985). Dopamine is

[4] This chapter previously appeared as an article in Proceedings of the National Academy of Sciences (U.S.A). The original citation is as follows: Hashemi P, Dankoski EC, Lama R, Wood KM, Takmakov P, and Wightman RM. "Brain dopamine and serotonin differ in regulation and its consequences." *Proc. Natl. Acad. Sci. U.S.A.* 109, 29 (Jul 2012): pp 11510-5.

easily oxidized, and electrochemical methods such as fast-scan cyclic voltammetry can be used for detection (Robinson, Hermans, Seipel, & Wightman, 2008). A carbon-fiber microelectrode is placed in the brain region of interest. The shape of the cyclic voltammogram identifies dopamine and its amplitude can be used to calculate concentration. Each cyclic voltammogram can be collected in less than 10 ms, enabling fast, repetitive acquisition. Successive recordings of fluctuations in dopamine concentration lead to visualization of dopaminergic transmission events with sub-second temporal resolution. This method has shown that electrical stimulations of dopaminergic axons immediately evoke dopamine release that is rapidly uptaken by the dopamine transporter (DAT). During behavior, receipt of unexpected rewards (J. J. Day, Roitman, Wightman, & Carelli, 2007) or cues that predict reward (Owesson-White, Cheer, Beyene, Carelli, & Wightman, 2008) result in transient changes in dopamine concentration. These transients arise from the spontaneous firing of dopaminergic neurons in the ventral tegmental area and are regulated by the same mechanisms as electrically evoked release (Sombers, Beyene, Carelli, & Wightman, 2009).

Similar sub-second characterizations of 5-HT transmission are possible because 5-HT is also easily oxidized. However, voltammetric detection of 5-HT is complicated by oxidative products that foul the electrode surface, lowering sensitivity and temporal resolution (Jackson et al., 1995). Furthermore, 5-hydroxyindole acetic acid (5-HIAA), the primary metabolite of 5-HT, can similarly degrade the electrode surface. To minimize these issues, we have modified the detection waveform to prevent formation of oxidation products that foul the electrode surface. We also electrodeposit Nafion, a cation exchange polymer, on the carbon fiber to decrease sensitivity to 5-HIAA (G.A. Gerhardt, A.F. Oke, G. Nagy, B. Moghaddam, & R.N. Adams, 1984; Hashemi et al., 2009). Using these modifications, we

have demonstrated that stimulated 5-HT release can be measured in the substantia nigra pars reticulata (SNr) by stimulating the MFB (Hashemi et al., 2011) at a location that also evokes dopamine release (Millar et al., 1985).

This work characterizes and compares factors that regulate extracellular concentrations of 5-HT and dopamine. In-house hardware and software developments enable application of two different waveforms at separate electrodes in different brain regions (Zachek, Takmakov, Moody, Wightman, & McCarty, 2009). Using simultaneous dopamine and 5-HT measurements evoked by a common stimulation, physiological and pharmacological manipulations of release amplitude and uptake properties were evaluated. We find that distinctly different processes govern dopamine and 5-HT dynamics. Taken together, these results show that mechanisms controlling 5-HT in the extracellular space are more stringent than those of dopamine.

Methods

For full experimental procedures, see Supplemental Information.

Surgical Procedures

Stereotaxic surgeries for voltammetric measurements were performed as previously described (Hashemi et al., 2009). Briefly, Nafion-modified carbon-fiber microelectrodes were implanted in the SNr and in NAc. A bipolar stainless steel stimulating electrode was implanted into the MFB. As noted, heart rate, breathing, and body temperature were monitored in some animals (see Supplemental Information).

Voltammetric Procedures

Quad UEI potentiostats described previously (Zachek, Takmakov, Moody, et al., 2009) were modified by enabling independent control of the potential on two pairs of operational amplifiers in the head stage. A data acquisition system capable of generating two independent waveforms and collecting from two sets of channels was previously described (Zachek, Takmakov, Moody, et al., 2009). All potentials reported are against Ag/AgCl.

Drugs and Reagents

Pharmaceutical grade pargyline hydrochloride, NSD 1015 (3-hydroxybenzylhydrazine dihydrochloride), GBR 12909 dihydrochloride, raclopride, methiothepin, citalopram and tetrabenazine were administered interperitoneally.

Data Analysis

Two-tailed Student's T-tests were performed on paired data sets. $p<0.05$ was taken as significant. Error bars are given as ±SEM. Two-way ANOVA was used for the analysis of body temperature and heart rate.

Results

Simultaneous Dopamine and 5-HT Release Evoked by a Common Stimulation

A carbon-fiber microelectrode was placed in the NAc of each rat and the dopamine waveform was applied. A second microelectrode was placed in the ipsilateral SNr and utilized the 5-HT waveform. Both waveforms are illustrated in Figure 4.1 (left panel). Release was evoked in both brain regions by electrically stimulating the ipsilateral MFB (60 Hz, 2 s duration, biphasic pulses, 2 ms each phase, 350 μA), shown in the color plots in

Figure 4.1. Each color plot encodes 300 cyclic voltammograms recorded over 30 s around the stimulation (initiated at 5 s, vertical black line). The shape of the cyclic voltammograms (upper current-voltage curve, left panel) recorded in the NAc and SNr identify dopamine and 5-HT, respectively. Strikingly, the amplitude of stimulated dopamine is approximately 300 times greater than 5-HT. The uptake rates of the neurotransmitters are more comparable. Dopamine and 5-HT transporters follow Michaelis-Menten kinetics. At low concentrations the rate constant for dopamine uptake in the NAc ($k = V_{max}/K_m$) is ~ 14 s^{-1} (P. A. Garris & Wightman, 1994), and in the SNr, it is ~4 s^{-1} for 5-HT uptake (Hashemi et al., 2011).

We first examined dopamine and 5-HT release as a function of the stimulating electrode's dorsoventral position. Figure 4.1 (right panel) shows the normalized amplitude of evoked 5-HT in the SNr and dopamine in the NAc obtained at varying stimulating electrode locations as it was lowered in 0.5 mm increments from -6 to -10.5 mm through the MFB. Stars indicate that significant release was evoked in that location ($p<0.05$). Both 5-HT and dopamine release were maximal with the stimulating electrode at -8.5 mm. The 5-HT response profile was broader, with measurable release at stimulation electrode depths between 7.0 – 10.0 mm below dura, whereas dopamine could only be recorded between 8.0 – 9.0 mm below dura.

Effect of stimulation parameters on release

We varied stimulus parameters in the MFB to examine their effects on release relative to that obtained with our maximal conditions (depth, 8.5 mm from dura, 60 Hz, 2 s duration, biphasic pulses, 2 ms each phase, 350 µA). Dopamine and 5-HT release are both sensitive to stimulus pulse width (Millar et al., 1985), reaching a maximum at 2 ms (Figure 4.2A).

Dopamine release increases with stimulus intensity up to 350 µA with 2 ms wide pulses (Wiedemann, Garris, Near, & Wightman, 1992), and 5-HT responds similarly (Figure 4.2B). Stimulated dopamine release diminishes when stimulations are repeated rapidly (Montague et al., 2004). Using maximal stimulation trains repeated every minute, we found that dopamine release decreased with consecutive stimulations, dropping to 38 ± 7 % of the maximum normalized value ($n=6$, $p<0.05$) after the 20^{th} stimulation (Figure 4.2C). In contrast, maximal 5-HT release did not show signs of depletion.

Pharmacology of Synthesis, Packaging, Release, Uptake and Metabolism

Various aspects of dopamine transmission, including synthesis (Millar et al., 1985), packaging (Owesson-White et al., 2012), autoreceptor regulation of release (Gonon & Buda, 1985), uptake (P. A. Garris & Wightman, 1994; P.A. Garris & Wightman, 1995), and metabolism (J.A. Stamford, Z.L. Kruk, & J. Millar, 1988), were characterized with pharmacology and *in vivo* voltammetry. In this study, we compared the dopaminergic and serotonergic responses to these manipulations. The averaged predrug and drug responses of stimulated 5-HT release are shown in the top rows of Figures 4.3 and 4.4 and the responses for dopamine to equivalent treatments are shown immediately below. Histograms with amplitude and $t_{1/2}$ (both expressed relative to predrug value) are displayed in the bottom two rows, respectively. Where the response to pharmacological treatment is significantly different from pre-drug, statistical significance ($p<0.05$) is noted with a star. Stimulation duration is indicated by horizontal bars below each concentration vs. time plot

We investigated the role of synthesis on dopamine and 5-HT release by administering NSD 1015 (100 mg kg^{-1}), an aromatic amino acid decarboxylase inhibitor (Figure 4.3, left

column). Inhibition of decarboxylase results in accumulation of L-DOPA and 5-hydroxytryptophan (Carlsson, Davis, Kehr, Lindqvist, & Atack, 1972). Sixty minutes following NSD 1015 administration, dopamine release was reduced to 18.0 ± 4.5 % of its original amplitude (n=6, $p<0.05$). In contrast, 5-HT release was reduced to 48.1 ± 2.8 % of its pre-treatment amplitude at the same time point (n=6, $p<0.01$). There were no significant effects of NSD 1015 on the $t_{1/2}$ of dopamine or 5-HT.

Dopamine and 5-HT are both released via exocytosis from vesicular stores. We investigated the significance of rapid vesicular packaging in both systems by comparing the effects of a vesicular monoamine transporter 2 (VMAT2) inhibitor, tetrabenazine (10 mg kg^{-1}) (Quinn, Shore, & Brodie, 1959; Zheng, Dwoskin, & Crooks, 2006). Tetrabenazine significantly reduced dopamine release to 6.3 ± 3.0 % of its predrug value 60 minutes after its administration (n=5, $p<0.05$, Figure 4.3, center column). Effects on 5-HT release were not significant (71.6% ± 8.8 % of predrug value, n=5). However, the time delay between stimulation onset and maximum signal increased from 2.21 ± 0.15 seconds to 3.52 ± 0.34 seconds (n=5, $p<0.05$) after tetrabenazine administration. Tetrabenazine reduced dopamine release close to the limit of detection, therefore, $t_{1/2}$ analyses for statistical significance were not possible. The $t_{1/2}$ of 5-HT was significantly increased from 1.9 + 0.25 seconds to 2.59 ± 0.43 seconds (135 ± 21% of original; n=5, $p<0.05$).

To examine autoreceptor control of release at 5-HT terminals in the SNr, we administered methiothepin (20 mg kg^{-1}), a non-selective 5-HT 1a and 1b receptor antagonist (Monachon et al., 1972). Stimulated 5-HT release increased to 161 ± 10 % of its original (Figure 4.3, right column) (n=6, $p<0.05$). We administered raclopride, a D2 receptor antagonist, to examine the effects of autoreceptors in the dopaminergic system (Kohler, Hall,

Ogren, & Gawell, 1985). Raclopride (2 mg kg-^{1}) increased stimulated dopamine release to 184 ± 34 % (n=6, $p<0.05$) of the predrug value. While raclopride had no significant effects on $t_{1/2}$ for dopamine, methiothepin significantly increased $t_{1/2}$ for 5-HT from 1.36 ± 0.17 seconds to 1.99 ± 0.24 seconds (n=6, $p<0.05$).

Figure 4.4 (left panel) shows the effects of inhibition of the 5-HT uptake transporter (SERT) and DAT. SERT was inhibited with the selective serotonin reuptake inhibitor citalopram (10 mg kg^{-1}) (Hyttel, 1982) **(i),** while GBR 12909 (15 mg kg^{-1}), was used to inhibit DAT (**ii**) (Andersen, 1989). Citalopram significantly increased stimulated 5-HT amplitude to 476 ± 134 % of its original value (n=6, $p<0.05$) and significantly increased $t_{1/2}$ from 2.27 ± 0.07 s to 7.35 ± 1.46 seconds (n=6, $p<0.05$). GBR 12909 significantly increased stimulated dopamine amplitude to 279 ± 70 % of its predrug value (n=6, $p<0.05$) and significantly increased $t_{1/2}$ from 0.86 ± 0.14 seconds to 2.12 ± 0.2 seconds (n=6, $p<0.05$).

Figure 4.4 (right panel) compares the effects of monoamine oxidase (MAO) inhibition with pargyline (75 mg kg^{-1}) on dopamine and 5-HT stimulated release (J.A. Stamford et al., 1988). 5-HT release amplitude increased to 349 ± 60 % of its original value (n=6, $p<0.05$) while dopamine release did not increase significantly (175.1 ± 27.3 %, n=6, $p>0.05$). There were no significant effects of pargyline on dopamine $t_{1/2}$, however, the 5-HT $t_{1/2}$ significantly increased from 1.58 ± 0.07 seconds to 2.97 ± 0.49 seconds (n=6, $p<0.05$).

SSRI and MAOI administration

Figure 4.5 shows spontaneous efflux of dopamine (A) and 5-HT (B) occurring after respiratory arrest caused by administration of citalopram (10 mg kg^{-1}) followed by pargyline (150 mg kg^{-1}). The concentration of dopamine efflux at its peak averaged 37.7 ± 3.4 µM

(n=4), while 5-HT efflux was significantly lower at 0.296 ± 0.080 μM (n=4, $p<0.001$) (Figure 4.5C). The time elapsed between onset and peak of efflux also differed significantly, averaging 77 ± 4 s for dopamine and 266 ± 50 s for 5-HT (n=4 for each, $p<0.01$) (Figure 4.5F). Figures 4.5D and 4.5E compare responses of body temperature and heart rate between anaesthetized rats that received electrical stimulation (ES) and two injections of saline 35 minutes apart (n=4, white) or ES followed by citalopram (T1) and pargyline (T2) (n=6, black). Pargyline administration coincides with a significant decrease in body temperature (D) and heart rate (E) that persists throughout the remainder of the experiment ($p<0.05$).

Discussion

5-HT Release Regulation is More Stringent Than for Dopamine

In this work electrical stimulation of the MFB simultaneously evoked dopamine release in the NAc and 5-HT release in the SNr. Stimulation at a common site that releases different neurotransmitters provides a way to compare dynamic alterations in their regulatory mechanisms (Park, Takmakov, & Wightman, 2011). A particularly noteworthy finding was that dopamine release was approximately 300 times greater than 5-HT release despite similar tissue content in the two regions examined (90 ng/mg protein for dopamine in the NAc (P. A. Garris & Wightman, 1994) and 21 ng mg^{-1} protein for 5-HT in the SNr (Palkovits et al., 1974)). Thus, in spite of comparable stores, the releasable pool of 5-HT in the SNr is miniscule compared to the releasable pool of dopamine in the NAc. Distinct storage and releasable pools for both 5-HT and dopamine have been described (Shields & Eccleston, 1973; Shore, 1976), but the large difference in their relative size had not previously been appreciated. Moreover, we previously noted that evoked release of 5-HT in the SNr is much lower *in vivo* compared to its electrically evoked release from SNr slice preparations

(Hashemi et al., 2011). This suggests that *in vivo* 5-HT release is subject to tighter control mechanisms than both 5-HT in slices and dopamine *in vivo*.

To identify possible mechanisms for these differences, we explored the effects of the electrical stimulation on the dopamine and 5-HT axons that course through the MFB. Dopaminergic and serotonergic fiber bundles responded similarly to the stimulation parameters tested, giving greater release with wide electrical pulses and large current amplitudes (Figure 4.2). These properties are consistent with our predictions, given that both fibers are unmyelinated (Beaudet & Descarries, 1981; Grace & Bunney, 1983). Varying the dorsoventral location of the stimulating electrode revealed that 5-HT release can be evoked over greater region than dopamine, suggesting that serotonergic fibers have a broader topographic distribution. However, this is not sufficient to explain the 300-fold greater release of dopamine because even direct stimulation of serotonergic cell bodies in the dorsal raphe evokes comparably low 5-HT release (Hashemi et al., 2011).

The disparity between 5-HT and dopamine release amplitudes is attributed to differences in the readily releasable pool. Dopamine release was sensitive to repetitive application of stimulation trains, exhibiting a fatigue in release that did not occur for 5-HT in the SNr. The diminished release of dopamine after repeated stimulations has been attributed to depletion of the releasable pool (Yavich & MacDonald, 2000). In contrast, some 5-HT may be stored in dense core vesicles (Van Bockstaele & Pickel, 1993) or other compartments that do not exocytose. This would produce effects consistent with a small quantity of 5-HT available for release.

Dopamine Release is Synthesis and Packaging Sensitive While 5-HT is an Uptake/Metabolism Controlled System

Several of the pharmacological agents investigated in this work (Figures 4.3 and 4.4) inhibit the same processes in dopaminergic and serotonergic neurons. For example, inhibition of aromatic amino acid decarboxylase with NSD 1015 inhibits synthesis of both 5-HT and dopamine (Carlsson et al., 1972). Because the preceding experiments suggest that the releasable pool of dopamine is more sensitive to depletion, we predicted that releasable 5-HT would also be less sensitive to synthesis inhibition, and this was found to be the case. 5-HT and dopamine are both packaged into vesicles via the action of VMAT2 (Henry, Sagne, Bedet, & Gasnier, 1998), and inhibition of this transporter with tetrabenazine resulted in a greater decrease in dopamine release than 5-HT. We propose that a smaller releasable pool contributes to lower release amplitudes, which in turn reduces the requirement for packaging in serotonergic terminals. This is supported by the comparatively moderate response of 5-HT to manipulations that affect synthesis and packaging. There was, however, a significant increase in the $t_{1/2}$ for 5-HT clearance. An increase in cytoplasmic 5-HT caused by VMAT2 inhibition could decrease uptake rates by altering the concentration-dependent driving force for SERT, a common feature of amine transporters (Torres & Amara, 2007). There was a delay in the onset of 5-HT release that may be indication of tetrabenazine-insensitive vesicular pools, possibly dense core vesicles, compensating for the demand on release.

Following release, one fate for monoamines is metabolic degradation by MAO (Jain, Sands, & Von Korff, 1973). Prior work has shown that there is a small increase in dopamine release following MAO inhibition, presumably because repackaging into vesicles becomes more likely during a reduction in metabolic degradation (J.A. Stamford et al., 1988).

However, the increase in stimulated 5-HT release following MAO inhibition is greater than 3-fold, indicating that serotonergic neurons have greater regulation by MAO. Moreover, while MAO inhibition had no effect on the rate of dopamine clearance, a significant increase in the $t_{1/2}$ of the 5-HT signal indicates that this treatment caused a reduction in 5-HT reuptake rate. Similar to inhibition of VMAT2, MAO inhibition could alter the driving force of SERT, resulting in decreased rate of uptake.

Another means for extracellular regulation is uptake via transporters. However, because different receptors and transporters regulate dopamine and 5-HT release, it was necessary to administer different agents to evaluate these control points. We found that both neurotransmitter systems were sensitive to selective inhibition of their transporters (Figure 4.4D), results consistent with previous work (Budygin, Kilpatrick, Gainetdinov, & Wightman, 2000; Hyttel, 1982). 5-HT autoreceptors are known to suppress 5-HT release in a manner similar to the regulation of dopamine release by the dopamine autoreceptor in the NAc (Chaput, Blier, & de Montigny, 1986; Sesack, Aoki, & Pickel, 1994; Threlfell et al., 2010). We used methiothepin, a non-selective 5-HT autoreceptor antagonist to target the multiple 5-HT autoreceptors (Barnes & Sharp, 1999). Following raclopride and methiothepin, release of dopamine and 5-HT, respectively, was moderately increased. This suggests that regulation by 5-HT autoreceptors is not responsible for the differences between 5-HT and dopamine release. The increase in the $t_{1/2}$ of the 5-HT signal after methiothepin administration is consistent with the suggestion by Daws and colleagues that 5-HT_{1B} autoreceptors modulate 5-HT clearance (Daws, Gerhardt, & Frazer, 1999; Daws et al., 2000).

Disrupting 5-HT Control Mechanisms Results in Serotonin Syndrome

Within 2.5 hours of SERT and MAO inhibition respiratory arrest was followed by spontaneous efflux of dopamine and 5-HT (Figure 4.5A and B). Synchronized dopamine and 5-HT efflux likely reflects reversal of their transporters, which use secondary active transport coupled to the respiration-sensitive Na^+/K^+ ATPase (Torres & Amara, 2007). The spontaneous efflux preceding death resembles evoked release in that the maximum 5-HT amplitude is much lower than for dopamine (Figure 5C). Furthermore, 5-HT efflux is prolonged (Figure 4.5D) adding support to the concept that 5-HT is constrained more tightly with neurons. Following citalopram, pargyline administration led to decreases in heart rate and body temperature leading up to eventual death (Figure 4.5D and E). These findings concur with previous reports that combined administration of MAO and SERT, but not DAT, inhibitors cause fatalities in rats (Marley & Wozniak, 1984). In humans, this pharmacological combination is known to induce serotonin syndrome, which arises from excess serotonergic activity in the central nervous system (Izumi et al., 2006; Lane & Baldwin, 1997; Mitchell, 1997). Our findings reveal the consequences of serotonin syndrome in anesthetized animals.

Conclusions

In prior work we used a similar comparative approach to compare release of norepinephrine and dopamine evoked by a single stimulation, and found that their release and uptake characteristics were quite similar (Park et al., 2011). In this work, high time resolution recordings revealed much greater differences in regulation of dopamine and 5-HT. We found that 5-HT release is highly regulated and is dominated primarily by re-uptake/inactivation systems that could not be unraveled with slower monitoring techniques

such as microdialysis. Moreover, use electrochemical monitoring has revealed neurochemical processes that occur as a result of serotonin syndrome fatality.

Supplemental Methods

Animals

Sprague Dawley rats (male, 8-12 weeks, 250-350g) were purchased from Charles River Labs (Raleigh, NC, USA). All animal care was in accordance with the Guide for the Care and Use of Laboratory Animals and approved by the Institutional Animal Care and Use Committees of the University of North Carolina. Rats were housed in a 12:12 hour light cycles with controlled temperature and humidity. Rats were given *ad libitum* access to food and water.

Rats were anesthetized with urethane (15 g kg^{-1} rat weight) and positioned in a stereotaxic frame (David Kopf Instruments, Tujunga, CA, USA). Surgeries were performed as previously described (Hashemi et al., 2009) using stereotaxic coordinates referenced from bregma and taken from Paxinos and Watson's Rat Brain Atlas (Paxinos & Watson, 2007). Nafion-modified carbon-fiber microelectrodes were implanted in the SNR (stereotaxic coordinates AP -4.8 to -5.2; ML+2.0; DV -7.3) and in NAc (stereotaxic coordinates AP +2.0 to +2.3; ML +2.0; DV -7.3). A bipolar stainless steel stimulating electrode, insulated to the tip (0.2mm diameter, Plastics One, Roanoke, VA, USA) was implanted into the MFB (AP -2.5to -2.8; ML 1.7; DV -8.0).

Voltammetric Procedures

Carbon-fiber microelectrodes were fabricated by aspiration of a single 2.5-µm carbon fiber (T-650, Thornel, Amoco Co.) into a glass capillary with a 0.6mm external diameter and 0.4 mm internal diameter (A-M Systems, Inc., Sequim, WA). A micropipette puller (Narishige, Tokyo, Japan) was used to form a carbon-glass seal. The exposed carbon fiber was cut to approximately 100 µm in length and soaked in isopropyl alcohol (IPA) for 30 minutes to clean the surface (Cahill et al., 1996). The procedure for electrodeposition of Nafion was previously described (Hashemi et al., 2009). The reference electrodes were chloridized silver wire (0.5mm diameter, Sigma-Aldrich) in 0.1 M HCl. All potentials reported are against Ag/AgCl.

Quad UEI potentiostats (University of North Carolina Department of Chemistry Electronics Shop), described previously (Zachek, Takmakov, Park, Wightman, & McCarty, 2009), were modified by enabling independent control of the potential on two pairs of operational amplifiers in the head stage chip. A data acquisition system capable of generating two independent waveforms and collecting from two sets of channels was previously described (Zachek, Takmakov, Moody, et al., 2009). One NI 6251M card was used for generation of "5-HT waveform" (-0.1 to 1.0 V with a resting potential of 0.2 V at 1000 Vs^{-1} at 10 Hz) as described elsewhere (Jackson et al., 1995) and for data collection from the microelectrode placed in the SNR. The other NI-6251M card was used for generation of "dopamine waveform" (-0.4 to 1.3 V with a resting potential of -0.4 V at 400 Vs^{-1} at 10 Hz) and data collection from the microelectrode placed in the nucleus accumbens core (NAc).

Drugs and Reagents

Chemicals were purchased from Sigma-Aldrich (St. Louis, MO, USA) at pharmaceutical quality. Doses were selected from literature sources. Pargyline hydrochloride (75 mg/kg or 150 mg/kg) (Millar et al., 1985), NSD 1015 (100 mg/kg) (Muck-Seler & Diksic, 1995), GBR 12909 dihydrochloride (15 mg/kg) (Reid, Hsu, & Berger, 1997), raclopride (2 mg kg^{-1}) (Park et al., 2009), methiothepin (10 mg kg^{-1}) (Monachon et al., 1972), and citalopram (10 mg kg^{-1}) (Hashemi et al., 2009) were dissolved in saline and injected intraperitoneally at a volume of 0.6 ml kg^{-1}. Tetrabenazine (10 mg/kg) (Larsson & Komisaruk, 1972) was first dissolved in 0.2 ml 20% ethanol and diluted in saline and injected intraperitoneally at a volume of 0.6 ml kg^{-1}. Prior to drug administration, the voltammetric responses were evaluated following an i.p injection of the vehicle. There were no significant changes. For all drugs except pargyline, readings were taken 60 minutes after i.p administration. Readings were taken 90 minutes after pargyline administration to ensure enough time for the full effects to occur (Millar et al., 1985; J. A. Stamford, Z. L. Kruk, & J. Millar, 1988).

Monitoring of Physiological Conditions

A SurgiVet V3395 TPR (Temperature, Pulse Rate, and Respiration) monitor was used to record the rat's body temperature and heart rate every 5 minutes throughout experiments. Heart rate was measured using a SpO_2 digital oximetry probe (range 20-350 beats per minute, accuracy ±2%). For consistent results, the oximeter probe was positioned under a shaved region of the rat's body. Body temperature was measured using a temperature probe (range 32-140ºF, accuracy ± 1ºF) positioned under the length of the

animal. Heart rate and temperature are reported as a percentage of baseline, a minimum of 30 minutes in between completion of stereotactic surgery and onset of electrical stimulations. Breathing was monitored by observation throughout the experiment as use of the respiration sensor was not possible with the animal positioned in a stereotaxic frame.

Data Analysis

In this work we used $t_{1/2}$ to describe neurotransmitter clearance rates. It is defined as the time to go from the maximum evoked concentration to half of the maximal value.

Two-tailed Student's T-tests were performed on paired data sets, $p<0.05$ was taken as significant.

Two-way ANOVAs were performed on heart rate and temperature data sets using Bonferroni post-hoc tests to determine significance at each time point. $p<0.05$ was taken as significant.

Support

The authors thank the department of Chemistry Electronics Facility who designed and fabricated the instrumentation for these experiments. This research was supported by the NIH (Grant NS15841 to R.M.W.).

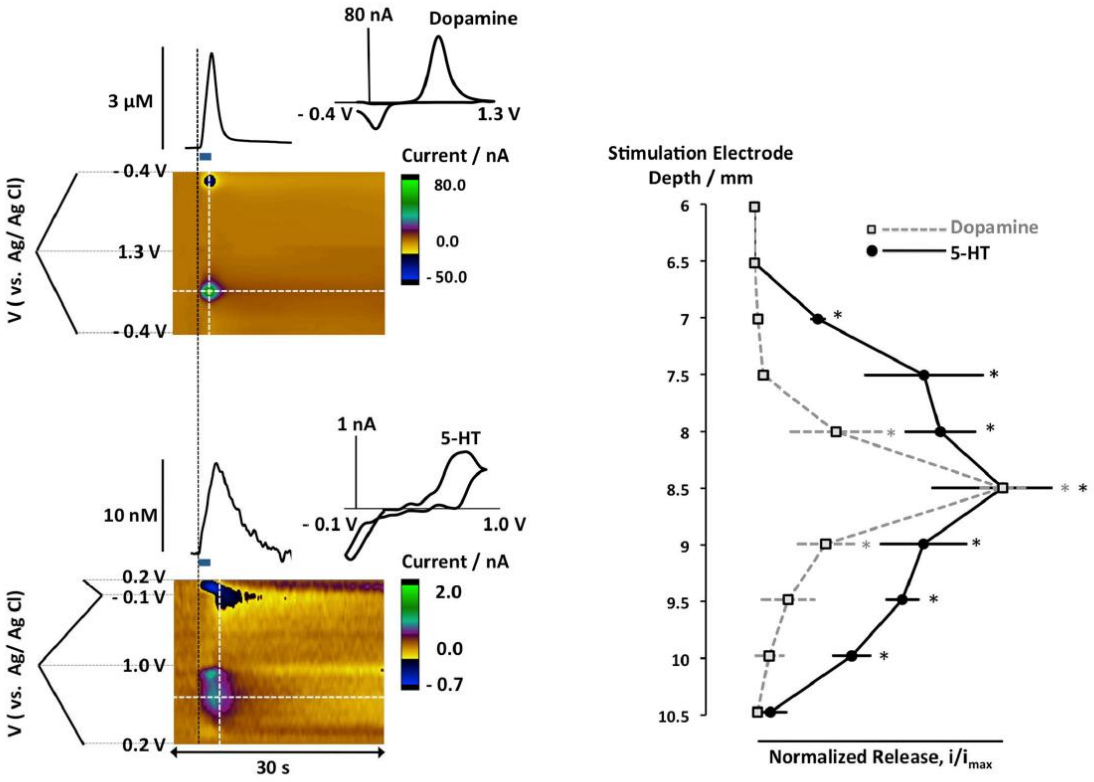

Figure 4.1 Comparison of dopamine and serotonin release evoked by electrical stimulation of MFB. Left panel: Representative color plots with potential on the y-axis, time on the x–axis, and the current in false color. Horizontal white dashed line was used to construct the current vs. time traces plotted above the color plots. Stimulation onset (dashed black vertical line) and duration is represented by the blue bar under the current vs. time traces. Cyclic voltammograms taken at the vertical white dashed lines are inset. Right panel: averaged, normalized responses recorded in the NAc (dopamine) and SNr (5-HT) as the stimulating electrode was lowered down a vertical tract to the MFB (n=6). Stars indicate normalized 5-HT maximal release values that are significantly different from the corresponding dopamine normalized release values ($p<0.05$).

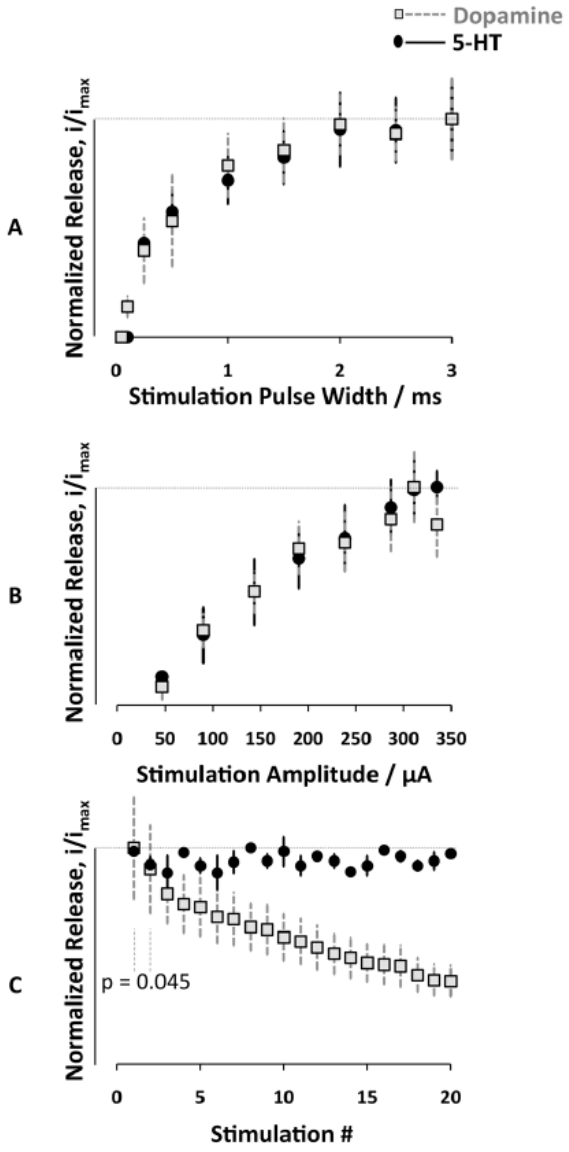

Figure 4.2 Comparison of dopamine and serotonin release evoked by varying stimulation parameters. Averaged, normalized dopamine and 5-HT maximal release with (A) variation of stimulation pulse width and (B) stimulation current amplitude (n=6 for each transmitter). (C) Averaged, normalized dopamine and 5-HT responses to repeated stimulation trains (n=6). Stimulations were 120 biphasic pulses at 60Hz, 350 µA and 2ms delivered once every 60 seconds for 20 minutes.

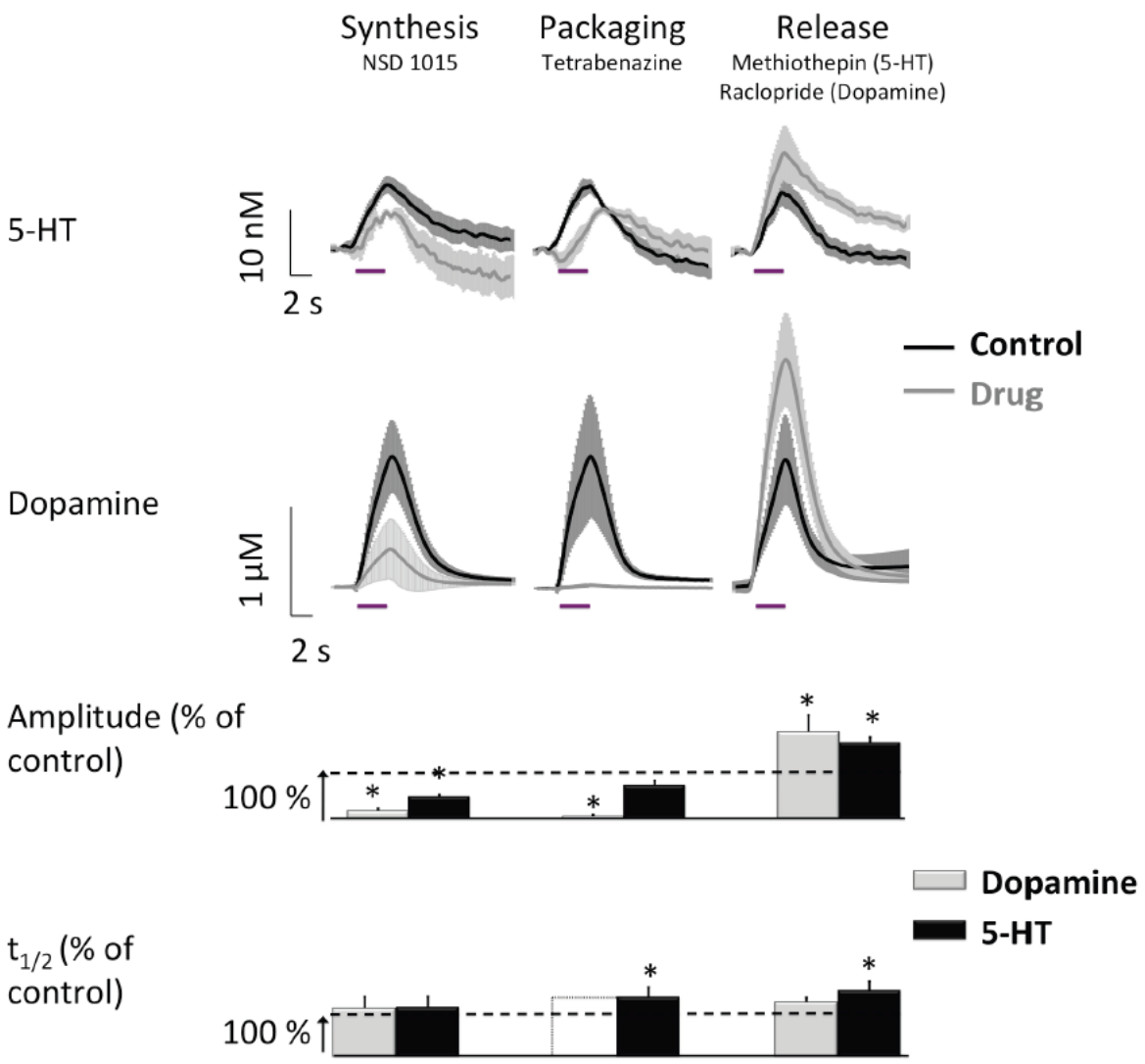

Figure 4.3 Effects of manipulating dopamine and serotonin synthesis, packaging and release. Comparison of averaged responses of 5-HT in the SNr (top; n=5) and dopamine in the NAc (below, n=6) to pharmacological inhibition of synthesis, packaging and release (left to right). Synthesis was inhibited with NSD 1015 and vesicular packaging was inhibited with tetrabenazine. Release was increased by autoreceptor antagonists (methiothepin for 5-HT and raclopride for dopamine). The two bottom rows show histograms of the percent change in amplitude and $t_{1/2}$ induced by the drug 60 min after its administration. Stars on the histogram indicate a significant change from pre-drug values ($p<0.05$).

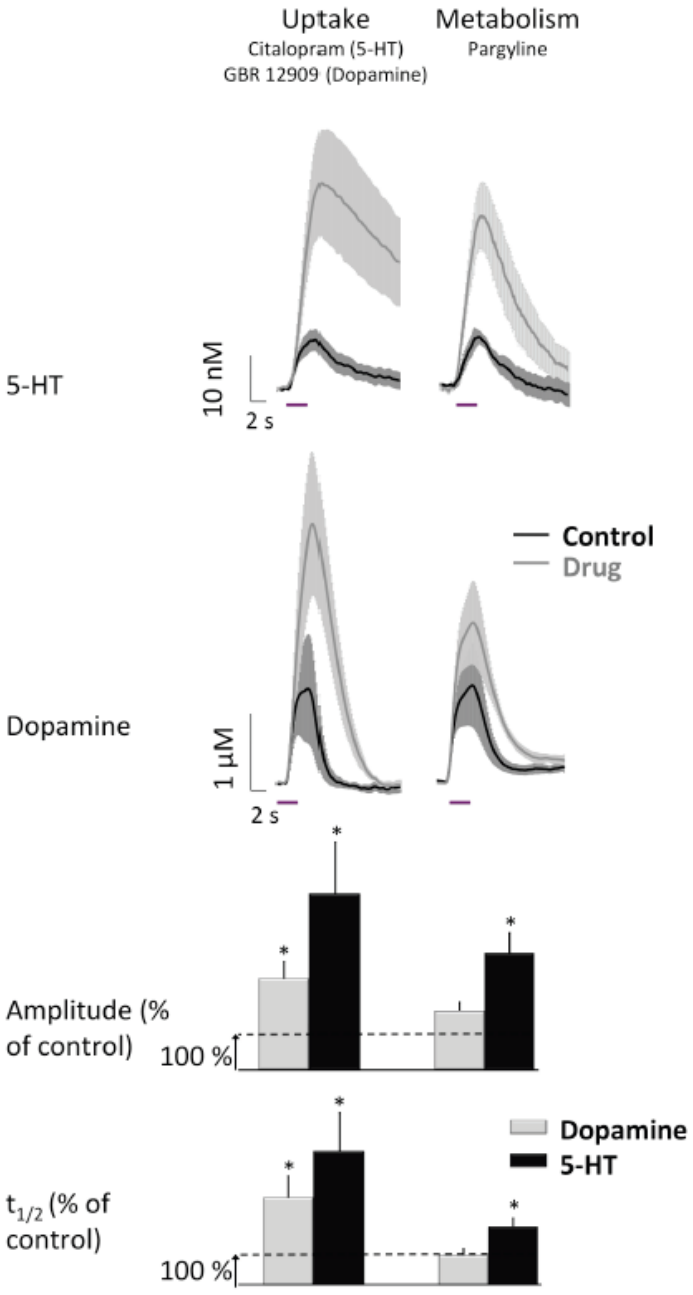

Figure 4.4 Effects of uptake and MAO inhibitors on dopamine and serotonin release. Comparison of averaged responses of 5-HT in the SNr (top; n=5) and dopamine in the NAc (below; n=6) to pharmacological inhibition of uptake and metabolism by MAO. Uptake was inhibited by GBR 12909 for dopamine and citalopram for 5-HT. Pargyline inhibited MAO and is effective for both neurotransmitters. The two bottom rows show histograms displaying the percent change in amplitude and $t_{1/2}$. Stars on the histogram indicate a significant change from predrug values ($p<0.05$).

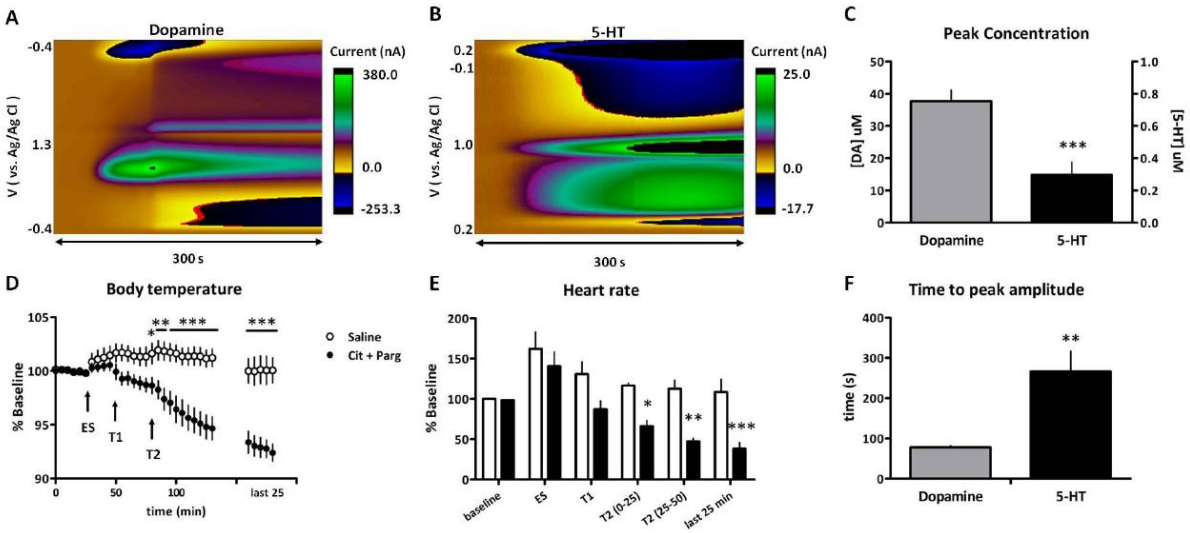

Figure 4.5 Dual uptake and MAO inhibition disregulates serotonin signaling. (A, B) Representative results from individual animals for dopamine (Monachon et al.) and 5-HT (SNr) efflux that both occur spontaneously immediately following respiratory arrest. (C) Maximal dopamine and 5-HT concentrations (n=4 for each). (D) Response of body temperature relative to baseline (0-25 min) during electrical stimulations (six 2-s stimulations, 5 min apart, ES), following citalopram (T1), and following pargyline (T2). Drug-treated animals shown in black circles (n=6) and saline controls shown in white circles (n=4). (E) Response of heart rate to electrical stimulations (ES), citalopram (T1), and pargyline (T2). Drug-treated animals shown in black bars (n=4), saline controls shown in white circles (n=4). (F) Mean time between onset of efflux and peak of efflux for dopamine and 5-HT (n=4). Stars on graphs indicate significant differences between groups (*, $p<0.05$; **, $p<0.01$; ***, $p<0.001$).

CHAPTER 5: THE DORSAL RAPHE NUCLEUS MEDIATES SSRI-INDUCED FACILITATION OF SEROTONIN SIGNALING

Introduction

Nearly 1 in 8 adults in the United States will suffer from depression in their lifetimes, and over half will seek medical treatment for their symptoms (Kessler et al., 2003). Enhancing serotonin signaling is a common goal of these treatments because hypofunction of the serotonergic system is widely believed to underlie depressive symptoms (Jacobsen, Medvedev, & Caron, 2012). The most commonly-prescribed pharmacotherapies for depression are selective serotonin reuptake inhibitors (SSRIs), which increase serotonin levels by reducing serotonin transporter (SERT) function. However, given that 3-6 weeks lapse before clinical improvements are observed, it is believed that SSRIs exert their effects via plasticity in serotonergic function and its downstream targets (Blier & de Montigny, 1998). This plasticity arises from two key effects of acute SSRI exposure: increases in extracellular serotonin levels, and reduced spontaneous firing of serotonergic neurons (Pineyro & Blier, 1999). The former is a consequence of a functional shift in the release and uptake equilibrium due to reductions in SERT function. The latter arises due to increased activation of 5-HT1a autoreceptors, which inhibit excitation of serotonergic neurons (Blier et al., 1998). Sustained increases in serotonin levels during chronic SSRI treatment leads to functional desensitization of these autoreceptors, and this desensitization is a critical component in the therapeutic effects of SSRI treatment (Bortolozzi et al., 2012; Ferres-Coy et al., 2013).

In this work, we use fast-scan cyclic voltammetry (FSCV) to examine how serotonin release is affected by acute SERT inhibition. Previously, we reported that serotonin evoked *in vivo* is remarkably lower in concentration than that evoked in brain slices (Bunin et al., 1998; Hashemi et al., 2011), and we demonstrated that SERT function is critical to maintaining physiological release and uptake equilibria *in vivo* (Hashemi et al., 2012). To better understand how SERT function may contribute to limited release *in vivo*, we examined how citalopram (CIT), a commonly-prescribed SSRI, alters serotonin release evoked by stimulations ranging in frequency. Varying stimulation frequency is one way to differentiate between effects on release *vs*. uptake in measurements of neurotransmission (Wightman & Zimmerman, 1990). Although seroto'nin release is consistently frequency-dependent in brain slices, we were surprised to find that it was not frequency-dependent *in vivo*. Moreover, acute SSRI treatment with CIT produced frequency-dependent release. We show evidence that CIT-induced enhancement of serotonin release is anatomically dissociable from changes in uptake, and implicate the dorsal raphe nucleus (DRN) in mediating these effects. This work demonstrates that SSRIs can rapidly alter serotonin signaling in distal brain regions by inhibiting SERT activity in the DRN. This novel property of SSRIs may provide important clues into how the acute effects of SSRIs translate into therapeutic efficacy during chronic treatment.

Materials and Methods

Animals

All experiments were conducted in accordance with protocols approved by University of North Carolina at Chapel Hill (UNC-CH) Institution Animal Care and Use Committee. Male C57Bl6/J WT and Slc6a4 homozygous knock-out mice were received from Jackson

Laboratories (Bar Harbor, ME) at 5-6 weeks of age and housed in groups of 4 for a minimum of 2 weeks after arrival. Mice were provided with food and water ad libitum and kept on a 12-hour-day/light cycle.

Electrochemistry

Carbon-fiber microelectrodes were fabricated as previously described (Cahill et al., 1996). Carbon fibers were aspirated into a glass capillary (external diameter: 0.6, internal diameter: 0.4) and pulled on a vertical capillary puller (Narashige, Japan) so that glass formed a tapered seal with carbon fiber. The exposed length of carbon fiber was then trimmed to 150 µM. To enhance sensitivity to serotonin, Nafion (5% in methanol, Sigma-Aldrich, St. Louis, MO) was applied to microelectrodes in a dip-coating process. Briefly, the tip of each electrode was dipped into Nafion solution then baked at 70 ºC for 10 minutes to evaporate solvent. This was repeated 7 times to obtain the the desired Nafion thickness. Electrodes were post-calibrated in a flow-injection system to obtain *in vitro* calibration factors as previously described (Hashemi et al., 2009).

Application of waveform, data collection, and stimulation application were controlled by Tarheel CV software via an in-house manufactured potentiostat (UEI, UNC-CH Electronics Facility). Voltammetric measurement of *in vivo* serotonin release has been previously described (Hashemi et al., 2009). For serotonin detection, a voltage waveform scanning from -0.1 to 1 V at 1000 V/s was applied at a rate of 10 Hz and held at 0.2 V between scans (Jackson et al., 1995).

In vivo experiments

Mice were anaesthetized with urethane (2 mg/g, i.p.) prior to stereotaxic surgery. A stainless-steel bipolar stimulating electrode (PlasticsOne, Roanoke, VA) was implanted into the DRN (AP: -4.1, ML: 0.0, DV: -2.5 to -2.7 mm) and a carbon-fiber microelectrode was lowered into the SNpr (AP -3.2, ML: +1.5, DV -4.0 to -4.2 mm). An Ag/AgCl reference electrode was secured in the contralateral hemisphere.

Detection of electrically evoked serotonin was optimized by moving stimulating electrode and carbon-fiber microelectrode in 0.1 mm increments within the given coordinate ranges. At the end of every experiment, CIT (10 mg/kg, i.p.) was administered to pharmacologically validate the signal recorded. In a few experiments, clearance was unaffected by CIT. This was attributed to unsuccessful targeting of the SNpr or DRN, and these experiments were excluded from statistical analyses.

For microinfusion experiments, prior to stimulation electrode implantation, a microinjection needle was lowered into the DRN, and approximately 25 µL of saline or CIT (800 mM, in saline) was ejected into the targeted region. After 15 minutes, the microinjector needle was removed and stimulating electrode was implanted as described above. Because of its close proximity to the cerebral aqueduct, misplacement of microinjector needle resulted in brainwide CIT exposure. A large increase in clearance half-life clearly demonstrated the failure of the microinfusion procedure, and these experiments were excluded from analyses.

Drugs and reagents

Citalopram hydrobromide and urethane were purchased from Sigma-Aldrich (St. Louis, MO) and used as received. Nafion (10% in mixed alcohols) was purchased from

Sigma-Aldrich and concentrated in a rotovap to replace solvent with methanol. Intraperitoneal-injected drugs were administered at a volume of 0.01 mL/g body weight.

Data analysis

Results are average values ± SEM except when representative data is presented. Trends in maximum evoked amplitude ($[5\text{-HT}]_{max}$), release rate, clearance half-life ($t_{1/2}$), and net overflow were analyzed using a repeated measures ANOVA with Tukey's multiple comparisons post-hoc analysis.

Release rate, $t_{1/2}$, and net overflow were calculated using concentration traces evoked by 20-60 Hz stimulations in each subject. Release rate was calculated by fitting lines to the rising phase of serotonin release, approximately the first 2 s. Adjustments of the fitting frame of up to 0.1 s were made to avoid stimulation artifacts and to ensure linear behavior (R^2>0.70). Clearance half rate ($t_{1/2}$) was calculated in Clampfit (Molecular Devices, LLC, USA) as the decay time between 100% and 50% evoked concentration. Net overflow was calculated in Clampfit using the integral under the curve for the first 15 seconds following the stimulation event. $t_{1/2}$ and net overflow analyses have been shown to correlate well with kinetic models of neurotransmitter release (Yorgason, Espana, & Jones, 2011).

Results

Serotonin release evoked in vivo varies with stimulation pulse number, but not frequency

Serotonin release was measured in the SNpr during stimulation of the DRN. A representative color plot identifies serotonin evoked after a 325 μA, 60 Hz, 1 s stimulation (Figure 5.1A). The concentration trace obtained at the oxidation potential for serotonin (Figure 5.1B) shows its release during the stimulation followed by its subsequent clearance.

In brain slices, prior work showed that serotonin release evoked in the SNpr by an adjacent stimulating electrode is pulse- and frequency-dependent. This was confirmed in the present work, where we found that $[5\text{-HT}]_{max}$ doubled when comparing release evoked by 20 Hz and 60 Hz stimulations in the SNpr (n=5). To characterize the responsiveness of serotonin release to different stimulation parameters *in vivo*, we compared $[5\text{-HT}]_{max}$ evoked by stimulations of the DRN that varied in pulse number and frequency. In dramatic contrast to the slice results, varying stimulation frequency *in vivo* did not affect $[5\text{-HT}]_{max}$ (Figure 5.1C). However, $[5\text{-HT}]_{max}$ was significantly affected by varying stimulation pulse number (Figure 5.1D; repeated measures ANOVA, $F(4,16)=9.374$, $P<0.001$). To rule out an effect of stimulus duration on pulse-dependence, we covaried pulse number with frequency to fix the total stimulus presentation time at 1 s. Again, increasing pulse number correlated with increasing $[5\text{-HT}]_{max}$ (Figure 5.1E; $F(4,24)=18.49$, $P<0.0001$). This confirms that evoked release can be manipulated by varying stimulation pulse number, but not frequency.

To determine what aspects of signaling contributed to lack of frequency-dependence, we examined how stimulation frequency affected release rate, $t_{1/2,}$ (a measure of uptake; Yorgason, Espana, & Jones, 2011) and net overflow in serotonin concentration traces. We found no effect of frequency on $t_{1/2}$ (Figure 5.1G). This was expected, as clearance rate should be unaffected by physiological stimulation. However, although stimulation frequency should directly correlate to the rate of neurotransmitter release (R.M. Wightman et al., 1988), no differences were observed in evoked release rate (Figure 5.1F). The consequence of this frequency insensitivity is that net overflow evoked by 20-60 Hz stimulations is identical (Figure 5.1H), such that in this range of frequencies, transient increases in extracellular serotonin do not differ.

SERT inhibition enhances serotonin release in a frequency-dependent manner

We then looked at the effects of CIT (10 mg/kg, i.p.) on serotonin dynamics. Unexpectedly, after CIT treatment, $[5\text{-HT}]_{max}$ was significantly affected by stimulation frequency *in vivo* (Figure 5.2A; repeated measures ANOVA, $F(4,20)=16.56$, $P<0.0001$). To confirm that this effect of CIT was not due to a non-selective effect of the drug, we administered CIT in mice whose copies of SERT (Slc6a4) had been genetically deleted (SERT-/- mice). Baseline serotonin release in SERT-/- mice was also frequency-independent, and CIT had no effect on $[5\text{-HT}]_{max}$ or $t_{1/2}$ in SERT-/- mice at any frequency. Moreover, serotonin release evoked by 20 Hz stimulations looked nearly identical to CIT-treated wild-type mice (Figure 5.2B). This suggests that the dosage of citalopram in these experiments is sufficient to saturate SERT. Tellingly, $[5\text{-HT}]_{max}$ is significantly enhanced in CIT-treated wild-type mice compared to SERT-/- mice (Figure 5.2C). This suggests that acute SERT inhibition has an excitatory, frequency-dependent effect on serotonin signaling.

After we confirmed that CIT effects on $[5\text{-HT}]_{max}$ were selective for SERT, we examined concentration traces in wild-type mice to determine what aspects of neurotransmission contributed to frequency-dependent differences. Across all stimulation frequencies, $t_{1/2}$ was consistent. However, rate of evoked release varied significantly with stimulation frequency (Figure 5.2C; repeated measures ANOVA, $F(5,20)=24.18$, $P<0.0001$), suggesting that acute CIT treatment unexpectedly modified regulation of serotonin release. As a result of this enhancement in release rate, net evoked release is also frequency dependent (Figure 5.2E, repeated measures ANOVA, $F(5,20)=18.16$, $P<0.0001$). The finding that CIT enhances serotonin signaling in a frequency-dependent manner has not been previously reported and may be a major component of its therapeutic efficacy.

Inhibiting SERT in DRN enhances serotonin release in a frequency-dependent manner

Data presented above shows effects of CIT and other uptake inhibitors on $[5\text{-HT}]_{max}$ and $t_{1/2}$ after the effects of the drug have stabilized. For example, after 30 minutes, CIT effects are stable and remain consistent for up to 2 hours. However, the onset of CIT effects follows an interesting pattern that provides additional insights concerning its release-enhancing mechanisms. To characterize CIT onset, 60 Hz, 1 s stimulations were applied at 2 minute intervals and changes in $[5\text{-HT}]_{max}$ and $t_{1/2}$ relative to pre-drug release were determined. Figure 4A compares the response of these measurements for the first 16 minutes following CIT exposure. While $t_{1/2}$ does not increase for up to 12 minutes after SSRI exposure, $[5\text{-HT}]_{max}$ doubles within the first 6 minutes. Representative traces illustrating the separate effects on $[5\text{-HT}]_{max}$ and $t_{1/2}$ can be seen in Figure 5.3B. The apparent disassociation of changes in $[5\text{-HT}]_{max}$ from $t_{1/2}$ suggests that the acute effects of CIT on serotonin release may occur in a different anatomical location from where we measured uptake. Since we do not observe effects on $[5\text{-HT}]_{max}$ in brain slices, where serotonergic terminals are severed from cell bodies, we hypothesized that high-affinity SERT inhibition in the DRN contributed to these excitatory effects.

To test whether the DRN mediated CIT effects on $[5\text{-HT}]_{max}$ in the SNpr, we microinfused saline (μ-SAL) or CIT (μ-CIT) directly into the DRN and compared the effect of stimulation frequency on evoked release (Figure 5.3C). To confirm that CIT microinfusions did not access the cerebral aqueduct, which would enable drug to spread rapidly throughout the brain, we compared $t_{1/2}$ of serotonin release evoked by 60 Hz stimulations between μ-SAL and μ-CIT. No difference between μ-SAL and μ-CIT were

observed at baseline or in their response to i.p. CIT (10 mg/kg). Thus, microinfusions were limited to a localized area and did not alter SERT activity in the SNpr.

Next, we compared $[5\text{-HT}]_{max}$ evoked by varying stimulation frequencies. There was no effect of stimulation frequency in μ-SAL mice. However, there was a significant effect of stimulation frequency in μ-CIT mice (Figure 5.3D; repeated measures ANOVA, $F(2,8)=11.62$, $P<0.01$). When we compared μ-CIT with μ-SAL, there was a significant effect of treatment (repeated measures ANOVA, $F(1,16)=12.58$, $P<0.05$) and frequency x treatment interaction ($F(4,16)=10.10$, $P<0.001$). Post-hoc analyses revealed significant differences between $[5\text{-HT}]_{max}$ at 40 Hz ($P<0.05$), 50 Hz ($P<0.01$), and 60 Hz ($P<0.001$).

Discussion

Under normal conditions, serotonin signaling is under robust regulation from multiple inhibitory elements. The extent of this regulation is illustrated by a nearly 50-fold difference between serotonin concentrations evoked in brain slices vs. *in vivo* in the SNpr (Bunin et al., 1998; Hashemi et al., 2011; John & Jones, 2007a). This difference implies that some elements controlling serotonin release require intact circuitry. In spite of limited release, uptake by SERT remains relatively similar between *in vivo* and brain slice preparations (Daws & Toney, 2007). Since uptake that occurs during and between stimulus pulses shapes dynamic release as well as maximal evoked concentrations (R.M. Wightman et al., 1988), similarities in SERT function predict similarities in frequency-dependent release. As predicted by this model, in brain slices, $[5\text{-HT}]_{max}$ is frequency-dependent (Bunin & Wightman, 1998; Iravani & Kruk, 1997; O'Connor & Kruk, 1991b). Surprisingly, stimulation frequency did not affect serotonin release *in vivo* (Figure 5.1), even though other measures of stimulation intensity correlate well to findings in slices (Figure 5.1C-D). However, this result

is not totally unfounded in our understanding of serotonergic function. Serotonergic neurons in the DRN predominantly fire at a rate of 1-5 Hz (Pineyro & Blier, 1999). Burst-firing can occur at frequencies up to 100 Hz (Hajos et al., 1995), but its prevalence is correlated with behavioral arousal (Jacobs, 1991; Jacobs & Fornal, 1999). GABAergic inputs to the DRN are also behavioral state-dependent and may contribute to limitations in firing rate (Levine & Jacobs, 1992). Lack of frequency-dependence may reflect serotonergic function during low-arousal states, a theory consistent with our anaesthetized preparation.

Models of neurotransmission predict that slower stimulation frequencies will be most affected by changes in transporter function, because uptake occurs for a longer proportion of their release period (Wightman & Zimmerman, 1990). In our experiments, $[5\text{-HT}]_{max}$ and release rate were unaffected by stimulation frequency, so we anticipated that SERT inhibition would have similar effects on $[5\text{-HT}]_{max}$ across all stimulation frequencies. Instead, CIT enhanced serotonin release in a frequency-dependent manner, with the highest $[5\text{-HT}]_{max}$ and release rate occurring at 50 Hz or 60 Hz in all subjects (Figure 5.2A). Interestingly, at high frequencies, CIT treatment enhanced serotonin release in wild-type mice compared to SERT-/-. This suggests that frequency-dependent effects on release may not be a direct effect of reduced clearance in the SNpr, but due to SERT-mediated changes elsewhere. Differences in frequency sensitivity between CIT-treated wild-type *vs.* SERT-/- mice likely reflect developmental compensations for SERT deletion, potentially in autoreceptor populations and secondary transport systems (Gobbi, Murphy, Lesch, & Blier, 2001; Thompson et al., 2011). We have previously shown that loss of DAT expression significantly alters autoreceptor function (Jones et al., 1999).

In all wild-type mice, CIT effects on $[5\text{-HT}]_{max}$ preceded effects on $t_{1/2}$ (Figure 5.3A). This effect of CIT has not previously been shown because it can only be measured using a technique with temporal and spatial resolution commensurate with neurotransmission, such as FSCV. It suggests that SSRI-induced changes in release are dissociable from changes in uptake. Since CIT exposure does not affect $[5\text{-HT}]_{max}$ in brain slices, where terminal release sites are severed from their neurons, we hypothesized that CIT effects on $[5\text{-HT}]_{max}$ *in vivo* were mediated in the DRN. Using microinjections targeted to the DRN, we found CIT effects on $[5\text{-HT}]_{max}$ were indeed mediated by the DRN, while its effects on uptake were not (Figure 5.3). One possible mechanism for SERT-selective effects of CIT on release is desensitization of autoreceptors. Although desensitization is classically thought to occur after 3-6 week exposure to SSRIs, 5-HT1a receptors can rapidly internalize after acute exposure to SSRIs or 5-HT1a agonists (Riad, Watkins, Doucet, Hamon, & Descarries, 2001; Riad et al., 2004). In the case of acute SERT inhibition, 5-HT1a receptors may desensitize as a response to extremely high local serotonin levels, enabling faster firing rates. Alternatively, acute SERT inhibition may maximally activate autoreceptors and other 5-HT-mediated inhibitory circuitry, creating a "ceiling effect" for inhibitory control. Under normal conditions, inhibitory control probably upregulates in response to excitatory inputs to the DRN. However, SSRIs have substantial effects on serotonin signaling in the DRN (Bunin et al., 1998). CIT acutely increases serotonin levels 400% in the DRN, compared to approximately 200% in other forebrain regions (R. Invernizzi et al., 1992). If rising ambient serotonin levels maximize inhibitory feedback, unchecked responses to excitatory input would result in dramatic enhancements to transient serotonergic activity. This could explain paradoxical findings that acute SSRI treatment induces activity-dependent increases brainwide serotonin

levels and simultaneously prohibit serotonergic firing (Gartside et al., 1995; Hajos et al., 1995; Perry & Fuller, 1992).

In this work, we demonstrate novel properties of serotonin signaling and its response to SERT inhibition that have implications for the clinical efficacy of SSRIs. First, we show that serotonin release is not frequency-dependent *in vivo*. Although this finding was not expected based on prior voltammetric studies in brain slices, it may reflect behavioral state-dependent regulation of serotonin signaling. Our experimental method may model serotonin signaling during low-arousal states, where regulation of serotonergic signaling may be most robust. Next, we showed that SSRIs induce frequency-dependent release by selectively inhibiting SERT function, suggesting that serotonergic burst-firing is enabled after acute SSRI use. The ability to burst-fire in states of low arousal may underlie certain side effects of SSRI treatment, such as irregular sleep patterns (Bridoux, Laloux, Derambure, Bordet, & Monaca Charley, 2013; Katai et al., 2013). Finally, we found that the effects of SSRIs on forebrain release, but not uptake, were mediated by their effects in the DRN. SSRI-induced changes in ambient serotonin levels and enhancement of serotonin signaling related to burst-firing may coordinate during treatment to produce antidepressant outcomes. Acute increases in burst-firing may be masked by increases in ambient serotonin levels. However, as these levels normalize over the chronic treatment period, enhancements in serotonin release may register as larger, clearer signals throughout the brain. Therefore, a better understanding of how SSRIs can rapidly modify regulation of serotonergic activity may lead to more effective therapies for depression and related disorders.

Support

Douglas Kirkpatrick and Dr. Susan Carroll contributed data to this chapter. The authors would like to acknowledge technical support from the UNC Electronics Facility and Meg Fox, Nina Owesson-White, and Anna Belle for helpful methodological discussions.

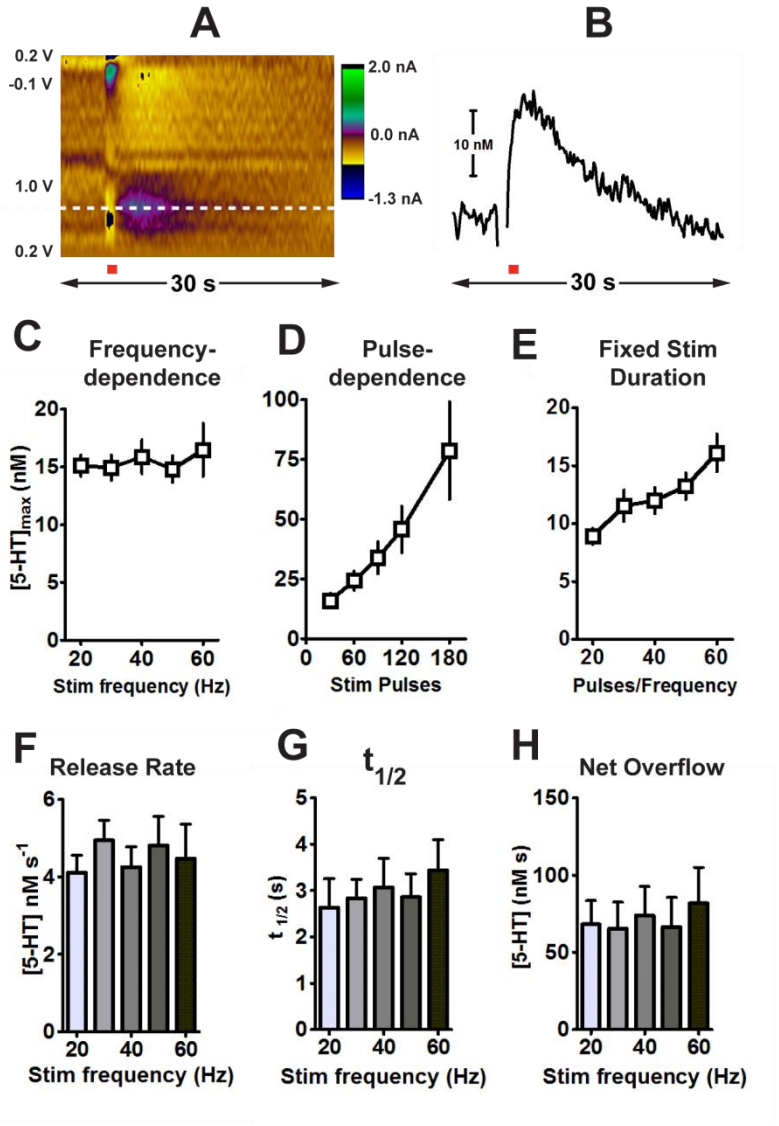

Figure 5.1 Serotonin release is not frequency-dependent *in vivo*. (A) Representative color plot showing serotonin release evoked in SNpr by a 60 Hz, 1 s stimulation of DRN. Color plot shows time (x-axis) vs. voltage waveform potential (y-axis), with change in current plotted in pseudocolor. Stimulus duration indicated by red bar. Peak oxidation potential for serotonin indicated by white dashed line. (B) Concentration trace obtained at the oxidation potential for serotonin and calculated using an *in vitro* post-calibration factor. Stimulus duration indicated by red bar. (C) Average $[5\text{-HT}]_{max}$ for 60 pulse stimulation trains applied at 20- 60 Hz (n=6). (D) Average $[5\text{-HT}]_{max}$ for stimulation pulse trains 30, 60, 90, 120, and 180 pulses in length (n=5). (E) Average $[5\text{-HT}]_{max}$ to stimulations of 1 s duration (n=7). (F) Average rate of change in serotonin concentration evoked by 60 pulse stimulation trains applied at 20- 60 Hz (n=6). (G) Average clearance half-life for these stimulations (n=6). (H) Average net overflow (area under concentration trace) of evoked serotonin release (n=6).

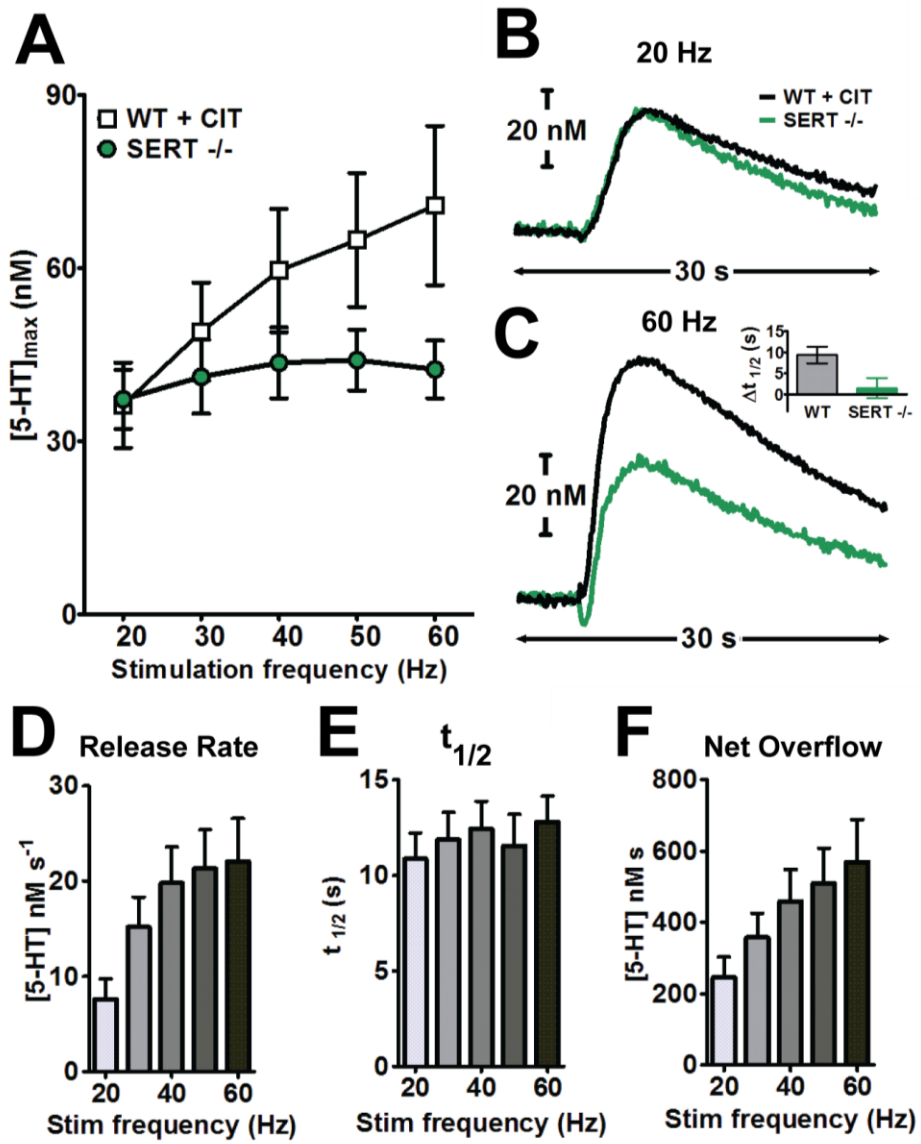

Figure 5.2 Inhibiting SERT induces frequency-dependent serotonin release. (A) Average [5-HT]$_{max}$ of CIT-treated WT (white squares) and SERT-/- mice (green circles) evoked by 60 pulse stimulations ranging from 20-60 Hz. (B) Average concentration trace showing serotonin release evoked by 20 Hz stimulations in CIT-treated WT or SERT-/- mice. (C) Average concentration trace showing serotonin release evoked by 60 Hz stimulations in CIT-treated WT (black) or SERT-/- mice (green). Inset shows change in clearance half-life compared to pre-drug values. (D) Rate of serotonin release evoked in WT mice by stimulations varying in frequency from 20-60 Hz. (E) Clearance half-life of serotonin release evoked by stimulations of varying frequency. (F) Net overflow of serotonin release evoked by stimulations of varying frequency. (WT, n=6; SERT-/-, n=5)

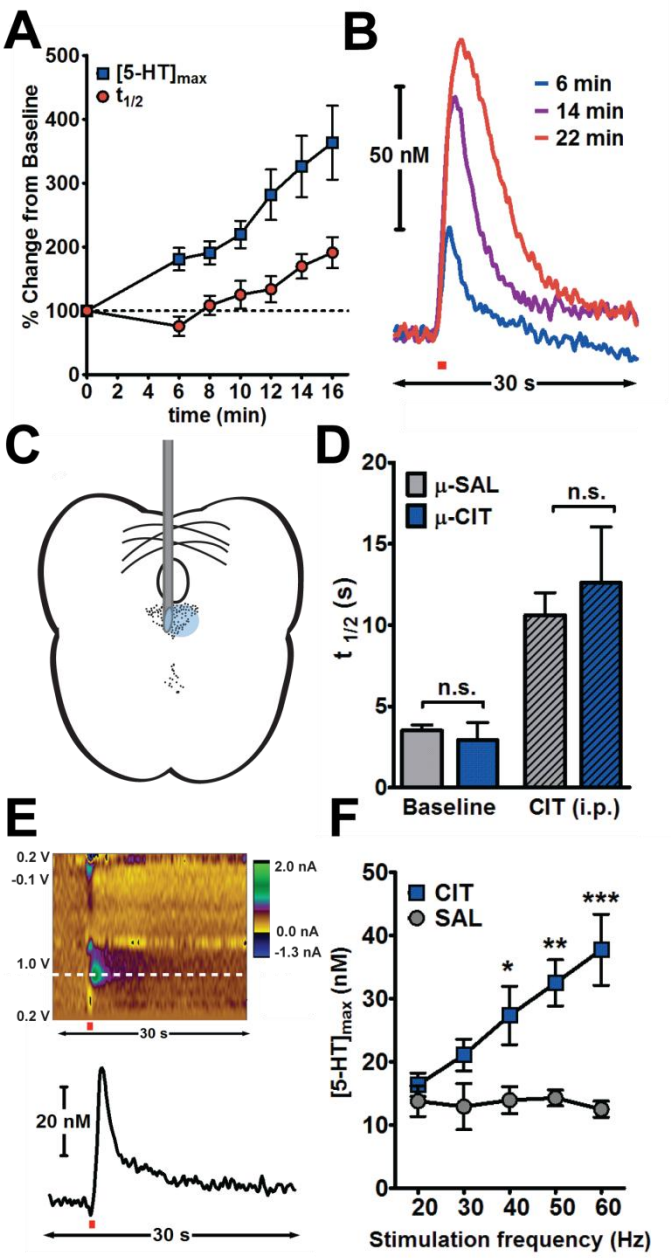

Figure 5.3 DRN mediates enhancement of serotonin signaling by SSRIs. (A) Average response of $[5\text{-HT}]_{max}$ (blue squares) and $t_{1/2}$ (red circles) to acute CIT treatment. Values shown are percent increase from pre-drug release. (B) Representative concentration traces showing serotonin release 6 minutes, 14 minutes, and 22 minutes after acute CIT treatment. Red bar indicates stimulus duration. (C) Illustration showing targeting of the DRN for microinfusions of CIT. (D) Representative color plot (top) and concentration trace (bottom) showing serotonin release evoked by 60 Hz, 1 s stimulation after microinfusion of CIT into DRN. (E) Comparison of average $t_{1/2}$ in saline microinfused (gray) and CIT microinfused subjects (blue) before and after acute CIT challenge (10 mg/kg, i.p.). (F) Average response of $[5\text{-HT}]_{max}$ in saline microinfused (gray circles) and CIT microinfused (blue squares) subjects.

CHAPTER 6: FACILITATION OF SEROTONIN SIGNALING BY SSRIs IS ATTENUATED BY SOCIAL ISOLATION

Introduction

Disorders involving depression and anxiety, including major depression and obsessive compulsive disorder (OCD), have high rates of comorbidity and are frequently attributed to hypofunction of the serotonergic system (Bespalov, van Gaalen, & Gross, 2010; Jacobsen et al., 2012). The most commonly prescribed medications in the treatment of depression and OCD are selective serotonin reuptake inhibitors (SSRIs), which inhibit serotonin's transporter (SERT). Acute SERT inhibition increases brain-wide serotonin levels and depresses firing of serotonergic neurons (Blier & de Montigny, 1998). Clinically, 3-6 weeks of continuous SSRI treatment are required before symptoms of depression and OCD begin to improve (de Montigny, Pineyro, Chaput, & Blier, 1992). This gap between treatment onset and therapeutic response suggests that the mechanism by which SSRIs exert anti-depressive and anxiolytic effects is not only due to an increase in ambient serotonin, but to an adaptive response in neural systems to sustained increases in serotonin levels. Indeed, a multitude of changes in gene expression, receptor sensitivity, neurochemical signaling, and functional activity coincide with the therapeutic window of SSRI therapy (Bespalov et al., 2010; Blier & de Montigny, 1998; de Montigny et al., 1992).

Although it is common to treat depression and OCD with SSRIs, the effectiveness of the treatment is also notoriously variable between individuals. Reports estimate that over 60% of depressed individuals and 40-60% of individuals with OCD are resistant to

improvement while on SSRI therapy (Brandl, Muller, & Richter, 2012; Gaynes et al., 2008). Depressed individuals with comorbid anxiety disorders have poorer outcomes on all types of antidepressant medication when compared with non-anxious depressed individuals (Fava et al., 2008). The serotonergic system is highly sensitive to stress, and genetic variability in its function contributes to stress resilience and responsiveness to SSRI therapy (Chaouloff, Berton, & Mormede, 1999; Oreland, Nordquist, Hallman, Harro, & Nilsson, 2010; Uher, 2011). Clinical research suggests that ongoing stress, including the absence of social support networks, can contribute to treatment-resistant depression and anxiety (Karelina & DeVries, 2011).Thus, improving pharmacotherapies for depression and OCD will likely require an understanding of how stress and anxiety interact with SSRI treatments. Social isolation is a form of chronic mild stress that replicates naturalistic environmental stressors for rodents and has been suggested as an animal model for depressive disorders (Nestler & Hyman, 2010; Wiborg, 2013). In mice, social isolation significantly upregulates the function of the hypothalamic-pituitary-adrenal (HPA) axis, altering levels of glucocorticoid (Ferres-Coy et al.) and corticotropin releasing factor (CRF) in various brain regions (Backstrom & Winberg, 2013; Blanchard, McKittrick, & Blanchard, 2001; Valzelli, 1973). The HPA axis also regulates serotonin signaling and the effects of antidepressants (Barden, 1996, 2004; Pariante & Miller, 2001). Understanding how social isolation alters serotonin signaling in mice, particularly in response to SSRIs, may provide clues about how stress influences treatment-resistant depression and OCD.

SSRI treatment changes serotonin metabolism, receptors, and transporters in a way that that could facilitate serotonergic activity. However, prior to this work, the effects of chronic SSRIs on endogenous *in vivo* serotonin release and uptake have not been reported.

We used fast-scan cyclic voltammetry (FSCV) to monitor serotonin signaling and alterations in its dynamics induced by chronic citalopram (CIT). FSCV is an electrochemical method with sufficient chemical resolution necessary to detect serotonin (Hashemi et al., 2009) and sufficient temporal resolution to resolve the processes of release from neuronal uptake (Hashemi et al., 2012). We have established that FSCV can monitor serotonin release *in vivo*, specifically in the substantia nigra *pars reticulata* (SNpr), which receives a dense serotonergic projection from the dorsal raphe nucleus (DRN). Here, we use FSCV to evaluate the effects of 20-day CIT exposure on serotonin signaling in pair-housed and single-housed mice. We found robust behavioral and neurochemical differences in the effects of SSRI treatment between these groups.

Materials and Methods

Animals

All experiments were performed in compliance with the University of North Carolina at Chapel Hill (UNC) Institutional Animal Care and Use Committee. Subjects were C57BL/6J male mice (4-5 weeks in age and 20-27 g at arrival from Jackson Laboratory, Bar Harbor, ME), initially housed in groups of 4. After one week of acclimation, 40 mice were housed individually, and 36 mice were housed in pairs. All subjects were kept on a 12-hour-day/light cycle and given *ad libitum* access to food and water.

Chronic CIT Treatment

To eliminate stress contribution from daily injections, citalopram hydrobromide (CIT; Roxane Laboratories) or vehicle (VEH) was administered via water bottles for 20 days. Briefly, water consumption was monitored for 7 days to establish a baseline for each subject

or pair of subjects. The concentration of CIT added to water during the treatment period was adjusted to 15 mg/kg/day (per oral) based on subject weights and previous-day consumption volumes throughout treatment. CIT was obtained in a sweetened oral solution formulation; therefore, VEH-treated animals received water containing D-Sorbitol (1.68 g/5 mL; Sigma Aldrich) to match the concentration of CIT solution. Comparisons of overall consumption can be found in **Supplemental Figure 1A-B**. On day 21, treatment was discontinued, and mice were given bottles containing only water.

Marble-Burying Assay

On day 21, 20 marbles were arranged in a 4 x 5 grid in a (34 x 20.5 x 13.5 cm) cage containing 5 cm of bedding. Mice were placed inside the cage for 30 minutes, after which the number of buried marbles (<2/3 visible above bedding) were counted.

Open field test

4-5 hours following the marble-burying assay on day 21, mice were evaluated for activity in an open field chamber (41 x 41 x 30 cm) crossed by a grid of photobeams (VersaMax system, AccuScan Instruments). Counts were taken of the number of photobeams broken during the trial in 5-minute intervals across one hour, with separate measures for total distance traveled, fine movements (repeated breaking of the same set of photobeams), and rearing movements (vertical activity). Time spent in the center region of the open field was also recorded.

Detection of Evoked 5-HT Release

24 hours after withdrawal of CIT or VEH solutions, mice were evaluated for CIT-induced changes in electrically-evoked serotonin release, using previously described methods (Hashemi et al., 2009). See Supplemental Information for more details.

Drugs and Reagents

Citalopram hydrobromide (obtained as oral solution, 10 mg/5 mL; Roxane Laboratories) was diluted in sterile saline (0.9%) for acute administration, or diluted with water for chronic treatment. Nomifensine maleate salt and urethane (Sigma-Aldrich, St. Louis, MO) were dissolved in sterile saline (0.9%). Intraperitoneal-injected drugs (for acute treatments) were administered at a volume of 0.01 mL/g body weight. All reagents were purchased from Sigma-Aldrich and used as received.

Data analysis

Results are average values ± SEM. Behavioral data were analyzed using a 2-way or repeated measures ANOVA with Bonferroni post-hoc analyses. Trends in maximum evoked amplitude ($[5\text{-HT}]_{max}$) were analyzed using a repeated measures ANOVA with Sidak multiple comparisons post-hoc analysis.

Release rate was calculated by fitting lines to the rising phase of serotonin release for each stimulation frequency (for each subject). Clearance half rate ($t_{1/2}$) was calculated in Clampfit (Molecular Devices, LLC, USA) as the decay time between 100% and 50% evoked concentration for each subject and averaged. Net overflow was calculated in Clampfit using the integral under the curve for the first 15 seconds following the stimulation event for each

stimulation frequency (for each subject). $t_{1/2}$ and net overflow analyses have been shown to correlate well with kinetic models of neurotransmitter release (Yorgason et al., 2011). Groups were compared using a 2-way ANOVA with Bonferroni post-hoc analysis.

To verify whether evoked serotonin release was frequency-dependent, $[5\text{-HT}]_{max}$ evoked at each stimulation frequency was normalized within-subjects to $[5\text{-HT}]_{max}$ evoked by 20 Hz stimulations. A line was fit to each group of normalized values and a hypothesis test determined whether the regression coefficient (slope) was significantly different from zero. Treatment groups described as having frequency-dependent release meet criteria by having a slope that is significantly different from zero.

Results

Electrical stimulation of the dorsal raphe nucleus evokes serotonin release in the substantia nigra pars reticulata

To verify the chemical origin of signals measured using our recording electrode coordinate, we tested the acute effects of a norepinephrine/dopamine uptake inhibitor (nomifensine, 5 mg/kg, i.p.) and an SSRI (CIT, 10 mg/kg, i.p.) on evoked release. In previous studies, a similar nomifensine dosage had robust effects on dopamine signals but was low enough to avoid non-selective effects (Robinson & Wightman, 2004). Likewise, the selected CIT dosage has been used with robust results on serotonin signaling in prior studies (Hashemi et al., 2012; Hashemi et al., 2009). Color plots and traces show serotonin release at baseline (Figure 6.1A), unaltered 30 minutes after nomifensine (Figure 6.1B), and increased in amplitude and $t_{1/2}$ 30 minutes after CIT (Figure 6.1C). This response pharmacologically confirms that signals measured at this location are serotonergic, without

contribution from catecholamines. Representative histology shows the location of the stereotaxic coordinate used for carbon-fiber electrode placement (Figure 6.1D). Because electrolytic lesions from Nafion-coated carbon-fiber microelectrodes are difficult to locate, we did histology following electrolytic lesions with tungsten wires at the same stereotaxic coordinate. Inset shows the contralateral SNpr, illustrating its dense serotonergic terminal field.

Anxiety-like behavior is reduced by chronic CIT treatment

We selected the treatment period and dosage for chronic citalopram (cCIT) based on prior studies that used oral SSRI administration and found robust neurochemical effects (Davidson & Stamford, 1997a, 2000). We used the marble-burying assay, a standard index of anxiety-like behavior, since previous studies had found that chronic SSRI treatment in mice leads to reductions in buried marbles (Arora et al. 2013; Ichimaru et al. 1995). We also performed an open field test for CIT effects on overall activity, as well as additional measures of anxiety-like behavior (Jiao, Nitzke, Doukas, Seiglie, & Dulawa, 2011; Strekalova et al., 2013).

In line with previous reports (Arora, Bhowmik, Khanam, & Vohora, 2013; Ichimaru, Egawa, & Sawa, 1995), we found that cCIT decreased the number of marbles buried (Figure 6.2A). These effects of SSRI treatment were only significant in paired-housed, and not single-housed, mice (post-hoc analyses following 2-way ANOVA, main effect of treatment, $F(1,72)=9.7$, $P<0.01$). In the OF test, cCIT did not significantly affect general locomotion in either housing group (Figure 6.2B-C), confirming previous findings on CIT effects in C57BL/6 mice (Jiao et al., 2011; Strekalova et al., 2013). However, cCIT led to highly

significant decreases in time spent in the center region of the open field, in comparison to VEH (Figure 6.2D; main effect of treatment, $F(1,72)=19.0$, $P<0.0001$). cCIT also led to mild reductions in fine movements, an index of repetitive and stereotyped behavior (Figure 6.2E; main effect of treatment, $F(1,72)=10.0$, $P<0.01$). Rearing movements, another measure of active exploration in the open field, were decreased by cCIT, although this effect was only significant in the pair-housed mice (Figure 6.2E; post-hoc analyses following main effect of treatment, $F(1,68)=9.5$, $P<0.01$). Overall, cCIT had anxiolytic effects in the marble-burying assay, but not in the OF test, with more significant effects in the pair-housed mice.

cCIT increases serotonin release in pair-housed mice

Serotonin release exhibits robust dependence on stimulation frequency when examined in brain slices (Dankoski & Wightman, 2013) . This is the result of uptake occurring throughout stimulation pulse trains and has been described using Michaelis-Menten models of neurotransmission (Bunin et al., 1998; Dreyer, Herrik, Berg, & Hounsgaard, 2010). Table 6.1 compares maximal release ($[5\text{-HT}]_{max}$) evoked by a range of stimulation frequencies (20-60 Hz, 60 pulses each). In marked contrast to the slice results, we found that *in vivo* serotonin signaling was not frequency-dependent under baseline conditions. No significant effect of cCIT or frequency was found when comparing $[5\text{-HT}]_{max}$ in single-housed mice. However, cCIT increased $[5\text{-HT}]_{max}$ in pair-housed mice (repeated measures ANOVA, main effect of treatment, $F(1,12)=5.4$, $P<0.05$), with main effects of stimulation frequency ($F(4,48)=3.9$, $P<0.01$), as well as a treatment x frequency interaction ($F(4,48)=5.9$, $P<0.001$). Post-hoc analysis revealed significant differences at 50 Hz and 60 Hz ($P<0.05$).

After an acute CIT challenge (Table 6.1, bottom), the effects of cCIT in pair-housed mice were maintained and intensified (repeated measures ANOVA; main effect of treatment, $F(1,12)=9.8$, $P<0.01$; frequency, $F(4,48)=68.9$, $P<0.0001$, and treatment x frequency interaction, $F(4,48)=7.6$, $P<0.0001$). Post-hoc analyses revealed differences between VEH and cCIT pair-housed mice at stimulus frequencies of 30 Hz, 40 Hz (both at $P<0.05$), 50 Hz, and 60 Hz (both at $P<0.01$). Changes in $[5\text{-HT}]_{max}$ are not correlated with a change in local serotonin content (Figure 6.S1C). Therefore, functional changes in neurotransmission must underlie the effects of cCIT treatment.

Increased $[5\text{-HT}]_{max}$ in cCIT pair-housed mice is due to facilitation of release

To determine what underlies changes in $[5\text{-HT}]_{max}$, we analyzed the rate of release, clearance half-life ($t_{1/2}$), and net overflow in serotonin concentration traces evoked by 60 Hz, 1s stimulations (Figure 6.3). Figure 6.3A-B shows average concentration traces of serotonin release at 60 Hz (concentration traces for all stimulation frequencies are in Figure 6.S2). cCIT treatment increased release rate (2-way ANOVA, main effect of treatment $F(1,25)=6.1$, $P<0.05$), and there was an interaction between treatment and housing ($F(1,25)=4.6$, $P<0.05$) (Figure 3C). Post-hoc analysis revealed differences in 60 Hz release rate between pair-housed VEH and cCIT mice (7.4 ± 1.1 nM s^{-1} *vs* 19.2 ± 3.1 nM s^{-1}, n=6 and n=8, respectively, $p<0.01$), but not between single-housed VEH and cCIT mice.

Surprisingly, clearance ($t_{1/2}$) of evoked serotonin was unaltered by housing or cCIT treatment (Figure 6.3D). This demonstrates that increases in $[5\text{-HT}]_{max}$ (Table 6.1) were due to facilitation of release following cCIT treatment. Similar results have been obtained in previous voltammetric studies (Davidson & Stamford, 1997a, 2000); however, our result

conflicts with the work of Benmansour et al. (1999), who found that baseline SERT function was impaired by chronic SSRI treatment. Their study was conducted in the hippocampus and measured SERT function using high concentrations of exogenously applied serotonin, critical differences which may explain this discrepancy.

In the present study, cCIT increased net overflow (Figure 6.3E, 2-way ANOVA, $F(1,25)=6.6$, $P<0.05$) and post-hoc analysis showed differences between VEH and CIT treatment in pair-housed (0.11 ± 0.02 µM s *vs* 0.22 ± 0.04 µM s, n=6 and n=8, respectively, $P<0.05$) but not single-housed mice. Additional post-hoc analysis comparing effect of housing found differences between cCIT single- *vs* pair-housed mice (0.14 ± 0.01 µM s *vs* 0.22 ± 0.04 µM s, n=9 and n=8, respectively, $P<0.05$). Taken together, these data show that facilitation of serotonin release is a major contributor to the enhanced serotonergic neurotransmission in pair-housed cCIT mice, whereas uptake is unaffected.

Because differences in release rate and $t_{1/2}$ were only apparent in release evoked by higher-frequency stimulations, we developed an assay to quantitatively establish frequency-dependence, described in **Methods**. Only serotonin release in pair-housed cCIT mice met the criteria for frequency-dependence (Figure 6.3F; hypothesis test for regression slope, $F(1,38)=14.4$, $p<0.001$). Frequency-dependent facilitation in pair-housed cCIT mice is a major shift in the dynamic regulation of serotonin release.

Acute uptake inhibition enhances facilitation of serotonin release in cCIT pair-housed mice

Next, we examined how cCIT treatment altered responses to CIT itself (Figure 6.4). Mice were withdrawn from CIT or VEH for 24 hours, sufficient to metabolize all remaining drug (Fredricson Overo, 1982). An acute challenge dose of CIT (10 mg/kg, i.p.) was

administered at the end of each experiment. Differences in uptake are evident when comparing average concentration traces evoked by 60 Hz, 60 pulse stimulations (Figure 6.4A-B). In all groups, $t_{1/2}$ increased, but to a lesser extent in cCIT mice (2-way ANOVA, $F(1,25)=7.4$, $P<0.05$) (Figure 6.4D). This finding concurs with Benmansour et al. (1999), who found that SERT function was less responsive to uptake inhibitors after chronic SSRI treatment.

Post-hoc analysis revealed differences in release rate between pair-housed VEH and cCIT mice (14.3 ± 2.5 nM s^{-1} *vs* 26.9 ± 3.8 nM s^{-1}, n=6 and n=8, respectively, $p<0.05$) (Figure 4C). Acute CIT also increased net overflow in cCIT mice (main effect of treatment, $F(1,25)=6.0$, $P<0.05$), with significant main effect of housing ($F(1,25)=4.50$, $P<0.05$) and a treatment x housing interaction ($F(1,25)=8.5$, $P<0.01$) (Figure 6.4E). Post-hoc analysis of net overflow revealed differences between VEH and cCIT in pair-housed mice (0.53 ± 0.06 µM s *vs* 1.13 ± 0.15 µM s, n=6 and n=8, respectively, $P<0.01$) and also between single- and pair-housed cCIT mice (0.57 ± 0.09 µM s *vs* 1.13 ± 0.15 µM s, n=9 and n=8, respectively, $P<0.01$). The overall increase in release rate and net overflow after acute CIT was expected, due to SSRI-induced reductions in uptake (Wightman & Zimmerman, 1990). Consistent with this, release rates measured in the various groups of mice varied in proportion to the pre-CIT release rates, and differences were still only observed in pair-housed mice.

We used a hypothesis test to quantitatively confirm frequency-dependence following acute CIT. Frequency-dependence was determined for all groups (Figure 6.4F, hypothesis test for regression slope; VEH-single, $F(1,28)=182.4$, $p<0.0001$; CIT-single, $F(1,38)=25.9$, $p<0.0001$; VEH-pair, $F(1,28)=96.2$, $p<0.0001$; CIT-pair, $F(1,43)=84.5$, $p<0.0001$). Although

all groups showed frequency-dependence following acute CIT, the magnitude of release at all frequencies was much greater in cCIT-treated paired animals (Table 6.1, bottom).

Discussion

Though SSRIs are commonly prescribed to treat disorders involving depression and anxiety, the mechanisms by which these agents exert therapeutic effects are not clear. Prior studies have examined how chronic SSRI treatment affects the serotonin system, but this is the first to compare effects of SSRI treatment on endogenous, *in vivo* release dynamics. Furthermore, this study directly addresses the interaction of social environment with serotonergic function in this context. Here, we found distinct differences in the effects of chronic SSRI treatment on serotonin signaling in single- *vs* pair-housed mice. We describe a novel effect of this treatment—the facilitation of serotonin signaling in a frequency-dependent fashion—and the ability to attenuate this outcome with concurrent social isolation.

Levels of neurotransmitter in the extracellular space are determined by a dynamic equilibrium between release and uptake (Dreyer et al., 2010). Previously, we reported that disruptions of serotonergic equilibria can be fatal, and release and uptake are both tightly controlled to maintain this balance (Hashemi et al., 2012). Further evidence of this control can be seen in Table 6.1 and Figure 6.3F: *in vivo* release is insensitive to the rate of stimulation. Spontaneous serotonergic burst-firing does occur during distinct behavioral states (Gartside et al., 2000; Jacobs, 1991);. Furthermore, serotonin neurons have the capacity for frequency-dependent release as measured in brain slices (Dankoski & Wightman, 2013), likely because inhibitory feedback from intact serotonergic neurons and other neuromodulatory systems are severed during slice preparation. Multiple inhibitory systems preserve the pacemaker-like firing (1-5 Hz) of serotonergic neurons. For instance,

somatodendritic 5-HT1a autoreceptors profoundly limit the firing rate of serotonergic neurons (Blier et al., 1998), and the DRN also receives complex feedback from prefrontal cortex (Celada, Puig, Casanovas, Guillazo, & Artigas, 2001).

Following chronic CIT treatment, $[5\text{-HT}]_{max}$ was frequency-dependent in pair-housed mice (Table 6.1). Our analysis showed this was due to increases in release rate, not $t_{1/2}$ (Figure 6.3C-D). Thus, cCIT increases the responsiveness of serotonergic neurons to higher stimulation frequencies. This could arise from 5-HT1a autoreceptor desensitization, a process that is well-documented following chronic SSRI exposure and is a critical component of their antidepressant effects (Celada, Bortolozzi, & Artigas, 2013; Ferres-Coy et al., 2013). Frequency-dependent signaling in cCIT-treated, pair-housed mice could arise from the suppression of autoreceptor feedback and would be a functional consequence of their desensitization. Even at low frequencies, cCIT substantively enhanced release in pair-housed mice after the acute CIT challenge. This indicates that during chronic treatment, baseline increases in release are intensified by ongoing uptake inhibition and may occur at low (1-5 Hz) firing rates. Increased release allows greater interaction of extracellular serotonin with its post-synaptic targets.

It could be hypothesized that chronic mild stress experienced by single-housed C57BL/6J mice would produce a depressive phenotype and intensify the effects of cCIT treatment when compared with VEH-treated counterparts. Surprisingly, social isolation blocked cCIT-induced facilitation of serotonin release, but did not induce changes in VEH-treated mice. Many behavioral and neurochemical effects of social isolation are correlated with an upregulation of HPA axis activity, including brain-wide increases in CRF and CORT levels (Backstrom & Winberg; Blanchard et al., 2001). C57BL/6J mice are a resilient strain,

and under ordinary conditions, these increases may not be behaviorally or neurochemically significant (Voikar, Polus, Vasar, & Rauvala, 2005). However, chronic SSRI treatment increases negative feedback to the HPA axis, reducing its function (Barden, 1996, 2004; Pariante & Miller, 2001). SSRI-induced changes in HPA axis activity directly affect serotonergic activity (Celada, Puig, Amargos-Bosch, Adell, & Artigas, 2004; Celada et al., 2001; Johnson, Grant, Ingram, & Gartside, 2007; Kirby et al., 2008). Isolation-induced increases in HPA axis function could negate the opposing effects of chronic SSRI exposure. Thus, social isolation and cCIT treatment may work against each other so that serotonin signaling is not altered in single-housed mice. Our finding that cCIT led to significant reductions in marble-burying in the paired-housed, but not the single-housed, mice provides additional evidence for lower sensitivity to SSRI effects with chronic social isolation.

Plasticity in serotonergic function and its downstream targets underlies the efficacy of SSRI therapies for depression and OCD (Blier & de Montigny, 1998). However, prior studies have not characterized the changes in endogenous serotonin dynamics that occur during the therapeutic period of SSRI treatment. In this study, we used *in vivo* measurements to show that 20-day CIT treatment facilitates serotonin release in a frequency-dependent manner without altering SERT function. Prior studies have shown that autoreceptor desensitization occurs with the onset of therapeutic effects. Here, we demonstrate a consequence of this desensitization, revealing profound increases in evoked terminal serotonin release at all frequencies, a major mechanistic change that may contribute to the therapeutic actions of SSRIs. The observation that individually housing animals can entirely block this effect in both baseline and challenge conditions indicates that ongoing stress during SSRI treatment is an important variable in individual outcomes. This work shows that

plasticity in the serotonergic system is sensitive to environmental stress, and this can influence the effects of SSRI therapies.

Supplemental Methods

Carbon-fiber microelectrode construction and calibration

Carbon-fiber microelectrodes were assembled as previously described (Cahill et al., 1996). To enhance sensitivity to serotonin, Nafion (5% in methanol, Sigma-Aldrich) was applied to the electrodes using a dip-coating procedure. Briefly, microelectrodes were dipped into Nafion solution individually then baked at 70ºC for 10 minutes, for seven repetitions. An electrode calibration standard was determined by post-calibrating electrodes *in vitro* in phosphate buffered saline.

Detection of Evoked 5-HT release

On day 22, after 24 hours of withdrawal from CIT or VEH treatment, mice were anaesthetized with urethane (2 mg/g body weight in saline, i.p.) for stereotaxic surgery. A bipolar, stainless steel stimulating electrode (PlasticsOne, Roanoke, VA, USA) was implanted in the DRN (AP: -4.4, ML: 0.0, DV: -2.5 mm) and a carbon-fiber microelectrode was positioned into the SNpr (AP: -3.2, ML: +1.5). Serotonin release evoked by electrical stimulation of the DRN (325 μA biphasic pulses, 2 ms each phase, 20-60 Hz, 20-60 pulses) and optimized in the SNpr for maximal release between -4.0 and -4.2 mm dorsoventral from skull. Electrical stimulations were fixed-number of pulses (60 pulses, 20-60 Hz). To ensure stability of signal across experimental time course, 135 seconds elapsed between each stimulus presentation.

After baseline measurements were collected, an acute challenge dose of CIT (10 mg/kg i.p., Sigma-Aldrich) was administered to verify the identity of the measured signal as serotonin. Serotonin was identified by its unique cyclic voltammogram as well as its pronounced increase in evoked response following CIT challenge.

Because of technical difficulties lesioning with Nafion-coated carbon-fiber microelectrodes, representative histology was performed by lesioning with a tungsten electrode using a typical SNpr recording coordinate (AP: -3.2, ML: +1.5, DV: -4.1 mm). Immunohistochemistry was then performed as described below.

Immunohistochemistry

Mice were anesthetized with urethane and then perfused with 4% paraformaldehyde in PBS. Samples were incubated in 10, 20, and then 30% sucrose in PBS before being cut at 40 µm using a freezing-sliding microtome (Leica). Sections were collected, rinsed and blocked with 5% normal donkey serum and 0.2% Triton X-100 in PBS. Sections were then incubated in this blocking solution with primary antibody for 48 hours at 4°C. The primary antibodies used in this study were mouse anti-NeuN (1:500, MAB377, Millipore), rabbit anti-GFAP (1:1500, A2052, Sigma-Aldrich), and rabbit anti-5-HT (1:500, sc-13024, Santa Cruz Biotechnology). Secondary detection was performed with Alexa Fluor 488, 546, or 647 conjugated donkey anti-rabbit or anti-mouse antibodies (Invitrogen). Mounted sections were imaged on a Zeiss LSM 710 confocal microscope using 20×/0.8 NA objective.

Tissue content analysis

Mice were anesthetized with ethyl ether, decapitated, and the brain was rapidly removed and placed on ice. Coronal sections (300 µm thick) containing the SNpr were collected with a

Lancer Vibratome (World Precision Instruments, Sarasota, FL) in ice cold artificial cerebral spinal fluid (aCSF). The aCSF contained (in mM) 126 NaCl, 25 $NaHCO_3$, 2.45 KCl, 12 NaH_2PO_4, 1.2 $MgCl_2$, 2.4 $CaCl_2$, 20 HEPES, and 11 glucose. The pH of the buffer was adjusted to 7.4 and saturated with 95% O_2 /5% CO_2. The SNpr was excised with a 1 mm punch, and tissue was pooled such that each sample contained 5-8 mg total tissue from 3 mice. The samples were mixed with 200 µL of 0.1 N $HClO_4$ containing 1 µM hydroquinone, the internal standard, and subsequently homogenized using a sonic dismembrator (Fisher Scientific, Model 60, Pittsburgh, PA). The homogenate was then spun down at 6000 rpm for 10 minutes, and the supernatant was removed and filtered using a 0.2 µm syringe filter (Millex-LG). High performance liquid chromatography was performed using the methods of Mefford and Lähdesmäki *et al* (Lahdesmaki et al., 2002; Mefford, 1981). Briefly, 20 µL injections were made onto a revered-phase column (5 µm, 4.6 x 5 mm, Waters Atlantis). The mobile phase consisted of 0.1 M citric acid, 1 mM sodium hexylsulfate, 0.1 mM EDTA (pH = 3), and 10% methanol organic modifier at a flow rate of 1.0 mL/min. Neurotransmitters were detected with a thin layer radial electrochemical cell (BASi, West Lafayette, IN) at a potential of +800 mV vs Ag/AgCl. Data was collected at 60 Hz using a LabVIEW stripchart recorder program (Jorgenson Lab, UNC-CH) and homebuilt electronics. The peak area of the analyte was ratioed to the peak area of the internal standard, and the analyte concentration in the tissue was calculated.

Funding and Disclosure

This research was supported by an NIH grant to R.M.W. (NS 015841) and by the UNC Intellectual and Developmental Disabilities Research Center, funded by NICHD (U54 HD079124). The authors declare no competing financial interests in relation to this work.

Support

Meg Fox, Dr. Kara Agster, and Dr. Sheryl Moy contributed to data collection and experimental design in this chapter. The authors thank Dr. Rylan Larsen for assistance with confocal imaging and Nicholas Garcia for statistical expertise. We also acknowledge support from UNC Microscopy Core and the UNC Electronics Facility.

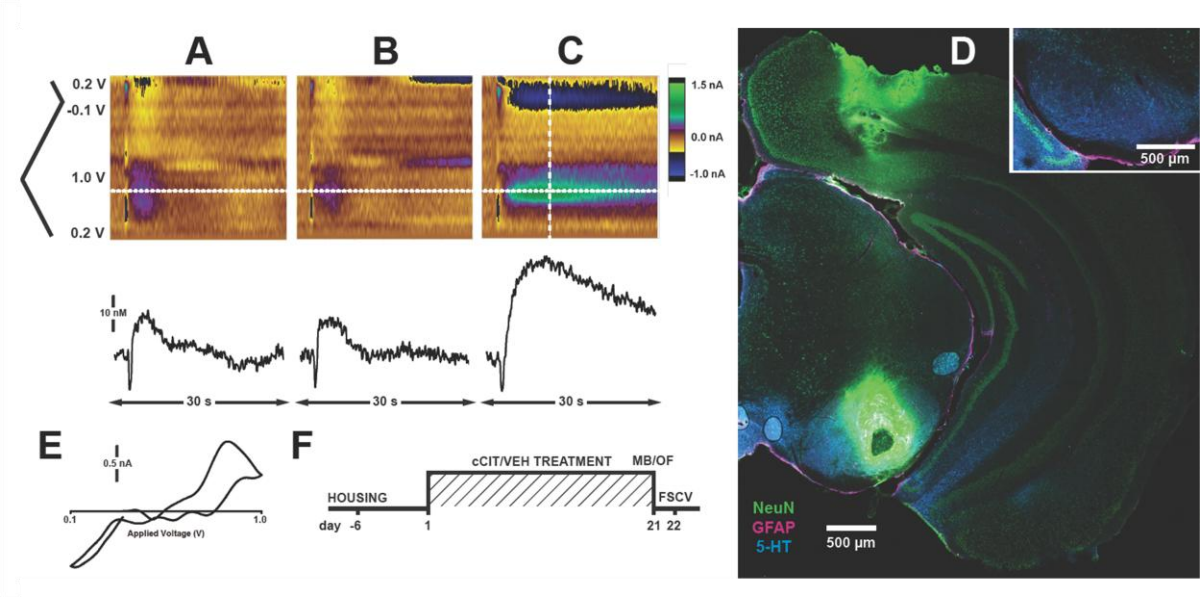

Figure 6.1 Voltammetric determination of serotonin release in the substantia nigra *pars reticulata* of the mouse brain. (A-C) Representative color plots (top) and concentration vs. time traces (bottom) showing electrically-evoked serotonin release (A) prior to drug treatment, (B) 30 minutes after administration of nomifensine (5 mg/kg, i.p.), and (C) 30 minutes after administration of citalopram (CIT, 10 mg/kg, i.p.). Traces were obtained from the oxidation current of serotonin, indicated by the dotted white line on the color plots, at approximately 0.8 V. (D) Representative histology from lesion showing targeted dorsoventral location of recording electrodes in SNpr. Green, NeuN; Magenta, GFAP; Blue, 5-HT. Inset shows contralateral SNpr containing dense serotonergic terminals. (E) Representative current-voltage trace taken at time point indicated by the dashed line in color plot C. (F) Timeline of experiments outlined in this paper: Mice were transferred to single- or pair-housing one week prior to chronic CIT (cCIT) treatment. CIT (15 mg/kg/day) or vehicle (VEH) was administered via water bottles for 20 days. On day 21, marble burying and open field assays were performed and animals were withdrawn from CIT or VEH for 24 hours. On day 22, anaesthetized voltammetry experiments were performed. Data shown are means ± SEM.

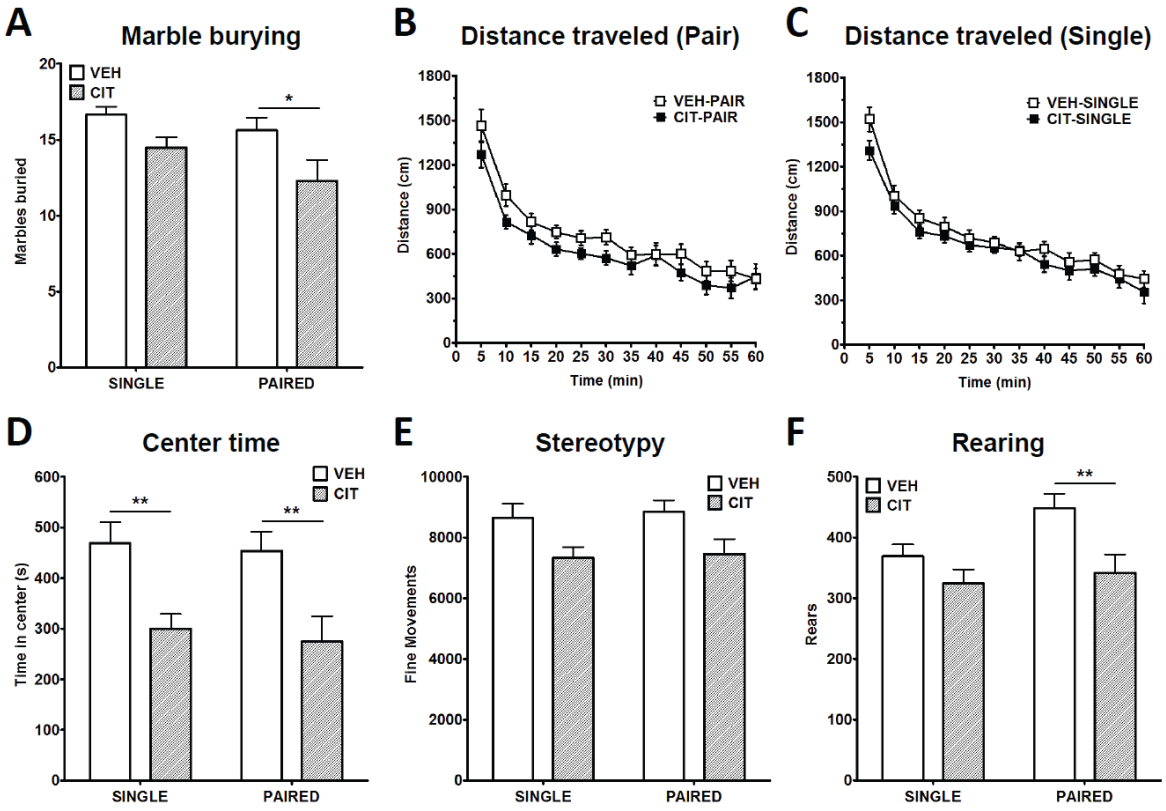

Figure 6.2 Effects of cCIT or VEH treatment on marble-burying and OF assays in pair- and single-housed mice. (**A**) Number of marbles (out of 20) buried during a 30 minute marble-burying assay. (**B-C**) Distance traveled across a 60 minute OF test. (**D**) Time spent in center of the OF chamber. (**E**) Fine movements during OF testing. (**F**) Incidences of rearing during OF testing. Data shown are means ± SEM. Bonferroni post-hoc analysis: **p<0.01, *p<0.05.

	20 Hz (nM)	30 Hz (nM)	40 Hz (nM)	50 Hz (nM)	60 Hz (nM)
Baseline					
Single-housed					
VEH (n=6)	16.4±2.0	15.9±1.2	16.7±1.2	16.8±1.2	17.2±1.4
CIT (n=9)	22.3±2.6	20.4±1.8	20.8±2.7	21.5±2.3	21.9±2.0
Pair-housed					
VEH (n=6)	17.6±2.4	16.1±1.2	16.2±2.1	16.2±0.9	16.4±1.5
CIT (n=8)	21.8±2.7	26.1±3.6	29.3±4.9	32.3±4.9*	32.2±5.5*
Citalopram challenge					
Single-housed					
VEH (n=6)	32.3±4.3	40.0±5.5	45.6±6.2	52.0±6.7	54.0±7.1
CIT (n=9)	37.2±7.2	44.9±8.4	49.5±8.9	53.9±8.7	54.9±8.5
Pair-housed					
VEH (n=6)	26.6±3.7	35.3±5.0	40.8±5.2	46.2±5.4	48.4±4.6
CIT (n=8)	54.1±7.1	68.0±8.3*	78.3±9.3*	87.4±10.7**	92.4±11.2**

*P<0.05, **P<0.01Sidak multiple comparisons test

Table 6.1 Maximal serotonin release ($[5\text{-HT}]_{max}$) measured in SNpr as evoked by electrical stimulation of DRN. Stimulation trains for each frequency were 60 pulses in length.

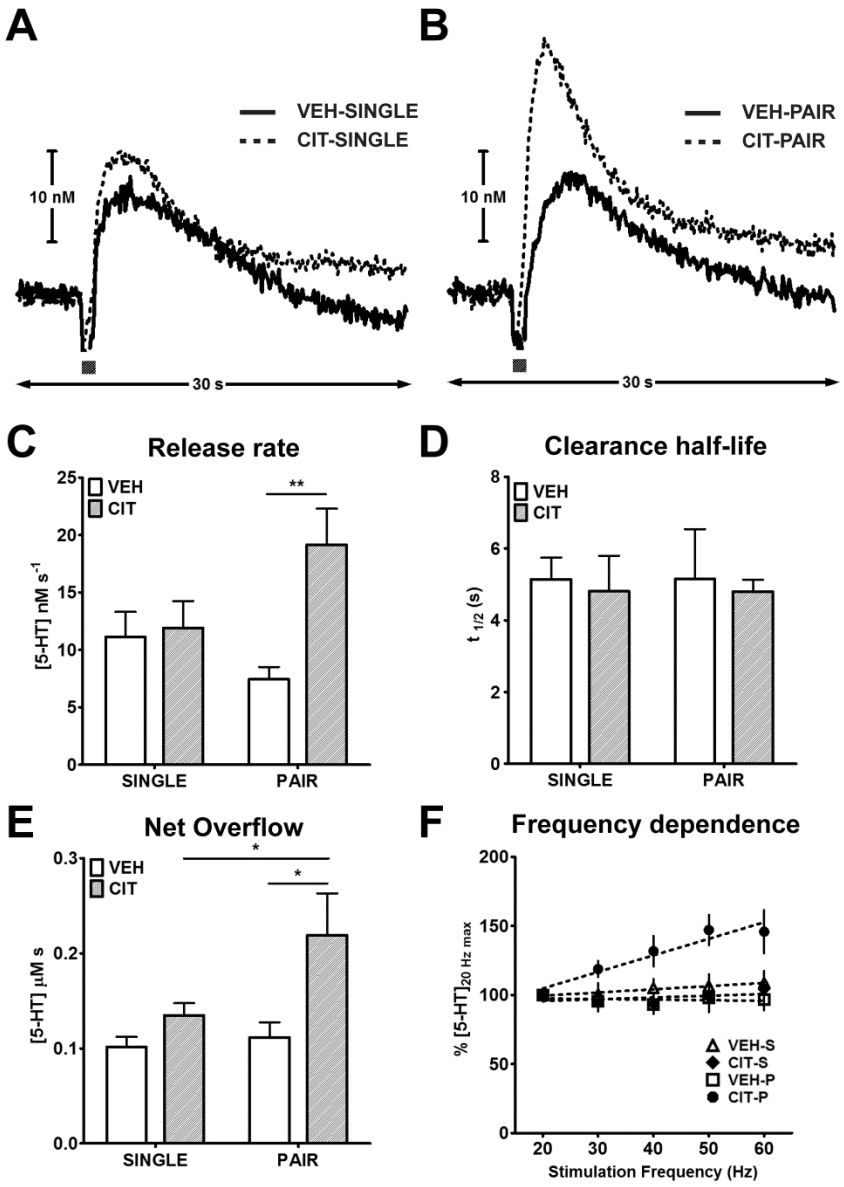

Figure 6.3. Comparison of serotonin release and uptake evoked by electrical stimulation of the DRN. (**A**-**B**) Averaged concentration vs. time traces of serotonin release evoked by a 60 Hz, 60 pulse stimulation of the DRN. Shaded bar below trace indicates the duration of stimulation. **(C**) Mean rate of change in [5-HT] during the rising phase of release evoked by 60 Hz, 60 pulse stimulation. (**D**) $t_{1/2}$ of evoked serotonin following 60 Hz, 60 pulse stimulation. (**E**) Mean net overflow (area under curve) following 60 Hz, 60 pulse stimulations. (**F**) Averages of normalized maximal release amplitudes evoked by 20 – 60 Hz stimulations. Dotted lines show best-fit linear regressions for each treatment group. Data shown are means ± SEM. Bonferroni post-hoc analysis: **p<0.01, *p<0.05.

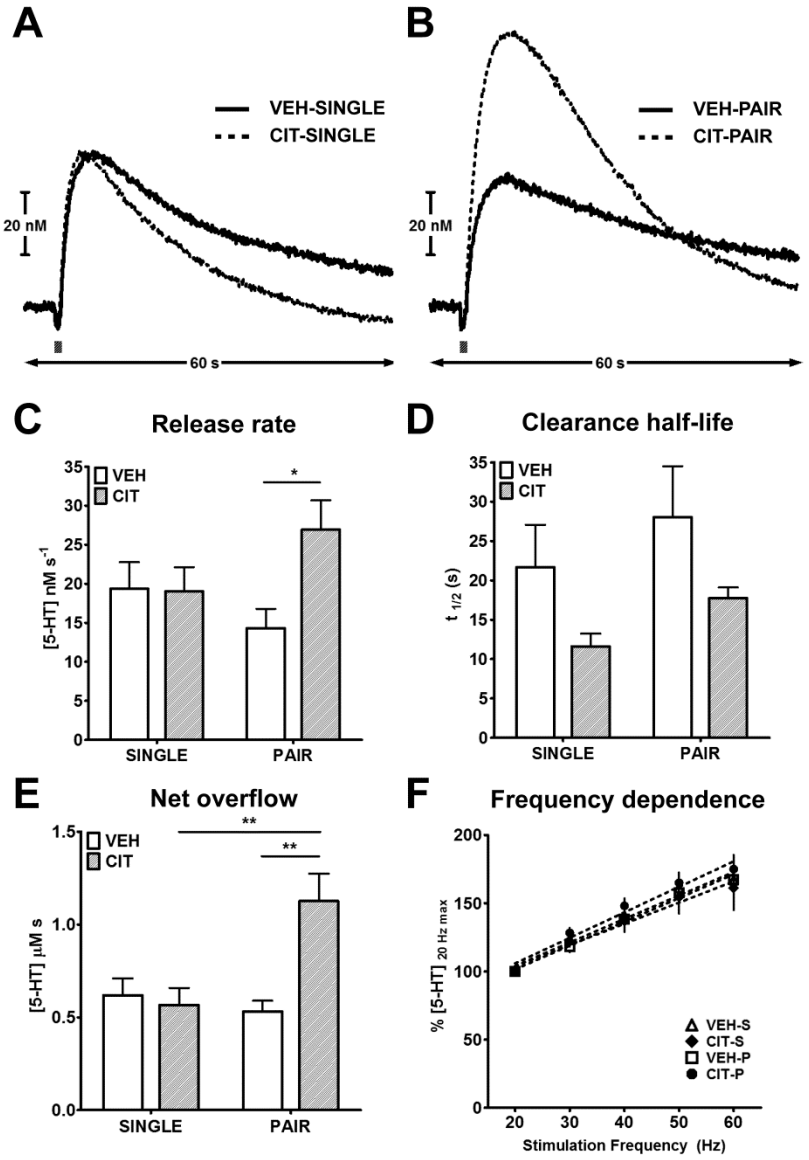

Figure 6.4 Comparison of electrically-evoked serotonin release following acute CIT challenge. (**A-B)** Averaged concentration vs. time traces of serotonin release evoked by a 60 Hz, 60 pulse stimulation of the DRN 30 minutes after acute CIT. Shaded bar below trace indicates the duration of stimulation. (**C**) Mean rate of change in [5-HT] during the rising phase of release evoked by 60 Hz, 60 pulse stimulation after acute CIT challenge. (**D**) Mean $t_{1/2}$ of evoked serotonin following 60 Hz, 60 pulse stimulations. (**E**) Mean area under curve (AUC) following 60 Hz, 60 pulse stimulations. (**F**) Averages of normalized maximal release amplitudes evoked by 20 – 60 Hz stimulations. Dotted lines show best-fit linear regressions for each treatment group. Data shown are means ± SEM. Bonferroni post-hoc analysis: **p<0.01, *p<0.05.

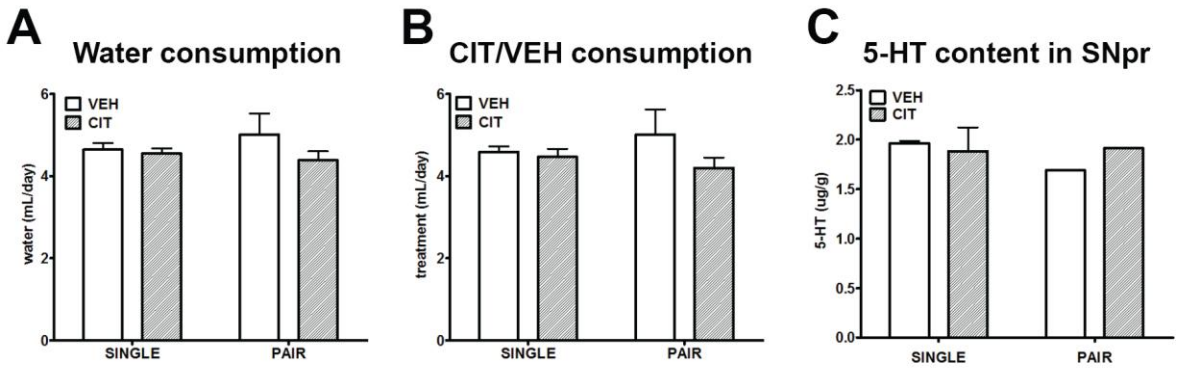

Figure 6.S1. Comparison of liquid consumption before and during CIT/VEH treatment and tissue content analysis. **(A)** Mean individual water volume consumed per day for the 7 days prior to treatment. **(B)** Mean individual liquid volume consumed per day during 20 days of CIT of VEH treatment. **(C)** Serotonin content analyzed using HPLC from tissue punches of SNpr.

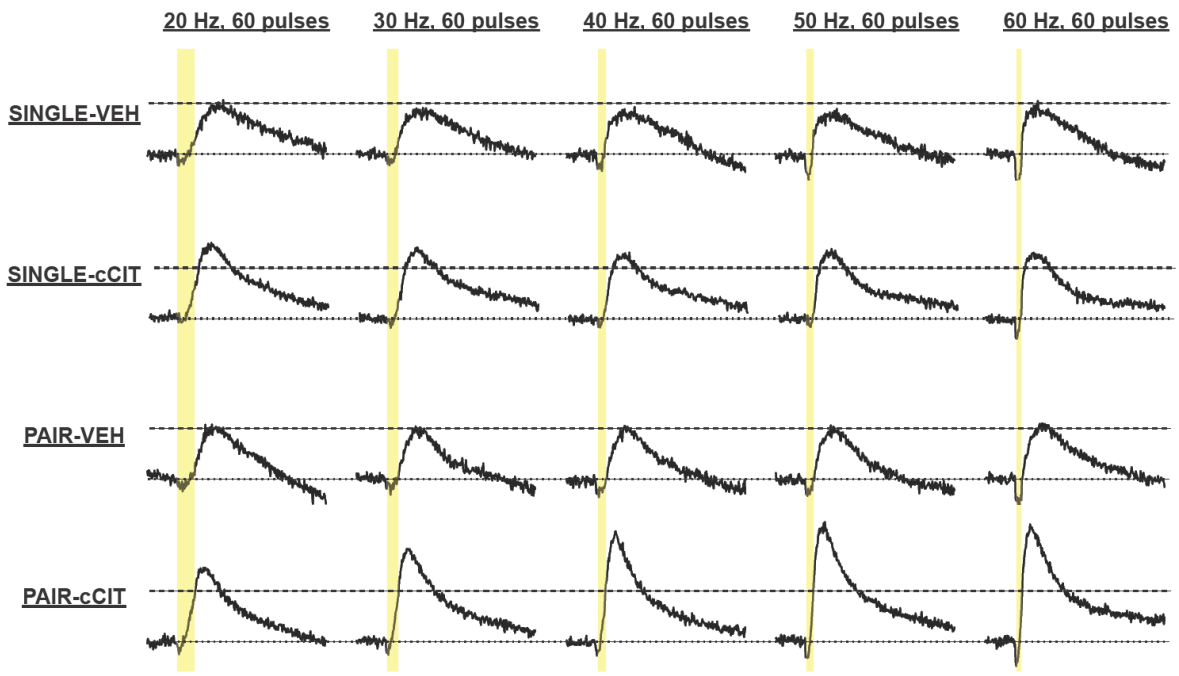

Figure 6.S2. 5-HT concentration traces evoked by each stimulation frequency. Duration of each 60 pulse stimulation train is denoted by the yellow bar over each trace: 20 Hz = 3 s, 30 Hz = 2 s, 40 Hz = 1.5 s, 50 Hz = 1.2 s, and 60 Hz = 1 s. Each trace shows 5 s prior to stimulation onset and 25 seconds after, for a total of 30 s. A dotted line indicates [5-HT]=0 nM (baseline) and the dashed line indicates [5-HT]=17 nM, the average $[5\text{-HT}]_{max}$ for 20 Hz release in VEH-treated single- and pair-housed mice. Serotonin release in VEH-treated mice looks kinetically similar across all frequencies. In single-housed cCIT mice, release is modestly increased, and the effect is similar across all frequencies. In contrast, enhancement of serotonin release in pair-housed cCIT mice intensifies with increasing stimulation frequency. Single-VEH (N=6), Single-cCIT (N=9), Pair-VEH (n=6), Pair-cCIT (n=8).

CHAPTER 7: CONCLUSION

Summary of findings

Fast-scan cyclic voltammetry of 5-HT

This work began with the goal of measuring serotonin release *in vivo*. Prior work had characterized a waveform that addressed a major obstacle in the electrochemical detection of serotonin: the electrode-fouling side-products formed by serotonin's oxidation and reduction (Jackson et al.). Unlike dopamine, which oxidizes and reduces predictably and with a clean cyclic voltammogram, there are over 30 products formed from serotonin's oxidation, and some of these polymerize and foul the surface of the carbon-fiber microelectrode. The result of this fouling is a deterioration of electrode sensitivity and temporal response. Jackson et al. (1995) condensed the voltage waveform used to measure dopamine so it did not scan as high or as low (-0.1 V to +1.0 V). Furthermore, the waveform was shifted so that between scans, the waveform was held at +0.2 V. Avoiding high and low potentials in this manner reduces the formation of fouling side-products. Additional fouling was avoided by kinetically out-running side-product formation: this is why the waveform scans at a faster speed than for dopamine (1000 V/s). The Jackson 5-HT waveform had been used successfully in brain slices to describe the release and uptake kinetics of serotonin (Bunin et al.), the extrasynaptic nature of its release (Bunin & Wightman), and had also been used to study serotonin release

in fly ventral nerve cord (Borue, Condron, & Venton, 2010; Borue, Cooper, Hirsh, Condron, & Venton, 2009)

In spite of these improvements, electrochemical detection of serotonin *in vivo* was still not possible. This was in part due to interference by metabolites of serotonin, specifically 5-hydroxyindoleacedic acid (5-HIAA). 5-HIAA is present at high levels in brain tissue and interferes with detection of serotonin due to its similar electrochemistry (Ross & Stenfors, 1997). Constant perfusion of buffer through brain slices reduces 5-HIAA to negligible levels, but methodological modifications were needed to avoid its detection *in vivo*. During the development of voltammetric methods to measure dopamine, anionic species such as ascorbic acid posed similar threats to the sensitivity and selectivity of dopamine detection. To exclude these anionic species, a cation-exchange polymer, Nafion, was applied to the carbon-fiber electrode in a dip-coating process (G. A. Gerhardt et al., 1984; Wiedemann et al., 1990). Nafion decreased sensitivity to anions like ascorbic acid, which in turn enhanced dopamine detection. Since 5-HIAA is an anion, and the serotonin molecule has a net positive charge, Nafion was also a good candidate for enhancing serotonin detection. We hypothesized that *in vivo* serotonin measurements would be possible using a combination of the modified Jackson 5-HT waveform and Nafion-coated microelectrodes.

Anatomical Choices for Serotonin Measurements

Although *in vitro* experiments confirmed that the Jackson 5-HT waveform and Nafion-coated electrodes heightened sensitivity and selectivity for serotonin, anatomical locations for stimulating and carbon-fiber microelectrodes still required optimization. In Chapter 2, we selected the dorsal raphe nucleus (DRN) as the site for electrical stimulation

because the majority of serotonergic neurons that send projections into forebrain are located there (Azmitia & Segal, 1978; Moore et al., 1978b). We selected the substantia nigra *pars reticulata* (SNpr) as the location for our recording electrode because its terminal serotonin field is second in density only to the DRN itself (Fibiger & Miller, 1977; Wirtshafter et al., 1987). Optimizing placement of the two electrodes in the target brain regions enabled the first measurements of *in vivo*, endogenous serotonin release (Hashemi et al.).

Although measuring serotonin release was now possible, a few problems still remained. Serotonin release evoked in brain slices of the SNpr was 50 times larger than serotonin release evoked *in vivo*. Additionally, electrical stimulation of the DRN had a low success rate, probably owing to its small size and location deep in the brainstem. In Chapter 3, we investigated whether stimulation of the medial forebrain bundle (MFB) could produce serotonin release that resembled release evoked by DRN stimulation. Ascending serotonergic projections run through the MFB and can be electrically stimulated to excite serotonergic neurons in the DRN (Hajos & Sharp). We demonstrated that electrical stimulation of the MFB could evoke serotonin release in the SNpr that closely resembled DRN-evoked release (Hashemi et al.). However, the MFB comprises a large number of projections, including those containing other electroactive neurotransmitters such as dopamine and norepinephrine. Although dopamine and norephinephrine did not contribute to release evoked in the SNpr by MFB stimulation, an oxidation peak on at the waveform's 'switching' potential (+1.0 V) suggested the presence of another electroactive molecule, histamine. In spite of less selectivity in evoked release, experimentation using the MFB stimulation site had a much higher success rate, and is utilized in Chapter 4.

In vivo modulation of serotonin release

In Chapter 4, we compared *in vivo* dopamine and serotonin signaling, evoked by a common stimulation of the MFB, to ascertain which biochemical mechanisms were most influential on their release. The same dorso-ventral location of the stimulating electrode evoked maximal release for both neurotransmitters; however, evoked dopamine concentrations were 300-fold greater than evoked serotonin concentrations. We observed that dopamine release declined rapidly after repeated stimulus presentation. Inhibition of synthesis and packaging also quickly depleted dopamine stores, suggesting that release is mostly limited by neurotransmitter availability. Serotonin release was not affected to the same extent as dopamine, possibly because its release was low enough to maintain a sufficient vesicular pool (Aghajanian et al.). Inhibition of serotonin's transporter (SERT) or monoamine oxidase (MAO), which metabolizes serotonin, enhanced serotonin release as well as decreased clearance rate. We hypothesized that clearance mechanisms, rather than synthesis and packaging mechanisms, play a large role in regulation of serotonin release *in vivo*. In support of this, we found that simultaneous inhibition of SERT and MAO caused rapid dysregulation of serotonin levels, resulting in death. We concluded that serotonin signaling is robustly regulated by clearance mechanisms to maintain viable extracellular levels (Hashemi et al.).

Role of SERT in dynamic modulation of serotonin signaling

Previously, our investigations of *in vivo* serotonin release showed that evoked concentrations were much lower *in vivo* than in brain slices. Chapter 5 demonstrates another major difference: serotonin release is positively correlated with stimulation frequency in brain slices, but not *in vivo*. Frequency-dependence has been described for *in vivo* dopamine release, and the effect is well-understood: longer inter-pulse intervals during low frequency

stimulations allow for more neurotransmitter uptake during the stimulus duration, so net release is lower (R.M. Wightman et al.). Accordingly, uptake inhibition affects dopamine release evoked by low frequency stimulations to a greater extent than high frequency stimulations. Because frequency dependence is a function of transporter activity, dopamine evoked by varying stimulation frequencies can be modeled using Michaelis-Menten kinetics for quantitative comparison of its dynamics (Wightman & Zimmerman). Lack of frequency-dependence in *in vivo* serotonin release was therefore a very surprising finding. More surprising was our observation that SERT inhibition by selective serotonin reuptake inhibitors (SSRIs) induced frequency-dependent release.

Chapter 5 investigates these unexpected effects of acute exposure to SSRIs. Although their effects on uptake are well-characterized, the observation that SSRIs enhance serotonin signaling in a frequency-dependent manner is unique. We hypothesized that the effects of SSRIs on serotonin release, but not uptake, were localized in the DRN. The DRN contains the highest SERT expression of any brain area, and serotonin levels there modulate feedback circuitry that inhibits serotonergic firing (Blier et al., 1998; Pineyro & Blier, 1999). Microinfusing an SSRI into the DRN replicated its systemic effects on release without affecting uptake. This suggests that SSRI-induced increases in DRN serotonin levels dysregulate local modulatory circuitry to favor responsiveness to high-frequency excitatory inputs. One way this could happen is via rapid desensitization of 5-HT1a autoreceptors, which has been shown after acute exposure to 5-HT1a agonists and SSRIs (Riad, Watkins, Doucet, Hamon, & Descarries, 2001; Riad et al., 2004). High extracellular concentrations of serotonin may similarly desensitize these autoreceptors, which would eliminate their restrictions of serotonergic firing rate. Alternatively, local increases in 5-HT may maximally

activate inhibitory feedback within the DRN that would normally escalate to relegate responsiveness to excitatory inputs. If inhibitory feedback cannot upregulate, stimulation frequency would have a more direct effect on serotonin release, as we observed. Additional experiments are needed to fully elucidate the mechanisms of SSRI effects in the DRN, and these future directions are discussed in a later section.

Effects of chronic SSRI treatment on serotonin signaling

Although SSRIs have robust acute effects, 3-6 weeks of chronic treatment are required before they exert clinical improvements in depression and anxiety-related disorders. Antidepressant effects of SSRIs likely depend on plasticity in serotonergic function and its targets during this time period (Branchi, 2011). We hypothesized that changes in serotonin signaling related to the acute effects of SSRIs may accompany the onset of antidepressant effects during chronic treatment. Chapter 6 describes how 20-day SSRI treatment improved behavioral indices of anxiety and enhanced serotonin release in pair-housed mice. As in Chapter 5, the effects on serotonin signaling were frequency-dependent, indicating that similar SERT-mediated mechanisms may underlie long-term effects of SSRI treatment. Interestingly, no enhancement of serotonin release was observed in singly-housed mice, suggesting that chronic mild stress during SSRI treatment can attenuate its effects. These findings underscore how SERT function modulates serotonin release in a way that is distinguishable from its effects on uptake. They also suggest that neurobiological systems involved in the transduction of stress may endogenously modulate SERT, and thus, the effects of stress may interact with both the pathophysiology and treatment of depressive disorders.

Discussion and Future Directions

Stimulation of the MFB and DRN evoke serotonin release with similar properties, and each stimulation location has advantages and disadvantages. The DRN in the rat brain extends barely over 1 mm in any dimension. As rats grow, their skulls increase in length and their brain does not, making bregma an unreliable predictor of DRN location in larger, older subjects. In contrast, the MFB is a large and developmentally stable target. In chapters 3 and 4 of this dissertation, MFB stimulation was used because of its much higher experimental success rate. However, electrical stimulations in this region evoke many kinds of neurotransmitter in many brain regions. When we began using this technique in mice (chapters 5 and 6), we found that the DRN and MFB were equally facile targets as long as age and weight ranges for mice were well-controlled (8-14 weeks, 25-30 g). The DRN is considered a superior electrical stimulation site because it offers some level of specificity.

Future work would benefit from an even more selective stimulation method. The dorsal raphe contains 30% GABAergic neurons, many of which contribute to local modulatory circuitry. In our experiments, it is unclear whether GABAergic circuitry is partly responsible for the effects of SSRIs on evoked serotonin signaling. Optogenetic stimulation of serotonin release has been successful in fly ventral nerve cord (Borue, Condron, & Venton, 2010; Borue, Cooper, Hirsh, Condron, & Venton, 2009), and has been employed in several mammalian studies, but not in combination with FSCV. Use of this cell-type selective technique could clarify whether SERT inhibition selectively modifies serotonergic activity. One proposed experiment would be to compare serotonergic neuronal firing as well as release evoked by electrical vs. optogenetic stimulations. Additionally, our work has concentrated on serotonin signaling in the SNpr to avoid interference from other electroactive

neurotransmitters, such as dopamine and norepinephrine. However, light-activation of serotonin neurons would enable chemically-selective measurements in other brain regions, including the nucleus accumbens and hippocampus, where serotonergic signaling is known to be important.

One further aspect of this work that remains unclear is the role of various serotonin receptors in mediating the effects of SSRIs in the DRN. Although presynaptic 5-HT1a receptors are abundantly implicated in the effects of SSRIs, postsynaptic 5-HT2a, 2c, and 7 receptors on DRN interneurons may also contribute to the local feedback circuitry that is modified by dramatic alterations in ambient serotonin levels. Though we have attempted to study the roles of these receptors with available agonists and antagonists, these agents have weak effects. This could be due to poor passage through the blood brain barrier, rapid metabolism, cycling of receptor pools, homeostatic feedback, or constitutive receptor activity. Use of designer receptors exclusively activated by designer drugs (DREADDs, or RASSLs) could better elucidate the effects of these receptors on serotonin signaling. Recently, the Roth lab at University of North Carolina – Chapel Hill has shown that chronic activation of a 5-HT1a-like designer receptor has antidepressant behavioral effects in mice (Dan Urban, personal communication). It would be interesting to compare the effects of this treatment to the enhancements in serotonergic signaling observed in chapter 6.

In this work, serotonin release was measured in both rat and mouse models. The mouse model was developed because it offers several distinct advantages. First, serotonin release can be evoked by stimulations of much lower intensity in mice compared to rats (325 μA, 60 pulses *vs.* 350 μA, 120 pulses). The serotonergic system is of comparable size in mice and rats, so increased density of neurons and fibers in the smaller mouse brain may be more

optimal for stimulating and measuring serotonin release. The effect of brain size in combination with inbreeding-driven consistency in the C57Bl/6J strain probably also contribute to increased success rate with DRN stimulation. Second, mouse models offer more options for genetic manipulation. We used this to our advantage to some extent with the SERT-/- mouse to show selectivity of SSRIs for SERT, but future work could make even better use of the mouse lines by employing optogenetic models and conditional knockouts. In particular, the hypothesis that desensitization of 5-HTa autoreceptors underlies enhancement of serotonin signaling after chronic SSRIs, discussed in chapter 6, could be addressed using CRE-lox recombination to delete presynaptic 5-HT1a receptors in adult mice.

Concluding Remarks

Serotonin is a molecule found in nearly all organisms: plants, single-celled animals, invertebrates, and vertebrates. In every organism, it is possible to identify serotonin's role in maintaining systemic homeostasis, whether it is to regulate the division of cells, capture free oxygen, stabilize microtubule structures, or influence neuronal excitability in the spinal cord and central nervous system (Azmitia, 2007). In the mammalian brain, less than 250,000 serotonin-synthesizing neurons cluster in tiny nuclei in the brainstem, and yet these neurons send projections to innervate nearly every region of the forebrain and basal ganglia. They constitute 1/1,000,000 of total brain cells, but they may account for 1/500 of all synaptic terminals (Molliver, 1987). Though in complex organisms, serotonin participates in a wide array of nervous system functions, ranging in complexity from regulation of breathing and body temperature to high-level cortical processing, its evolutionary history as a homeostatic force remains a constant predictor for its role in these processes (Abrams, Johnson, Hollis, &

Lowry, 2004). The work in this dissertation fits within the interpretive framework that emphasizes this role of equilibrium in serotonin signaling.

Many studies have shown that the serotonin system is resistant to changes in function, a property that is maintained by feedback from forebrain structures as well as local inhibitory circuitry (Blier et al., 1998; Pineyro & Blier, 1999). Our findings agree that serotonin signaling is subject to tremendous limitations by these feedback systems. Under normal conditions, released concentrations *in vivo* are low and seemingly relegated by the slow firing rate of serotonergic neurons. We have shown enhancement of release induced by acute and chronic SERT inhibition that could be interpreted as a loss of homeostatic function. In "The Wisdom of the Body" (1932), Sir Walter Cannon disabuses this notion, asserting that "slight instability is the necessary condition for the true stability of the organism." Flexibility, not rigidity, is the true hallmark of homeostasis, and it is an outstanding and fascinating property of all neural systems. Because many endogenous and naturally-occurring exogenous substances are able to modify serotonin transporter function, plasticity in serotonin signaling may be an adaptive response that transduces physiological states and environmental signals back to the nervous system. In the case of acute SSRIs, facilitation of serotonin signaling that coincides with increases in ambient serotonin levels is a temporary but dramatic dysregulation of the serotonin system. After 3-6 weeks of SSRI treatment, both ambient serotonin levels and serotonergic firing rates have normalized, but facilitation in signaling is sustained. Thus, by introducing instability to the serotonergic system, SSRIs may promote the plasticity in regulatory functions that result in their antidepressive effects.

REFERENCES

Abrams, J. K., Johnson, P. L., Hollis, J. H., & Lowry, C. A. (2004). Anatomic and functional topography of the dorsal raphe nucleus. *Ann N Y Acad Sci, 1018*, 46-57.

Adell, A., Celada, P., & Artigas, F. (2001). The role of 5-HT1B receptors in the regulation of serotonin cell firing and release in the rat brain. *J Neurochem, 79*(1), 172-182.

Aghajanian, G. K., Sprouse, J. S., Sheldon, P., & Rasmussen, K. (1990). Electrophysiology of the central serotonin system: receptor subtypes and transducer mechanisms. *Ann N Y Acad Sci, 600*, 93-103; discussion 103.

Aghajanian, G. K., & Wang, R. Y. (1978). Psychopharmacology: A Generation of Progress. In M. A. Lipton, A. DiMascio & K. F. Killiam (Eds.), (pp. 171-183). New York: Raven Press.

Aghajanian, G. K., Wang, R. Y., & Baraban, J. (1978). Serotonergic and non-serotonergic neurons of the dorsal raphe: reciprocal changes in firing induced by peripheral nerve stimulation. *Brain Res, 153*(1), 169-175.

Anden, N. E., Fuxe, K., & Ungerstedt, U. (1967). Monoamine pathways to the cerebellum and cerebral cortex. *Experientia, 23*(10), 838-839.

Andersen, P. H. (1989). The dopamine inhibitor GBR 12909: selectivity and molecular mechanism of action. *Eur J Pharmacol, 166*(3), 493-504.

Anichtchik, O. V., Huotari, M., Peitsaro, N., Haycock, J. W., Mannisto, P. T., & Panula, P. (2000). Modulation of histamine H3 receptors in the brain of 6-hydroxydopamine-lesioned rats. *Eur J Neurosci, 12*(11), 3823-3832.

Arora, T., Bhowmik, M., Khanam, R., & Vohora, D. (2013). Oxcarbazepine and fluoxetine protect against mouse models of obsessive compulsive disorder through modulation of cortical serotonin and CREB pathway. *Behav Brain Res, 247*, 146-152.

Arrang, J. M., Garbarg, M., Lancelot, J. C., Lecomte, J. M., Pollard, H., Robba, M., . . . Schwartz, J. C. (1987). Highly potent and selective ligands for histamine H3-receptors. *Nature, 327*(6118), 117-123.

Artigas, F., Perez, V., & Alvarez, E. (1994). Pindolol induces a rapid improvement of depressed patients treated with serotonin reuptake inhibitors. *Arch Gen Psychiatry, 51*(3), 248-251.

Azmitia, E. C. (2007). Serotonin and brain: evolution, neuroplasticity, and homeostasis. *Int Rev Neurobiol, 77*, 31-56.

Azmitia, E. C., & Segal, M. (1978). Autoradiographic Analysis of Differential Ascending Projections of Dorsal and Median Raphe Nuclei in Rat. *Journal of Comparative Neurology, 179*(3), 641-667.

Backstrom, T., & Winberg, S. (2013). Central corticotropin releasing factor and social stress. *Front Neurosci, 7*, 117.

Barden, N. (1996). Modulation of glucocorticoid receptor gene expression by antidepressant drugs. *Pharmacopsychiatry, 29*(1), 12-22.

Barden, N. (2004). Implication of the hypothalamic-pituitary-adrenal axis in the physiopathology of depression. *J Psychiatry Neurosci, 29*(3), 185-193.

Barnes, N. M., & Sharp, T. (1999). A review of central 5-HT receptors and their function. *Neuropharmacology, 38*(8), 1083-1152.

Baur, J. E., Kristensen, E. W., May, L. J., Wiedemann, D. J., & Wightman, R. M. (1988). Fast-scan voltammetry of biogenic amines. *Anal Chem., 60*, 1268-1272.

Beaudet, A., & Descarries, L. (1981). The fine structure of central serotonin neurons. *J Physiol (Paris), 77*(2-3), 193-203.

Beaven, M. A., & Shaff, R. E. (1979). New inhibitors of histamine-N-methyltransferase. *Biochem Pharmacol, 28*(2), 183-188.

Bel, N., & Artigas, F. (1992). Fluvoxamine preferentially increases extracellular 5-hydroxytryptamine in the raphe nuclei: an in vivo microdialysis study. *Eur J Pharmacol, 229*(1), 101-103.

Bell, J. L., McIlwain, H., & Thomas, J. (1956). The composition of isolated cerebral tissues; ascorbic acid and cozymase. *Biochem J, 64*(2), 332-335.

Bennett, J. P., Jr., Logan, W. J., & Snyder, S. H. (1973). Amino acids as central nervous transmitters: the influence of ions, amino acid analogues, and ontogeny on transport systems for L-glutamic and L-aspartic acids and glycine into central nervous synaptosomes of the rat. *J Neurochem, 21*(6), 1533-1550.

Bergquist, F., Shahabi, H. N., & Nissbrandt, H. (2003). Somatodendritic dopamine release in rat substantia nigra influences motor performance on the accelerating rod. *Brain Res, 973*(1), 81-91.

Bertrand, P. P., Hu, X., Mach, J., & Bertrand, R. L. (2008). Serotonin (5-HT) release and uptake measured by real-time electrochemical techniques in the rat ileum. *Am J Physiol Gastrointest Liver Physiol, 295*(6), G1228-1236.

Bespalov, A. Y., van Gaalen, M. M., & Gross, G. (2010). Antidepressant treatment in anxiety disorders. *Curr Top Behav Neurosci, 2*, 361-390.

Blakely, R. D., Berson, H. E., Fremeau, R. T., Jr., Caron, M. G., Peek, M. M., Prince, H. K., & Bradley, C. C. (1991). Cloning and expression of a functional serotonin transporter from rat brain. *Nature, 354*(6348), 66-70.

Blanchard, R. J., McKittrick, C. R., & Blanchard, D. C. (2001). Animal models of social stress: effects on behavior and brain neurochemical systems. *Physiol Behav, 73*(3), 261-271.

Blier, P., & de Montigny, C. (1998). Possible serotonergic mechanisms underlying the antidepressant and anti-obsessive-compulsive disorder responses. *Biol Psychiatry, 44*(5), 313-323.

Blier, P., de Montigny, C., & Chaput, Y. (1987). Modifications of the serotonin system by antidepressant treatments: implications for the therapeutic response in major depression. *J Clin Psychopharmacol, 7*(6 Suppl), 24S-35S.

Blier, P., de Montigny, C., & Chaput, Y. (1988). Electrophysiological assessment of the effects of antidepressant treatments on the efficacy of 5-HT neurotransmission. *Clin Neuropharmacol, 11 Suppl 2*, S1-10.

Blier, P., de Montigny, C., & Chaput, Y. (1990). A role for the serotonin system in the mechanism of action of antidepressant treatments: preclinical evidence. *J Clin Psychiatry, 51 Suppl*, 14-20; discussion 21.

Blier, P., Pineyro, G., el Mansari, M., Bergeron, R., & de Montigny, C. (1998). Role of somatodendritic 5-HT autoreceptors in modulating 5-HT neurotransmission. *Ann N Y Acad Sci, 861*, 204-216.

Boess, F. G., & Martin, I. L. (1994). Molecular biology of 5-HT receptors. *Neuropharmacology, 33*(3-4), 275-317.

Bortolozzi, A., Castane, A., Semakova, J., Santana, N., Alvarado, G., Cortes, R., . . . Artigas, F. (2012). Selective siRNA-mediated suppression of 5-HT1A autoreceptors evokes strong anti-depressant-like effects. *Mol Psychiatry, 17*(6), 612-623.

Borue, X., Condron, B., & Venton, B. J. (2010). Both synthesis and reuptake are critical for replenishing the releasable serotonin pool in Drosophila. *J Neurochem, 113*(1), 188-199.

Borue, X., Cooper, S., Hirsh, J., Condron, B., & Venton, B. J. (2009). Quantitative evaluation of serotonin release and clearance in Drosophila. *J Neurosci Methods, 179*(2), 300-308.

Bosker, F. J., Cremers, T. I., Jongsma, M. E., Westerink, B. H., Wikstrom, H. V., & den Boer, J. A. (2001). Acute and chronic effects of citalopram on postsynaptic 5-hydroxytryptamine(1A) receptor-mediated feedback: a microdialysis study in the amygdala. *J Neurochem, 76*(6), 1645-1653.

Bosker, F. J., Klompmakers, A. A., & Westenberg, H. G. (1995). Effects of single and repeated oral administration of fluvoxamine on extracellular serotonin in the median raphe nucleus and dorsal hippocampus of the rat. *Neuropharmacology, 34*(5), 501-508.

Bosker, F. J., van Esseveldt, K. E., Klompmakers, A. A., & Westenberg, H. G. (1995). Chronic treatment with fluvoxamine by osmotic minipumps fails to induce persistent functional changes in central 5-HT1A and 5-HT1B receptors, as measured by in vivo microdialysis in dorsal hippocampus of conscious rats. *Psychopharmacology (Berl), 117*(3), 358-363.

Boureau, Y. L., & Dayan, P. (2011). Opponency revisited: competition and cooperation between dopamine and serotonin. *Neuropsychopharmacology, 36*(1), 74-97. doi: npp2010151 [pii]

Branchi, I. (2011). The double edged sword of neural plasticity: increasing serotonin levels leads to both greater vulnerability to depression and improved capacity to recover. *Psychoneuroendocrinology, 36*(3), 339-351.

Brandl, E. J., Muller, D. J., & Richter, M. A. (2012). Pharmacogenetics of obsessive-compulsive disorders. *Pharmacogenomics, 13*(1), 71-81.

Brazell, M. P., Kasser, R. J., Renner, K. J., Feng, J., Moghaddam, B., & Adams, R. N. (1987). Electrocoating carbon fiber microelectrodes with Nafion improves selectivity for electroactive neurotransmitters. *J Neurosci Methods, 22*(2), 167-172.

Bridoux, A., Laloux, C., Derambure, P., Bordet, R., & Monaca Charley, C. (2013). The acute inhibition of rapid eye movement sleep by citalopram may impair spatial learning and passive avoidance in mice. *J Neural Transm, 120*(3), 383-389.

Brown, R. E., Stevens, D. R., & Haas, H. L. (2001). The physiology of brain histamine. *Prog Neurobiol, 63*(6), 637-672.

Budygin, E. A., Kilpatrick, M. R., Gainetdinov, R. R., & Wightman, R. M. (2000). Correlation between behavior and extracellular dopamine levels in rat striatum: comparison of microdialysis and fast-scan cyclic voltammetry. *Neurosci Lett, 281*(1), 9-12. doi: S0304-3940(00)00813-2 [pii]

Bull, D. R., Palij, P., Sheehan, M. J., Millar, J., Stamford, J. A., Kruk, Z. L., & Humphrey, P. P. (1990). Application of fast cyclic voltammetry to measurement of electrically evoked dopamine overflow from brain slices in vitro. *J Neurosci Methods, 32*(1), 37-44.

Bunin, M. A., Prioleau, C., Mailman, R. B., & Wightman, R. M. (1998). Release and uptake rates of 5-hydroxytryptamine in the dorsal raphe and substantia nigra reticulata of the rat brain. *J Neurochem, 70*(3), 1077-1087.

Bunin, M. A., & Wightman, R. M. (1998). Quantitative evaluation of 5-hydroxytryptamine (serotonin) neuronal release and uptake: an investigation of extrasynaptic transmission. *J Neurosci, 18*(13), 4854-4860.

Cahill, P. S., Walker, Q. D., Finnegan, J. M., Mickelson, G. E., Travis, E. R., & Wightman, R. M. (1996). Microelectrodes for the measurement of catecholamines in biological systems. *Anal Chem, 68*(18), 3180-3186.

Carlsson, A., Davis, J. N., Kehr, W., Lindqvist, M., & Atack, C. V. (1972). Simultaneous measurement of tyrosine and tryptophan hydroxylase activities in brain in vivo using an inhibitor of the aromatic amino acid decarboxylase. *Naunyn Schmiedebergs Arch Pharmacol, 275*(2), 153-168.

Casanovas, J. M., Lesourd, M., & Artigas, F. (1997). The effect of the selective 5-HT1A agonists alnespirone (S-20499) and 8-OH-DPAT on extracellular 5-hydroxytryptamine in different regions of rat brain. *Br J Pharmacol, 122*(4), 733-741.

Cases, O., Lebrand, C., Giros, B., Vitalis, T., De Maeyer, E., Caron, M. G., . . . Seif, I. (1998). Plasma membrane transporters of serotonin, dopamine, and norepinephrine mediate serotonin accumulation in atypical locations in the developing brain of monoamine oxidase A knock-outs. *J Neurosci, 18*(17), 6914-6927.

Cases, O., Seif, I., Grimsby, J., Gaspar, P., Chen, K., Pournin, S., . . . et al. (1995). Aggressive behavior and altered amounts of brain serotonin and norepinephrine in mice lacking MAOA. *Science, 268*(5218), 1763-1766.

Cechova, S., & Venton, B. J. (2008). Transient adenosine efflux in the rat caudate-putamen. *J Neurochem, 105*(4), 1253-1263.

Celada, P., Bortolozzi, A., & Artigas, F. (2013). Serotonin 5-HT1A receptors as targets for agents to treat psychiatric disorders: rationale and current status of research. *CNS Drugs, 27*(9), 703-716.

Celada, P., Puig, M., Amargos-Bosch, M., Adell, A., & Artigas, F. (2004). The therapeutic role of 5-HT1A and 5-HT2A receptors in depression. *J Psychiatry Neurosci, 29*(4), 252-265.

Celada, P., Puig, M. V., Casanovas, J. M., Guillazo, G., & Artigas, F. (2001). Control of dorsal raphe serotonergic neurons by the medial prefrontal cortex: Involvement of serotonin-1A, GABA(A), and glutamate receptors. *J Neurosci, 21*(24), 9917-9929.

Chaouloff, F., Berton, O., & Mormede, P. (1999). Serotonin and stress. *Neuropsychopharmacology, 21*(2 Suppl), 28S-32S.

Chaput, Y., Blier, P., & de Montigny, C. (1986). In vivo electrophysiological evidence for the regulatory role of autoreceptors on serotonergic terminals. *J Neurosci, 6*(10), 2796-2801.

Chaput, Y., de Montigny, C., & Blier, P. (1986). Effects of a selective 5-HT reuptake blocker, citalopram, on the sensitivity of 5-HT autoreceptors: electrophysiological studies in the rat brain. *Naunyn Schmiedebergs Arch Pharmacol, 333*(4), 342-348.

Chazal, G., & Ralston, H. J., 3rd. (1987). Serotonin-containing structures in the nucleus raphe dorsalis of the cat: an ultrastructural analysis of dendrites, presynaptic dendrites, and axon terminals. *J Comp Neurol, 259*(3), 317-329.

Clarke, W. P., Yocca, F. D., & Maayani, S. (1996). Lack of 5-hydroxytryptamine1A-mediated inhibition of adenylyl cyclase in dorsal raphe of male and female rats. *J Pharmacol Exp Ther, 277*(3), 1259-1266.

Corvaja, N., Doucet, G., & Bolam, J. P. (1993). Ultrastructure and synaptic targets of the raphe-nigral projection in the rat. *Neuroscience, 55*(2), 417-427.

Cragg, S. J., Hawkey, C. R., & Greenfield, S. A. (1997). Comparison of serotonin and dopamine release in substantia nigra and ventral tegmental area: region and species differences. *J Neurochem, 69*(6), 2378-2386.

Cremers, T. I., Spoelstra, E. N., de Boer, P., Bosker, F. J., Mork, A., den Boer, J. A., . . . Wikstrom, H. V. (2000). Desensitisation of 5-HT autoreceptors upon pharmacokinetically monitored chronic treatment with citalopram. *Eur J Pharmacol, 397*(2-3), 351-357.

Cumming, P., Shaw, C., & Vincent, S. R. (1991). High affinity histamine binding site is the H3 receptor: characterization and autoradiographic localization in rat brain. *Synapse, 8*(2), 144-151.

Dankoski, E. C., & Wightman, R. M. (2013). Monitoring serotonin signaling on a subsecond time scale. *Front Integr Neurosci, 7*, 44.

Davidson, C., & Stamford, J. A. (1995a). The effect of paroxetine on 5-HT efflux in the rat dorsal raphe nucleus is potentiated by both 5-HT1A and 5-HT1B/D receptor antagonists. *Neurosci Lett, 188*(1), 41-44.

Davidson, C., & Stamford, J. A. (1995b). Evidence that 5-hydroxytryptamine release in rat dorsal raphe nucleus is controlled by 5-HT1A, 5-HT1B and 5-HT1D autoreceptors. *Br J Pharmacol, 114*(6), 1107-1109.

Davidson, C., & Stamford, J. A. (1996). Serotonin efflux in the rat ventral lateral geniculate nucleus assessed by fast cyclic voltammetry is modulated by 5-HT1B and 5-HT1D autoreceptors. *Neuropharmacology, 35*(11), 1627-1634.

Davidson, C., & Stamford, J. A. (1997a). Chronic paroxetine desensitises 5-HT1D but not 5-HT1B autoreceptors in rat lateral geniculate nucleus. *Brain Res, 760*(1-2), 238-242.

Davidson, C., & Stamford, J. A. (1997b). Synergism of 5-HT 1B/D antagonists with paroxetine on serotonin efflux in rat ventral lateral geniculate nucleus slices. *Brain Res Bull, 43*(4), 405-409.

Davidson, C., & Stamford, J. A. (1998). Contrasting effects of chronic paroxetine on 5-HT1A control of dorsal raphe cell firing and 5-HT release. *Neuroreport, 9*(11), 2535-2538.

Davidson, C., & Stamford, J. A. (2000). Effect of chronic paroxetine treatment on 5-HT1B and 5-HT1D autoreceptors in rat dorsal raphe nucleus. *Neurochem Int, 36*(2), 91-96.

Daw, N. D., Kakade, S., & Dayan, P. (2002). Opponent interactions between serotonin and dopamine. *Neural Netw, 15*(4-6), 603-616. doi: S0893-6080(02)00052-7 [pii]

Daws, L. C. (2009). Unfaithful neurotransmitter transporters: focus on serotonin uptake and implications for antidepressant efficacy. *Pharmacol Ther, 121*(1), 89-99.

Daws, L. C., Gerhardt, G. A., & Frazer, A. (1999). 5-HT1B antagonists modulate clearance of extracellular serotonin in rat hippocampus. *Neurosci Lett, 266*(3), 165-168.

Daws, L. C., Gould, G. G., Teicher, S. D., Gerhardt, G. A., & Frazer, A. (2000). 5-HT(1B) receptor-mediated regulation of serotonin clearance in rat hippocampus in vivo. *J Neurochem, 75*(5), 2113-2122.

Daws, L. C., & Toney, G. M. (2007). High-Speed Chronoamperometry to Study Kinetics and Mechanisms for Serotonin Clearance In Vivo.

Day, H. E., Greenwood, B. N., Hammack, S. E., Watkins, L. R., Fleshner, M., Maier, S. F., & Campeau, S. (2004). Differential expression of 5HT-1A, alpha 1b adrenergic, CRF-R1, and CRF-R2 receptor mRNA in serotonergic, gamma-aminobutyric acidergic, and catecholaminergic cells of the rat dorsal raphe nucleus. *J Comp Neurol, 474*(3), 364-378.

Day, J. J., Roitman, M. F., Wightman, R. M., & Carelli, R. M. (2007). Associative learning mediates dynamic shifts in dopamine signaling in the nucleus accumbens. *Nat Neurosci, 10*(8), 1020-1028. doi: nn1923 [pii]

de Montigny, C., Pineyro, G., Chaput, Y., & Blier, P. (1992). Electrophysiological studies on the effect of long-term 5-HT reuptake inhibition on the function of 5-HT neurons. *Clin Neuropharmacol, 15 Suppl 1 Pt A*, 440A-441A.

Descarries, L., Audet, M. A., Doucet, G., Garcia, S., Oleskevich, S., Seguela, P., . . . Watkins, K. C. (1990). Morphology of central serotonin neurons. Brief review of quantified aspects of their distribution and ultrastructural relationships. *Ann N Y Acad Sci, 600*, 81-92.

Dewhurst, S. A., Croker, S. G., Ikeda, K., & McCaman, R. E. (1972). Metabolism of biogenic amines in Drosophila nervous tissue. *Comp Biochem Physiol B, 43*(4), 975-981.

Dib, B. (1994). New technique for cannulae implantation into the dorsal raphe nucleus using layer 5 of cerebellum reference in rat stereotaxic surgery. *Pharmacol Biochem Behav, 49*(3), 639-642.

Dong, S., Allen, J. A., Farrell, M., & Roth, B. L. (2010). A chemical-genetic approach for precise spatio-temporal control of cellular signaling. *Mol Biosyst, 6*(8), 1376-1380.

Dray, A., Gonye, T. J., Oakley, N. R., & Tanner, T. (1976). Evidence for the existence of a raphe projection to the substantia nigra in rat. *Brain Res, 113*(1), 45-57.

Dreyer, J. K., Herrik, K. F., Berg, R. W., & Hounsgaard, J. D. (2010). Influence of phasic and tonic dopamine release on receptor activation. *J Neurosci, 30*(42), 14273-14283. doi: 30/42/14273 [pii]

El Yacoubi, M., Bouali, S., Popa, D., Naudon, L., Leroux-Nicollet, I., Hamon, M., . . . Vaugeois, J. M. (2003). Behavioral, neurochemical, and electrophysiological characterization of a genetic mouse model of depression. *Proc Natl Acad Sci U S A, 100*(10), 6227-6232.

Evrard, A., Malagie, I., Laporte, A. M., Boni, C., Hanoun, N., Trillat, A. C., . . . Adrien, J. (2002). Altered regulation of the 5-HT system in the brain of MAO-A knock-out mice. *Eur J Neurosci, 15*(5), 841-851.

Fava, M., Rush, A. J., Alpert, J. E., Balasubramani, G. K., Wisniewski, S. R., Carmin, C. N., . . . Trivedi, M. H. (2008). Difference in treatment outcome in outpatients with anxious versus nonanxious depression: a STAR*D report. *Am J Psychiatry, 165*(3), 342-351.

Ferres-Coy, A., Santana, N., Castane, A., Cortes, R., Carmona, M. C., Toth, M., . . . Bortolozzi, A. (2013). Acute 5-HT(1)A autoreceptor knockdown increases antidepressant responses and serotonin release in stressful conditions. *Psychopharmacology (Berl), 225*(1), 61-74.

Fibiger, H. C., & Miller, J. J. (1977). Anatomical and Electrophysiological Investigation of Serotonergic Projection from Dorsal Raphe Nucleus to Substantia Nigra in Rat. *Neuroscience, 2*(6), 975-987.

Fredricson Overo, K. (1982). Kinetics of citalopram in test animals; drug exposure in safety studies. *Prog Neuropsychopharmacol Biol Psychiatry, 6*(3), 297-309.

Fuxe, K. (1965). Evidence for the Existence of Monoamine Neurons in the Central Nervous System. Iv. Distribution of Monoamine Nerve Terminals in the Central Nervous System. *Acta Physiol Scand Suppl*, SUPPL 247:237+.

Fuxe, K., Dahlstrom, A. B., Jonsson, G., Marcellino, D., Guescini, M., Dam, M., . . . Agnati, L. (2010). The discovery of central monoamine neurons gave volume transmission to the wired brain. *Prog Neurobiol, 90*(2), 82-100.

Garbarg, M., Barbin, G., Bischoff, S., Pollard, H., & Schwartz, J. C. (1976). Dual localization of histamine in an ascending neuronal pathway and in non-neuronal cells evidenced by lesions in the lateral hypothalamic area. *Brain Res, 106*(2), 333-348.

Garbarg, M., Barbin, G., Feger, J., & Schwartz, J. C. (1974). Histaminergic pathway in rat brain evidenced by lesions of the medial forebrain bundle. *Science, 186*(4166), 833-835.

Garcia, M., Floran, B., Arias-Montano, J. A., Young, J. M., & Aceves, J. (1997). Histamine H3 receptor activation selectively inhibits dopamine D1 receptor-dependent [3H]GABA release from depolarization-stimulated slices of rat substantia nigra pars reticulata. *Neuroscience, 80*(1), 241-249.

Garris, P. A., & Wightman, R. M. (1994). Different kinetics govern dopaminergic transmission in the amygdala, prefrontal cortex, and striatum: an in vivo voltammetric study. *J Neurosci, 14*(1), 442-450.

Garris, P. A., & Wightman, R. M. (1995). Regional differences in dopamine release, uptake, and diffusion measured by fast-scan cyclic voltammetry. In A. Boulton, G. Baker & R. N. Adams (Eds.), *Voltammetric Methods in Brain Systems* (pp. 179-220). Totowa, NJ: Humana.

Gartside, S. E., Hajos-Korcsok, E., Bagdy, E., Harsing, L. G., Jr., Sharp, T., & Hajos, M. (2000). Neurochemical and electrophysiological studies on the functional significance of burst firing in serotonergic neurons. *Neuroscience, 98*(2), 295-300.

Gartside, S. E., Umbers, V., Hajos, M., & Sharp, T. (1995). Interaction between a selective 5-HT1A receptor antagonist and an SSRI in vivo: effects on 5-HT cell firing and extracellular 5-HT. *Br J Pharmacol, 115*(6), 1064-1070.

Gaynes, B. N., Rush, A. J., Trivedi, M. H., Wisniewski, S. R., Spencer, D., & Fava, M. (2008). The STAR*D study: treating depression in the real world. *Cleve Clin J Med, 75*(1), 57-66.

Gerhardt, G., & Adams, R. N. (1982). Determination of Diffusion-Coefficients by Flow-Injection Analysis. *Anal Chem, 54*(14), 2618-2620.

Gerhardt, G. A., Oke, A. F., Nagy, G., Moghaddam, B., & Adams, R. N. (1984). Nafion-coated electrodes with high selectivity for CNS electrochemistry. *Brain Res, 290*(2), 390-395.

Gerhardt, G. A., Oke, A. F., Nagy, G., Moghaddam, B., & Adams, R. N. (1984). Nafion-coated electrodes with high selectivity for CNS electrochemistry. *Brain Res., 290*, 390-395.

Gobbi, G., Murphy, D. L., Lesch, K., & Blier, P. (2001). Modifications of the serotonergic system in mice lacking serotonin transporters: an in vivo electrophysiological study. *J Pharmacol Exp Ther, 296*(3), 987-995.

Gonon, F. G., & Buda, M. J. (1985). Regulation of dopamine release by impulse flow and by autoreceptors as studied by in vivo voltammetry in the rat striatum. *Neurosci., 14*, 765-774.

Grace, A. A., & Bunney, B. S. (1983). Intracellular and extracellular electrophysiology of nigral dopaminergic neurons--1. Identification and characterization. *Neuroscience, 10*(2), 301-315.

Haber, S. N., & Knutson, B. (2010). The reward circuit: linking primate anatomy and human imaging. *Neuropsychopharmacology, 35*(1), 4-26. doi: npp2009129 [pii]

Hafizi, S., Kruk, Z. L., & Stamford, J. A. (1990). Fast cyclic voltammetry: improved sensitivity to dopamine with extended oxidation scan limits. *J Neurosci Methods, 33*(1), 41-49.

Hagan, C. E., Schenk, J. O., & Neumaier, J. F. (2011). The contribution of low-affinity transport mechanisms to serotonin clearance in synaptosomes. *Synapse, 65*(10), 1015-1023.

Hajos-Korcsok, E., & Sharp, T. (2002). Electrical stimulation of the dorsal and median raphe nuclei increases extracellular noradrenaline in rat hippocampus: Evidence for a 5-HT-independent mechanism. *Pharmacol Biochem Behav, 71*(4), 807-813.

Hajos, M., Gartside, S. E., Villa, A. E., & Sharp, T. (1995). Evidence for a repetitive (burst) firing pattern in a sub-population of 5-hydroxytryptamine neurons in the dorsal and median raphe nuclei of the rat. *Neuroscience, 69*(1), 189-197.

Hajos, M., & Sharp, T. (1996). Burst-firing activity of presumed 5-HT neurones of the rat dorsal raphe nucleus: electrophysiological analysis by antidromic stimulation. *Brain Res, 740*(1-2), 162-168.

Halaris, A. E., Jones, B. E., & Moore, R. Y. (1976). Axonal-Transport in Serotonin Neurons of Midbrain Raphe. *Brain Res, 107*(3), 555-574.

Hashemi, P., Dankoski, E. C., Lama, R., Wood, K. M., Takmakov, P., & Wightman, R. M. (2012). Brain dopamine and serotonin differ in regulation and its consequences. *Proc Natl Acad Sci U S A, 109*(29), 11510-11515.

Hashemi, P., Dankoski, E. C., Petrovic, J., Keithley, R. B., & Wightman, R. M. (2009). Voltammetric detection of 5-hydroxytryptamine release in the rat brain. *Anal Chem, 81*(22), 9462-9471.

Hashemi, P., Dankoski, E. C., Wood, K. M., Ambrose, R. E., & Wightman, R. M. (2011). In vivo electrochemical evidence for simultaneous 5-HT and histamine release in the rat substantia nigra pars reticulata following medial forebrain bundle stimulation. *J Neurochem, 118*(5), 749-759. doi: 10.1111/j.1471-4159.2011.07352.x

Heeringa, M. J., & Abercrombie, E. D. (1995). Biochemistry of somatodendritic dopamine release in substantia nigra: an in vivo comparison with striatal dopamine release. *J Neurochem, 65*(1), 192-200.

Heien, M. L., Phillips, P. E., Stuber, G. D., Seipel, A. T., & Wightman, R. M. (2003). Overoxidation of carbon-fiber microelectrodes enhances dopamine adsorption and increases sensitivity. *Analyst, 128*(12), 1413-1419.

Henry, J. P., Sagne, C., Bedet, C., & Gasnier, B. (1998). The vesicular monoamine transporter: from chromaffin granule to brain. *Neurochem Int, 32*(3), 227-246. doi: S0197018697000922 [pii]

Herr, N. R., & Wightman, R. M. (2013). Improved techniques for examining rapid dopamine signaling with iontophoresis. *Front Biosci (Elite Ed), 5*, 249-257.

Hewton, R., Salem, A., & Irvine, R. J. (2007). Potentiation of 3,4-methylenedioxymethamphetamine-induced 5-HT release in the rat substantia nigra by clorgyline, a monoamine oxidase A inhibitor. *Clin Exp Pharmacol Physiol, 34*(10), 1051-1057.

Hjorth, S. (1993). Serotonin 5-HT1A autoreceptor blockade potentiates the ability of the 5-HT reuptake inhibitor citalopram to increase nerve terminal output of 5-HT in vivo: a microdialysis study. *J Neurochem, 60*(2), 776-779.

Hjorth, S., & Sharp, T. (1991). Effect of the 5-HT1A receptor agonist 8-OH-DPAT on the release of 5-HT in dorsal and median raphe-innervated rat brain regions as measured by in vivo microdialysis. *Life Sci, 48*(18), 1779-1786.

Hopwood, S. E., & Stamford, J. A. (2001). Multiple 5-HT(1) autoreceptor subtypes govern serotonin release in dorsal and median raphe nuclei. *Neuropharmacology, 40*(4), 508-519.

Hyttel, J. (1982). Citalopram--pharmacological profile of a specific serotonin uptake inhibitor with antidepressant activity. *Prog Neuropsychopharmacol Biol Psychiatry, 6*(3), 277-295.

Ichimaru, Y., Egawa, T., & Sawa, A. (1995). 5-HT1A-receptor subtype mediates the effect of fluvoxamine, a selective serotonin reuptake inhibitor, on marble-burying behavior in mice. *Jpn J Pharmacol, 68*(1), 65-70.

Imai, H., Steindler, D. A., & Kitai, S. T. (1986). The organization of divergent axonal projections from the midbrain raphe nuclei in the rat. *J Comp Neurol, 243*(3), 363-380.

Invernizzi, R., Belli, S., & Samanin, R. (1992). Citalopram's ability to increase the extracellular concentrations of serotonin in the dorsal raphe prevents the drug's effect in the frontal cortex. *Brain Res, 584*(1-2), 322-324.

Invernizzi, R., Bramante, M., & Samanin, R. (1995). Extracellular concentrations of serotonin in the dorsal hippocampus after acute and chronic treatment with citalopram. *Brain Res, 696*(1-2), 62-66.

Invernizzi, R. W., Pierucci, M., Calcagno, E., Di Giovanni, G., Di Matteo, V., Benigno, A., & Esposito, E. (2007). Selective activation of 5-HT(2C) receptors stimulates GABA-ergic function in the rat substantia nigra pars reticulata: a combined in vivo electrophysiological and neurochemical study. *Neuroscience, 144*(4), 1523-1535. doi: S0306-4522(06)01521-1 [pii]

Iravani, M. M., & Kruk, Z. L. (1997). Real-time measurement of stimulated 5-hydroxytryptamine release in rat substantia nigra pars reticulata brain slices. *Synapse, 25*(1), 93-102.

Iravani, M. M., Muscat, R., & Kruk, Z. L. (1999). MK-801 interaction with the 5-HT transporter: a real-time study in brain slices using fast cyclic voltammetry. *Synapse, 32*(3), 212-224.

Iversen, L. L. (1974). Uptake mechanisms for neurotransmitter amines. *Biochem Pharmacol, 23*(14), 1927-1935.

Izumi, T., Iwamoto, N., Kitaichi, Y., Kato, A., Inoue, T., & Koyama, T. (2006). Effects of co-administration of a selective serotonin reuptake inhibitor and monoamine oxidase inhibitors on 5-HT-related behavior in rats. *Eur J Pharmacol, 532*(3), 258-264. doi: S0014-2999(05)01344-0 [pii]

Jackson, B. P., Dietz, S. M., & Wightman, R. M. (1995). Fast-scan cyclic voltammetry of 5-hydroxytryptamine. *Anal Chem, 67*(6), 1115-1120.

Jacobs, B. L. (1991). Serotonin and behavior: emphasis on motor control. *J Clin Psychiatry, 52 Suppl*, 17-23.

Jacobs, B. L., & Fornal, C. A. (1999). Activity of serotonergic neurons in behaving animals. *Neuropsychopharmacology, 21*(2 Suppl), 9S-15S. doi: 10.1016/S0893-133X(99)00012-3

Jacobsen, J. P., Medvedev, I. O., & Caron, M. G. (2012). The 5-HT deficiency theory of depression: perspectives from a naturalistic 5-HT deficiency model, the tryptophan hydroxylase 2Arg439His knockin mouse. *Philos Trans R Soc Lond B Biol Sci, 367*(1601), 2444-2459.

Jain, M., Sands, F., & Von Korff, R. W. (1973). Monoamine oxidase activity measurements using radioactive substrates. *Anal Biochem, 52*(2), 542-554.

Jennings, K. A., Lesch, K. P., Sharp, T., & Cragg, S. J. (2010). Non-linear relationship between 5-HT transporter gene expression and frequency sensitivity of 5-HT signals. *J Neurochem, 115*(4), 965-973.

Jiao, J., Nitzke, A. M., Doukas, D. G., Seiglie, M. P., & Dulawa, S. C. (2011). Antidepressant response to chronic citalopram treatment in eight inbred mouse strains. *Psychopharmacology (Berl), 213*(2-3), 509-520.

John, C. E., Budygin, E. A., Mateo, Y., & Jones, S. R. (2006). Neurochemical characterization of the release and uptake of dopamine in ventral tegmental area and serotonin in substantia nigra of the mouse. *J Neurochem, 96*(1), 267-282.

John, C. E., & Jones, S. R. (2007a). Fast Scan Cyclic Voltammetry of Dopamine and Serotonin in Mouse Brain Slices.

John, C. E., & Jones, S. R. (2007b). Voltammetric characterization of the effect of monoamine uptake inhibitors and releasers on dopamine and serotonin uptake in mouse caudate-putamen and substantia nigra slices. *Neuropharmacology, 52*(8), 1596-1605.

Johnson, D. A., Grant, E. J., Ingram, C. D., & Gartside, S. E. (2007). Glucocorticoid receptor antagonists hasten and augment neurochemical responses to a selective serotonin reuptake inhibitor antidepressant. *Biol Psychiatry, 62*(11), 1228-1235.

Jones, S. R., Gainetdinov, R. R., Hu, X. T., Cooper, D. C., Wightman, R. M., White, F. J., & Caron, M. G. (1999). Loss of autoreceptor functions in mice lacking the dopamine transporter. *Nat Neurosci, 2*(7), 649-655.

Judge, S. J., & Gartside, S. E. (2006). Firing of 5-HT neurones in the dorsal and median raphe nucleus in vitro shows differential alpha1-adrenoceptor and 5-HT1A receptor modulation. *Neurochem Int, 48*(2), 100-107.

Karelina, K., & DeVries, A. C. (2011). Modeling social influences on human health. *Psychosom Med, 73*(1), 67-74.

Katai, Z., Adori, C., Kitka, T., Vas, S., Kalmar, L., Kostyalik, D., . . . Bagdy, G. (2013). Acute escitalopram treatment inhibits REM sleep rebound and activation of MCH-expressing

neurons in the lateral hypothalamus after long term selective REM sleep deprivation. *Psychopharmacology (Berl), 228*(3), 439-449.

Kawagoe, K. T., & Wightman, R. M. (1994). Characterization of amperometry for in vivo measurement of dopamine dynamics in the rat brain. *Talanta, 41*(6), 865-874.

Kessler, R. C., Berglund, P., Demler, O., Jin, R., Koretz, D., Merikangas, K. R., . . . Wang, P. S. (2003). The epidemiology of major depressive disorder: results from the National Comorbidity Survey Replication (NCS-R). *Jama, 289*(23), 3095-3105.

Kia, H. K., Brisorgueil, M. J., Hamon, M., Calas, A., & Verge, D. (1996). Ultrastructural localization of 5-hydroxytryptamine1A receptors in the rat brain. *J Neurosci Res, 46*(6), 697-708.

Kirby, L. G., Freeman-Daniels, E., Lemos, J. C., Nunan, J. D., Lamy, C., Akanwa, A., & Beck, S. G. (2008). Corticotropin-releasing factor increases GABA synaptic activity and induces inward current in 5-hydroxytryptamine dorsal raphe neurons. *J Neurosci, 28*(48), 12927-12937.

Kita, J. M., Kile, B. M., Parker, L. E., & Wightman, R. M. (2009). In vivo measurement of somatodendritic release of dopamine in the ventral tegmental area. *Synapse, 63*(11), 951-960.

Kohler, C., Hall, H., Ogren, S. O., & Gawell, L. (1985). Specific in vitro and in vivo binding of 3H-raclopride. A potent substituted benzamide drug with high affinity for dopamine D-2 receptors in the rat brain. *Biochem Pharmacol, 34*(13), 2251-2259.

Kohler, C., Swanson, L. W., Haglund, L., & Wu, J. Y. (1985). The cytoarchitecture, histochemistry and projections of the tuberomammillary nucleus in the rat. *Neuroscience, 16*(1), 85-110.

Korotkova, T. M., Haas, H. L., & Brown, R. E. (2002). Histamine excites GABAergic cells in the rat substantia nigra and ventral tegmental area in vitro. *Neurosci Lett, 320*(3), 133-136.

Kovacevic, T., Skelin, I., & Diksic, M. (2010). Chronic fluoxetine treatment has a larger effect on the density of a serotonin transporter in the Flinders Sensitive Line (FSL) rat model of depression than in normal rats. *Synapse, 64*(3), 231-240.

Kovachich, G. B., Aronson, C. E., Brunswick, D. J., & Frazer, A. (1988). Quantitative autoradiography of serotonin uptake sites in rat brain using [3H]cyanoimipramine. *Brain Res, 454*(1-2), 78-88.

Kreiss, D. S., & Lucki, I. (1994). Differential regulation of serotonin (5-HT) release in the striatum and hippocampus by 5-HT1A autoreceptors of the dorsal and median raphe nuclei. *J Pharmacol Exp Ther, 269*(3), 1268-1279.

Kreiss, D. S., & Lucki, I. (1997). Chronic administration of the 5-HT1A receptor agonist 8-OH-DPAT differentially desensitizes 5-HT1A autoreceptors of the dorsal and median raphe nuclei. *Synapse, 25*(2), 107-116.

Kristensen, E. W., Kuhr, W. G., & Wightman, R. M. (1987). Temporal characterization of perfluorinated ion exchange coated microvoltammeteric electrodes for in vivo use. *Anal.Chem., 59*, 1752-1757.

Kristensen, E. W., Wilson, R. L., & Wightman, R. M. (1986a). Dispersion in Flow-Injection Analysis Measured with Microvoltammetric Electrodes. *Anal Chem, 58*(4), 986-988.

Kristensen, E. W., Wilson, R. L., & Wightman, R. M. (1986b). Dispersion in Flow-Injection Analysis Measured with Microvoltammetric Electrodes. *Analytical Chemistry, 58*(4), 986-988.

Lahdesmaki, J., Sallinen, J., MacDonald, E., Kobilka, B. K., Fagerholm, V., & Scheinin, M. (2002). Behavioral and neurochemical characterization of alpha(2A)-adrenergic receptor knockout mice. *Neuroscience, 113*(2), 289-299.

Lama, R. D., Charlson, K., Anantharam, A., & Hashemi, P. (2012). Ultrafast detection and quantification of brain signaling molecules with carbon fiber microelectrodes. *Anal Chem, 84*(19), 8096-8101.

Lane, R., & Baldwin, D. (1997). Selective serotonin reuptake inhibitor-induced serotonin syndrome: review. *J Clin Psychopharmacol, 17*(3), 208-221.

Larsson, K., & Komisaruk, B. R. (1972). Abnormally fast vibrissa movements induced by tetrabenazine in rats. *Psychopharmacologia, 23*(3), 300-304.

Levine, E. S., & Jacobs, B. L. (1992). Neurochemical afferents controlling the activity of serotonergic neurons in the dorsal raphe nucleus: microiontophoretic studies in the awake cat. *J Neurosci, 12*(10), 4037-4044.

Limberger, N., Trout, S. J., Kruk, Z. L., & Starke, K. (1991). "Real time" measurement of endogenous dopamine release during short trains of pulses in slices of rat neostriatum and nucleus accumbens: role of autoinhibition. *Naunyn Schmiedebergs Arch Pharmacol, 344*(6), 623-629.

Marley, E., & Wozniak, K. M. (1984). Interactions of a non-selective monoamine oxidase inhibitor, phenelzine, with inhibitors of 5-hydroxytryptamine, dopamine or noradrenaline re-uptake. *Journal of psychiatric research, 18*(2), 173-189.

May, L. J., Kuhr, W. G., & Wightman, R. M. (1988). Differentiation of dopamine overflow and uptake processes in the extracellular fluid of the rat caudate nucleus with fast-scan in vivo voltammetry. *J Neurochem, 51*(4), 1060-1069.

Mefford, I. N. (1981). Application of high performance liquid chromatography with electrochemical detection to neurochemical analysis: measurement of catecholamines, serotonin and metabolites in rat brain. *J Neurosci Methods, 3*(3), 207-224.

Merrill, E. G., Wall, P. D., & Yaksh, T. L. (1978). Properties of two unmyelinated fibre tracts of the central nervous system: lateral Lissauer tract, and parallel fibres of the cerebellum. *J Physiol, 284*, 127-145.

Michael, D., Travis, E. R., & Wightman, R. M. (1998). Color images for fast-scan CV measurements in biological systems. *Anal Chem, 70*(17), 586A-592A.

Michael, D. J., Joseph, J. D., Kilpatrick, M. R., Travis, E. R., & Wightman, R. M. (1999). Improving data acquisition for fast-scan cyclic voltammetry. *Anal Chem, 71*(18), 3941-3947.

Miele, M., & Fillenz, M. (1996). In vivo determination of extracellular brain ascorbate. *J Neurosci Methods, 70*(1), 15-19.

Millar, J., Stamford, J. A., Kruk, Z. L., & Wightman, R. M. (1985). Electrochemical, pharmacological and electrophysiological evidence of rapid dopamine release and removal in the rat caudate nucleus following electrical stimulation of the median forebrain bundle. *Eur J Pharmacol, 109*(3), 341-348.

Miller, J. J., Richardson, T. L., Fibiger, H. C., & McLennan, H. (1975). Anatomical and electrophysiological identification of a projection from the mesencephalic raphe to the caudate-putamen in the rat. *Brain Res, 97*(1), 133-136.

Mitchell, P. B. (1997). Drug interactions of clinical significance with selective serotonin reuptake inhibitors. *Drug Saf, 17*(6), 390-406.

Molliver, M. E. (1987). Serotonergic neuronal systems: what their anatomic organization tells us about function. *J Clin Psychopharmacol, 7*(6 Suppl), 3S-23S.

Monachon, M. A., Burkard, W. P., Jalfre, M., & Haefely, W. (1972). Blockade of central 5-hydroxytryptamine receptors by methiothepin. *Naunyn Schmiedebergs Arch Pharmacol, 274*(2), 192-197.

Montague, P. R., McClure, S. M., Baldwin, P. R., Phillips, P. E., Budygin, E. A., Stuber, G. D., . . . Wightman, R. M. (2004). Dynamic gain control of dopamine delivery in freely moving animals. *J Neurosci, 24*(7), 1754-1759. doi: 10.1523/JNEUROSCI.4279-03.2004

Moore, R. Y., Halaris, A. E., & Jones, B. E. (1978a). Serotonin Neurons of Midbrain Raphe - Ascending Projections. *Journal of Comparative Neurology, 180*(3), 417-&.

Moore, R. Y., Halaris, A. E., & Jones, B. E. (1978b). Serotonin neurons of the midbrain raphe: ascending projections. *J Comp Neurol, 180*(3), 417-438.

Moret, C., & Briley, M. (1996). Effects of acute and repeated administration of citalopram on extracellular levels of serotonin in rat brain. *Eur J Pharmacol, 295*(2-3), 189-197.

Moret, C., & Briley, M. (1997). 5-HT autoreceptors in the regulation of 5-HT release from guinea pig raphe nucleus and hypothalamus. *Neuropharmacology, 36*(11-12), 1713-1723.

Mosko, S. S., Haubrich, D., & Jacobs, B. L. (1977). Serotonergic afferents to the dorsal raphe nucleus: evdience from HRP and synaptosomal uptake studies. *Brain Res, 119*(2), 269-290.

Moukhles, H., Bosler, O., Bolam, J. P., Vallee, A., Umbriaco, D., Geffard, M., & Doucet, G. (1997). Quantitative and morphometric data indicate precise cellular interactions between serotonin terminals and postsynaptic targets in rat substantia nigra. *Neuroscience, 76*(4), 1159-1171.

Muck-Seler, D., & Diksic, M. (1995). The acute effects of reserpine and NSD-1015 on the brain serotonin synthesis rate measured by an autoradiographic method. *Neuropsychopharmacology, 12*(3), 251-262. doi: 0893-133X(94)00084-D [pii]

Nestler, E. J., & Hyman, S. E. (2010). Animal models of neuropsychiatric disorders. *Nat Neurosci, 13*(10), 1161-1169.

O'Connor, J. J., & Kruk, Z. L. (1991a). Fast cyclic voltammetry can be used to measure stimulated endogenous 5-hydroxytryptamine release in untreated rat brain slices. *J Neurosci Methods, 38*(1), 25-33.

O'Connor, J. J., & Kruk, Z. L. (1991b). Frequency dependence of 5-HT autoreceptor function in rat dorsal raphe and suprachiasmatic nuclei studied using fast cyclic voltammetry. *Brain Res, 568*(1-2), 123-130.

O'Connor, J. J., & Kruk, Z. L. (1992). Pharmacological characteristics of 5-hydroxytryptamine autoreceptors in rat brain slices incorporating the dorsal raphe or the suprachiasmatic nucleus. *Br J Pharmacol, 106*(3), 524-532.

O'Connor, J. J., & Kruk, Z. L. (1994). Effects of 21 days treatment with fluoxetine on stimulated endogenous 5-hydroxytryptamine overflow in the rat dorsal raphe and suprachiasmatic nucleus studied using fast cyclic voltammetry in vitro. *Brain Res, 640*(1-2), 328-335.

Oh, E., Maejima, T., Liu, C., Deneris, E., & Herlitze, S. (2010). Substitution of 5-HT1A receptor signaling by a light-activated G protein-coupled receptor. *J Biol Chem, 285*(40), 30825-30836.

Ohno, Y. (2010). New insight into the therapeutic role of 5-HT1A receptors in central nervous system disorders. *Cent Nerv Syst Agents Med Chem, 10*(2), 148-157.

Oreland, L., Nordquist, N., Hallman, J., Harro, J., & Nilsson, K. W. (2010). Environment and the serotonergic system. *Eur Psychiatry, 25*(5), 304-306.

Owesson-White, C. A., Cheer, J. F., Beyene, M., Carelli, R. M., & Wightman, R. M. (2008). Dynamic changes in accumbens dopamine correlate with learning during intracranial self-stimulation. *Proc Natl Acad Sci U S A, 105*(33), 11957-11962. doi: 0803896105 [pii]

Owesson-White, C. A., Roitman, M. F., Sombers, L. A., Belle, A. M., Keithley, R. B., Peele, J. L., . . . Wightman, R. M. (2012). Sources contributing to the average extracellular concentration of dopamine in the nucleus accumbens. *J Neurochem, 121*(2), 252-262. doi: 10.1111/j.1471-4159.2012.07677.x

Owesson, C. A., Hopwood, S. E., Callado, L. F., Seif, I., McLaughlin, D. P., & Stamford, J. A. (2002). Altered presynaptic function in monoaminergic neurons of monoamine oxidase-A knockout mice. *Eur J Neurosci, 15*(9), 1516-1522.

Palkovits, M., Brownstein, M., & Saavedra, J. M. (1974). Serotonin content of the brain stem nuclei in the rat. *Brain Res, 80*(2), 237-249.

Panula, P., Pirvola, U., Auvinen, S., & Airaksinen, M. S. (1989). Histamine-immunoreactive nerve fibers in the rat brain. *Neuroscience, 28*(3), 585-610.

Parent, A., Descarries, L., & Beaudet, A. (1981). Organization of ascending serotonin systems in the adult rat brain. A radioautographic study after intraventricular administration of [3H]5-hydroxytryptamine. *Neuroscience, 6*(2), 115-138.

Pariante, C. M., & Miller, A. H. (2001). Glucocorticoid receptors in major depression: relevance to pathophysiology and treatment. *Biol Psychiatry, 49*(5), 391-404.

Park, J., Kile, B. M., & Wightman, R. M. (2009). In vivo voltammetric monitoring of norepinephrine release in the rat ventral bed nucleus of the stria terminalis and anteroventral thalamic nucleus. *Eur J Neurosci, 30*(11), 2121-2133.

Park, J., Quaiserova-Mocko, V., Patel, B. A., Novotny, M., Liu, A., Bian, X., . . . Swain, G. M. (2008). Diamond microelectrodes for in vitro electroanalytical measurements: current status and remaining challenges. *Analyst, 133*(1), 17-24.

Park, J., Takmakov, P., & Wightman, R. M. (2011). In vivo comparison of norepinephrine and dopamine release in rat brain by simultaneous measurements with fast-scan cyclic voltammetry. *J Neurochem, 119*(5), 932-944. doi: 10.1111/j.1471-4159.2011.07494.x

Patel, B. A., Bian, X., Quaiserova-Mocko, V., Galligan, J. J., & Swain, G. M. (2007). In vitro continuous amperometric monitoring of 5-hydroxytryptamine release from enterochromaffin cells of the guinea pig ileum. *Analyst, 132*(1), 41-47.

Paxinos, G., & Watson, C. (2007). *The Rat Brain in Stereotaxic Coordinates* (6th ed.): Elsevier.

Pazos, A., & Palacios, J. M. (1985). Quantitative autoradiographic mapping of serotonin receptors in the rat brain. I. Serotonin-1 receptors. *Brain Res, 346*(2), 205-230.

Pellegrino de Iraldi, A. (1992). Compartmentalization of monoaminergic synaptic vesicles in the storage and release of neurotransmitter. *Mol Neurobiol, 6*(4), 323-337.

Perry, K. W., & Fuller, R. W. (1992). Effect of fluoxetine on serotonin and dopamine concentration in microdialysis fluid from rat striatum. *Life Sci, 50*(22), 1683-1690.

Petty, F., Davis, L. L., Kabel, D., & Kramer, G. L. (1996). Serotonin dysfunction disorders: a behavioral neurochemistry perspective. *J Clin Psychiatry, 57 Suppl 8*, 11-16.

Phillips, P. E., Hancock, P. J., & Stamford, J. A. (2002). Time window of autoreceptor-mediated inhibition of limbic and striatal dopamine release. *Synapse, 44*(1), 15-22.

Phillips, P. E. M., & Wightman, R. M. (2003). Critical guidelines for validation of the selectivity of in-vivo chemical microsensors. *Trac-Trends in Analytical Chemistry, 22*(9), 509-514.

Pihel, K., Hsieh, S., Jorgenson, J. W., & Wightman, R. M. (1995). Electrochemical detection of histamine and 5-hydroxytryptamine at isolated mast cells. *Anal.Chem., 67*, 4514-4521.

Pihel, K., Hsieh, S., Jorgenson, J. W., & Wightman, R. M. (1998). Quantal corelease of histamine and 5-hydroxytryptamine from mast cells and the effects of prior incubation. *Biochemistry, 37*(4), 1046-1052.

Pineyro, G., & Blier, P. (1999). Autoregulation of serotonin neurons: role in antidepressant drug action. *Pharmacol Rev, 51*(3), 533-591.

Pineyro, G., Castanon, N., Hen, R., & Blier, P. (1995). Regulation of [3H]5-HT release in raphe, frontal cortex and hippocampus of 5-HT1B knock-out mice. *Neuroreport, 7*(1), 353-359.

Pollard, H., Llorens-Cortes, C., Barbin, G., Garbarg, M., & Schwartz, J. C. (1978). Histamine and histidine decarboxylase in brain stem nuclei: distribution and decrease after lesions. *Brain Res, 157*(1), 178-181.

Pollard, H., Moreau, J., Arrang, J. M., & Schwartz, J. C. (1993). A detailed autoradiographic mapping of histamine H3 receptors in rat brain areas. *Neuroscience, 52*(1), 169-189.

Quinn, G. P., Shore, P. A., & Brodie, B. B. (1959). Biochemical and pharmacological studies of RO 1-9569 (tetrabenazine), a nonindole tranquilizing agent with reserpine-like effects. *J Pharmacol Exp Ther, 127*, 103-109.

Ranganathan, S., Kuo, T.-C., & McCreery, R. L. (1999). Facile Preparation of Active Glassy Carbon Electrodes with Activated Carbon and Organic Solvents. *Anal Chem, 71*(16), 3574-3580.

Reid, M. S., Hsu, K., Jr., & Berger, S. P. (1997). Cocaine and amphetamine preferentially stimulate glutamate release in the limbic system: studies on the involvement of dopamine. *Synapse, 27*(2), 95-105. doi: 10.1002/(SICI)1098-2396(199710)27:2<95::AID-SYN1>3.0.CO;2-6 [pii]

Reubi, J. C., & Emson, P. C. (1978). Release and distribution of endogenous 5-HT in rat substantia nigra. *Brain Res, 139*(1), 164-168.

Riad, M., Watkins, K. C., Doucet, E., Hamon, M., & Descarries, L. (2001). Agonist-induced internalization of serotonin-1a receptors in the dorsal raphe nucleus (autoreceptors) but not hippocampus (heteroreceptors). *J Neurosci, 21*(21), 8378-8386.

Riad, M., Zimmer, L., Rbah, L., Watkins, K. C., Hamon, M., & Descarries, L. (2004). Acute treatment with the antidepressant fluoxetine internalizes 5-HT1A autoreceptors and reduces the in vivo binding of the PET radioligand [18F]MPPF in the nucleus raphe dorsalis of rat. *J Neurosci, 24*(23), 5420-5426.

Rice, M. E. (1999). Use of ascorbate in the preparation and maintenance of brain slices. *Methods, 18*(2), 144-149.

Rice, M. E., & Nicholson, C. (1989). Measurement of nanomolar dopamine diffusion using low-noise perfluorinated ionomer coated carbon fiber microelectrodes and high-speed cyclic voltammetry. *Anal Chem, 61*(17), 1805-1810.

Rice, M. E., Richards, C. D., Nedergaard, S., Hounsgaard, J., Nicholson, C., & Greenfield, S. A. (1994). Direct monitoring of dopamine and 5-HT release in substantia nigra and ventral tegmental area in vitro. *Exp Brain Res, 100*(3), 395-406.

Roberts, C., & Price, G. W. (2001). Interaction of serotonin autoreceptor antagonists in the rat dorsal raphe nucleus: an in vitro fast cyclic voltammetry study. *Neurosci Lett, 300*(1), 45-48.

Robinson, D. L., Hermans, A., Seipel, A. T., & Wightman, R. M. (2008). Monitoring rapid chemical communication in the brain. *Chem Rev, 108*(7), 2554-2584. doi: 10.1021/cr068081q

Robinson, D. L., & Wightman, R. M. (2004). Nomifensine amplifies subsecond dopamine signals in the ventral striatum of freely-moving rats. *J Neurochem, 90*(4), 894-903.

Robinson, D. L., & Wightman, R. M. (2007). Rapid dopamine release in freely moving rats. In A. C. Michael & L. M. Borland (Eds.), *Electrochemical Methods for Neuroscience* (pp. 17-36). Boca Raton, FL: CRC Press.

Rocha, L. S., & Carapuca, H. M. (2006). Ion-exchange voltammetry of dopamine at Nafion-coated glassy carbon electrodes: quantitative features of ion-exchange partition and reassessment on the oxidation mechanism of dopamine in the presence of excess ascorbic acid. *Bioelectrochemistry, 69*(2), 258-266.

Ross, S. B., & Stenfors, C. (1997). The forgotten 5-hydroxyindoleacetic acid. *J Neurochem, 69*(1), 437-439.

Rossi, D. V., Burke, T. F., McCasland, M., & Hensler, J. G. (2008). Serotonin-1A receptor function in the dorsal raphe nucleus following chronic administration of the selective serotonin reuptake inhibitor sertraline. *J Neurochem, 105*(4), 1091-1099.

Rueter, L. E., Fornal, C. A., & Jacobs, B. L. (1997). A critical review of 5-HT brain microdialysis and behavior. *Rev Neurosci, 8*(2), 117-137.

Sanford, A. L., Morton, S. W., Whitehouse, K. L., Oara, H. M., Lugo-Morales, L. Z., Roberts, J. G., & Sombers, L. A. (2010). Voltammetric Detection of Hydrogen Peroxide at Carbon Fiber Microelelctrodes. *Anal Chem, In press*.

Sari, Y. (2004). Serotonin1B receptors: from protein to physiological function and behavior. *Neurosci Biobehav Rev, 28*(6), 565-582.

Schenk, J. O., Miller, E., Gaddis, R., & Adams, R. N. (1982). Homeostatic control of ascorbate concentration in CNS extracellular fluid. *Brain Res, 253*(1-2), 353-356.

Schoups, A., Dillen, L., Claeys, M., Duchateau, A., Verbeuren, T. J., & De Potter, W. P. (1986). Characterization of serotonin receptors and lack of effect of antidepressant therapy on monoamine functions in various regions of the rabbit brain. *Eur J Pharmacol, 126*(3), 259-271.

Schultz, K. N., & Kennedy, R. T. (2008). Time-resolved microdialysis for in vivo neurochemical measurements and other applications. *Annu Rev Anal Chem (Palo Alto Calif), 1*, 627-661.

Schwartz, J. C., Arrang, J. M., Garbarg, M., Pollard, H., & Ruat, M. (1991). Histaminergic transmission in the mammalian brain. *Physiol Rev, 71*(1), 1-51.

Sesack, S. R., Aoki, C., & Pickel, V. M. (1994). Ultrastructural localization of D2 receptor-like immunoreactivity in midbrain dopamine neurons and their striatal targets. *J Neurosci, 14*(1), 88-106.

Shaskan, E. G., & Snyder, S. H. (1970). Kinetics of serotonin accumulation into slices from rat brain: relationship to catecholamine uptake. *J Pharmacol Exp Ther, 175*(2), 404-418.

Shields, P. J., & Eccleston, D. (1973). Evidence for the synthesis and storage of 5-hydroxytryptamine in two separate pools in the brain. *J Neurochem, 20*(3), 881-888.

Shore, P. A. (1976). Actions of amfonelic acid and other non-amphetamine stimulants on the dopamine neuron. *J Pharm Pharmacol, 28*(11), 855-857.

Silvani, A., Bojic, T., Cianci, T., Franzini, C., Lenzi, P., Lucchi, M. L., & Zoccoli, G. (2004). Brain capillary perfusion in the spontaneously hypertensive rat during the wake-sleep cycle. *Exp Brain Res, 154*(1), 44-49.

Smith, A. D., Olson, R. J., & Justice, J. B., Jr. (1992). Quantitative microdialysis of dopamine in the striatum: effect of circadian variation. *J Neurosci Methods, 44*(1), 33-41.

Sombers, L. A., Beyene, M., Carelli, R. M., & Wightman, R. M. (2009). Synaptic overflow of dopamine in the nucleus accumbens arises from neuronal activity in the ventral tegmental area. *J Neurosci, 29*(6), 1735-1742. doi: 29/6/1735 [pii]

Sprouse, J. S., & Aghajanian, G. K. (1987). Electrophysiological responses of serotoninergic dorsal raphe neurons to 5-HT1A and 5-HT1B agonists. *Synapse, 1*(1), 3-9.

Stamford, J. A. (1985). In vivo voltammetry: promise and perspective. *Brain Res, 357*(2), 119-135.

Stamford, J. A., Davidson, C., McLaughlin, D. P., & Hopwood, S. E. (2000). Control of dorsal raphe 5-HT function by multiple 5-HT(1) autoreceptors: parallel purposes or pointless plurality? *Trends Neurosci, 23*(10), 459-465.

Stamford, J. A., Kruk, Z. L., & Millar, J. (1988). Stimulated limbic and striatal dopamine release measured by fast cyclic voltammetry: anatomical, electrochemical and pharmacological characterisation. *Brain Res, 454*(1-2), 282-288. doi: 0006-8993(88)90828-1 [pii]

Stamford, J. A., Kruk, Z. L., & Millar, J. (1988). Stimulated limbic and striatal dopamine release measured by fast cyclic voltammetry: anatomical, electrochemical and pharmacological characterisation. *Brain Res, 454*(1-2), 282-288.

Stamford, J. A., Kruk, Z. L., & Millar, J. (1990). Striatal dopamine terminals release serotonin after 5-HTP pretreatment: in vivo voltammetric data. *Brain Res, 515*(1-2), 173-180.

Stamford, J. A., Kruk, Z. L., Millar, J., & Wightman, R. M. (1984). Striatal dopamine uptake in the rat: in vivo analysis by fast cyclic voltammetry. *Neurosci Lett, 51*(1), 133-138.

Steinbusch, H. W., Nieuwenhuys, R., Verhofstad, A. A., & Van der Kooy, D. (1981). The nucleus raphe dorsalis of the rat and its projection upon the caudatoputamen. A combined cytoarchitectonic, immunohistochemical and retrograde transport study. *J Physiol (Paris), 77*(2-3), 157-174.

Steinbusch, H. W., van der Kooy, D., Verhofstad, A. A., & Pellegrino, A. (1980). Serotonergic and non-serotonergic projections from the nucleus raphe dorsalis to the caudate-putamen complex in the rat, studied by a combined immunofluorescence and fluorescent retrograde axonal labeling technique. *Neurosci Lett, 19*(2), 137-142.

Stratford, T. R., & Wirtshafter, D. (1990). Ascending dopaminergic projections from the dorsal raphe nucleus in the rat. *Brain Res, 511*(1), 173-176.

Strekalova, T., Anthony, D. C., Dolgov, O., Anokhin, K., Kubatiev, A., Steinbusch, H. M., & Schroeter, C. (2013). The differential effects of chronic imipramine or citalopram

administration on physiological and behavioral outcomes in naive mice. *Behav Brain Res, 245*, 101-106.

Takmakov, P., McKinney, C. J., Carelli, R. M., & Wightman, R. M. (2011). Instrumentation for fast-scan cyclic voltammetry combined with electrophysiology for behavioral experiments in freely moving animals. *Rev Sci Instrum, 82*(7), 074302.

Takmakov, P., Zachek, M. K., Keithley, R. B., Walsh, P. L., Donley, C., McCarty, G. S., & Wightman, R. M. (2010). Carbon microelectrodes with a renewable surface. *Anal Chem, 82*(5), 2020-2028. doi: 10.1021/ac902753x

Thienprasert, A., & Singer, E. A. (1993). Electrically induced release of endogenous noradrenaline and dopamine from brain slices: pseudo-one-pulse stimulation utilized to study presynaptic autoinhibition. *Naunyn Schmiedebergs Arch Pharmacol, 348*(2), 119-126.

Thompson, B. J., Jessen, T., Henry, L. K., Field, J. R., Gamble, K. L., Gresch, P. J., . . . Blakely, R. D. (2011). Transgenic elimination of high-affinity antidepressant and cocaine sensitivity in the presynaptic serotonin transporter. *Proc Natl Acad Sci U S A, 108*(9), 3785-3790.

Thorre, K., Sarre, S., Ebinger, G., & Michotte, Y. (1997). Characterization of the extracellular serotonin release in the substantia nigra of the freely moving rat using microdialysis. *Brain Res, 772*(1-2), 29-36.

Threlfell, S., Cragg, S. J., Kallo, I., Turi, G. F., Coen, C. W., & Greenfield, S. A. (2004). Histamine H3 receptors inhibit serotonin release in substantia nigra pars reticulata. *J Neurosci, 24*(40), 8704-8710.

Threlfell, S., Greenfield, S. A., & Cragg, S. J. (2010). 5-HT(1B) receptor regulation of serotonin (5-HT) release by endogenous 5-HT in the substantia nigra. *Neuroscience, 165*(1), 212-220.

Torres, G. E., & Amara, S. G. (2007). Glutamate and monoamine transporters: new visions of form and function. *Current opinion in neurobiology, 17*(3), 304-312. doi: 10.1016/j.conb.2007.05.002

Uher, R. (2011). Genes, environment, and individual differences in responding to treatment for depression. *Harv Rev Psychiatry, 19*(3), 109-124.

Valzelli, L. (1973). The "isolation syndrome" in mice. *Psychopharmacologia, 31*(4), 305-320.

Van Bockstaele, E. J., & Pickel, V. M. (1993). Ultrastructure of serotonin-immunoreactive terminals in the core and shell of the rat nucleus accumbens: cellular substrates for interactions with catecholamine afferents. *J Comp Neurol, 334*(4), 603-617. doi: 10.1002/cne.903340408

van der Kooy, D., & Hattori, T. (1980). Dorsal raphe cells with collateral projections to the caudate-putamen and substantia nigra: a fluorescent retrograde double labeling study in the rat. *Brain Res, 186*(1), 1-7.

Vandermaelen, C. P., & Aghajanian, G. K. (1983). Electrophysiological and pharmacological characterization of serotonergic dorsal raphe neurons recorded extracellularly and intracellularly in rat brain slices. *Brain Res, 289*(1-2), 109-119.

Verge, D., Daval, G., Marcinkiewicz, M., Patey, A., el Mestikawy, S., Gozlan, H., & Hamon, M. (1986). Quantitative autoradiography of multiple 5-HT1 receptor subtypes in the brain of control or 5,7-dihydroxytryptamine-treated rats. *J Neurosci, 6*(12), 3474-3482.

Verge, D., Daval, G., Patey, A., Gozlan, H., el Mestikawy, S., & Hamon, M. (1985). Presynaptic 5-HT autoreceptors on serotonergic cell bodies and/or dendrites but not terminals are of the 5-HT1A subtype. *Eur J Pharmacol, 113*(3), 463-464.

Voikar, V., Polus, A., Vasar, E., & Rauvala, H. (2005). Long-term individual housing in C57BL/6J and DBA/2 mice: assessment of behavioral consequences. *Genes Brain Behav, 4*(4), 240-252.

Whishaw, I. Q., Cioe, J. D., Previsich, N., & Kolb, B. (1977). The variability of the interaural line vs the stability of bregma in rat stereotaxic surgery. *Physiol Behav, 19*(6), 719-722.

Wiborg, O. (2013). Chronic mild stress for modeling anhedonia. *Cell Tissue Res, 354*(1), 155-169.

Wiedemann, D. J., Basse-Tomusk, A., Wilson, R. L., Rebec, G. V., & Wightman, R. M. (1990). Interference by DOPAC and ascorbate during attempts to measure drug-induced changes in neostriatal dopamine with Nafion-coated, carbon-fiber electrodes. *J Neurosci Methods, 35*(1), 9-18.

Wiedemann, D. J., Garris, P. A., Near, J. A., & Wightman, R. M. (1992). Effect of chronic haloperidol treatment on stimulated synaptic overflow of dopamine in the rat striatum. *J Pharmacol Exp Ther, 261*(2), 574-579.

Wightman, R. M., Amatore, C., Engstrom, R. C., Hale, P. D., Kristensen, E. W., Kuhr, W. G., & May, L. J. (1988). Real-time characterization of dopamine overflow and uptake in the rat striatum. *Neuroscience, 25*(2), 513-523.

Wightman, R. M., Amatore, C., Engstrom, R. C., Hale, P. D., Kristensen, E. W., Kuhr, W. G., & May, L. J. (1988). Real-time characterization of dopamine overflow and uptake in the rat striatum. *Neuroscience, 25*(2), 513-523.

Wightman, R. M., & Zimmerman, J. B. (1990). Control of dopamine extracellular concentration in rat striatum by impulse flow and uptake. *Brain Res Brain Res Rev, 15*(2), 135-144.

Wirtshafter, D., Stratford, T. R., & Asin, K. E. (1987). Evidence that serotonergic projections to the substantia nigra in the rat arise in the dorsal, but not the median, raphe nucleus. *Neurosci Lett, 77*(3), 261-266.

Wrona, M. Z., & Dryhurst, G. (1990). Electrochemical Oxidation of 5-Hydroxytryptamine in Aqueous-Solution at Physiological Ph. *Bioorganic Chemistry, 18*(3), 291-317.

Wrona, M. Z., Lemordant, D., Lin, L., Blank, C. L., & Dryhurst, G. (1986). Oxidation of 5-hydroxytryptamine and 5,7-dihydroxytryptamine. A new oxidation pathway and formation of a novel neurotoxin. *J Med Chem, 29*(4), 499-505.

Yavich, L., & MacDonald, E. (2000). Dopamine release from pharmacologically distinct storage pools in rat striatum following stimulation at frequency of neuronal bursting. *Brain Res., 870*(1-2), 73-79.

Yocca, F. D., & Maayani, S. (1990). 5-HT receptors linked to adenylyl cyclase activity in mammalian brain. *Ann N Y Acad Sci, 600*, 212-223.

Yorgason, J. T., Espana, R. A., & Jones, S. R. (2011). Demon voltammetry and analysis software: analysis of cocaine-induced alterations in dopamine signaling using multiple kinetic measures. *J Neurosci Methods, 202*(2), 158-164.

Zachek, M. K., Takmakov, P., Moody, B., Wightman, R. M., & McCarty, G. S. (2009). Simultaneous decoupled detection of dopamine and oxygen using pyrolyzed carbon microarrays and fast-scan cyclic voltammetry. *Anal Chem, 81*(15), 6258-6265. doi: 10.1021/ac900790m

Zachek, M. K., Takmakov, P., Park, J., Wightman, R. M., & McCarty, G. S. (2009). Simultaneous monitoring of dopamine concentration at spatially different brain locations in vivo. *Biosens Bioelectron, 25*(5), 1179-1185.

Zheng, G., Dwoskin, L. P., & Crooks, P. A. (2006). Vesicular monoamine transporter 2: role as a novel target for drug development. *AAPS J, 8*(4), E682-692. doi: 10.1208/aapsj080478

Zhou, F. C., Tao-Cheng, J. H., Segu, L., Patel, T., & Wang, Y. (1998). Serotonin transporters are located on the axons beyond the synaptic junctions: anatomical and functional evidence. *Brain Res, 805*(1-2), 241-254.